Mechanisms of Growth and Chronic Disorders of Musculotendinous Tissues

by

Jonathan P. Gumucio

A dissertation submitted in partial fulfillment
of the requirements for the degree of
Doctor of Philosophy
(Molecular & Integrative Physiology)
from the University of Michigan
2017

Doctoral Committee:

Associate Professor Christopher L. Mendias, Chair
Professor Susan Brooks Herzog
Professor Jeffrey C. Horowitz
Professor Carey N. Lumeng
Professor Kathe A. Derwin, Cleveland Clinic

Jonathan P Gumucio

jgumucio@umich.edu

ORCID iD: 0000-0002-9074-3216

ACKNOWLEDGEMENTS

There are so many people to thank, and a little page here does such an injustice to them, but I will do my best. First, I'd like to thank my mentor, Chris Mendias, for his guidance, rigor, and friendship for the past six years. I have been working with you for even longer than this, and am glad we were able to ride this scientific wave together. I'd like to thank the rest of my committee, Susan Brooks for giving me my first job in science, Jeff Horowitz for being a great rotation mentor, Carey Lumeng for his guidance throughout my thesis and the prelim process, and Kathe Derwin, for her mentorship all the way from when I was just getting started as an undergrad scientist, and also being perhaps the best fellowship reviewer I've ever had.

I also want to thank my department/home, Molecular and Integrative Physiology. My graduate chairs, Ormond MacDougald, Scott Pletcher, and Sue Moenter have been incredible mentors, and helped me in real times of need, I won't forget what you've done for me. Also, our graduate coordinator, Michele Boggs, for taking care of us grad students and making sure we were well accommodated for. I need to also thank Bishr Omary, for his indelible support of me, I always felt very welcome meeting with you, even without an appointment. And the rest of my peers in MIP, you have been great friends and I hope to keep in touch, and I want to particularly thank Andrew Schwartz, Matt Taylor, and Danny Triner for being great friends and scientific confidants.

I want to thank the rest of my lab, there have been so many of you over the years, but thank you for the fun times, even late at night. Thank you to Kris Sugg, Stuart Roche, and Evan Lynch- you all deserve special mentions for your friendship and help.

Lastly, I want to thank my friends and family. I've had tremendous support and friendship during my time here, and there are too many of you for one acknowledgement section. I would be remiss if I didn't especially thank Cailen O'Shea, Mike Mikho, and Doug Van Pelt for being incredible support systems and friends for a very long time. I also want to especially thank Anna Pavlenko for helping me push through hard times, for her unwavering support of me and my goals, and her willingness to go on random road trips with me. And want to thank my parents Deb and Jorge, and brothers Nick and Jav. Being raised in a family of scientists was interesting for sure- I think I had a "committee" meeting every time I made it home for dinner. But in all seriousness, I couldn't have done it without you guys, thank you. None of this happens without you.

TABLE OF CONTENTS

LIST OF TABLES

LIST OF FIGURES

ABSTRACT

Musculoskeletal diseases affect over half of the United States population aged 18 or older, and over 75% of individuals 65 and older. Despite the prevalence and estimated economic burden of over $795 billion, little is known about the basic biology of some musculoskeletal tissues, nor the pathogenesis of certain musculoskeletal disorders. Understanding the biology of these tissues, as well as the mechanisms by which normal physiological functioning is lost will undoubtedly aid in the development of treatment strategies that help patients recover and return to normal life. The aims of this body of work was to i) address the lack of knowledge in basic tendon biology that restricts our ability to understand cellular and molecular changes to tendon following loading, and ii) address the mechanisms of the accumulation of pathological ectopic lipid with concomitant atrophy and fibrosis, termed myosteatosis, that occurs in chronic rotator cuff injuries. The studies in this dissertation fill in considerable gaps in the understanding of i) basic tendon biology and the role of the transcription factor, scleraxis, in adult tendon adaptation, and ii) the progression and consequences of myosteatosis on muscle metabolism and function. Scleraxis is a basic helix-loop-helix transcription factor required for the embryonic formation of tendon, but it was not known what the role of scleraxis was in adult tendon growth. We show that scleraxis is expressed in proliferative tendon fibroblasts, and is required for the proper growth and

adaptation of adult tendon to mechanical stimuli. Additionally, we show scleraxis may have a critical role in the differentiation of tendon progenitor cells. For myosteatosis, it was not known how lipid accumulated within torn rotator cuff muscles, or what pathways were activated by excess lipid. We show that myosteatosis arises from an initial acute inflammatory phase marked by dysfunctional mitochondria that are unable to oxidize lipid. This results in a buildup of lipid over time, which results in a chronic, sustained inflammatory environment, marked by oxidative stress, atrophy, and muscle dysfunction. Overall, this group of studies establishes several new directions for future research that apply to a much larger body of musculoskeletal disorders.

CHAPTER I

Introduction

BACKGROUND

Musculoskeletal injuries and disorders affect over half of the United States population over the age of 18, and roughly 75% of individuals 65 and older (53). Despite the prevalence and an estimated economic burden of over $795 billion, the basic biology of certain musculoskeletal tissues, nor the pathogenesis of certain musculoskeletal disorders was not known. This lack in knowledge of musculoskeletal issues presents a great opportunity for basic research into both the physiological functioning of musculoskeletal tissues, and identification of new pathways to target for treatment of musculoskeletal disorders. The studies in this dissertation aimed to i) address the lack of knowledge in basic tendon biology that restricts our ability to understand cellular and molecular changes to tendon following loading, and ii) address the mechanisms of the accumulation of pathological ectopic lipid with concomitant atrophy and fibrosis, termed myosteatosis, that occurs in chronic rotator cuff injuries.

Prolonged overloading and excessive overuse of musculotendinous structures leads to tissue stress and often bonafide clinical symptoms (28). Tendinopathies are painful disorders that can occur within almost any tendon in the body, and are degenerative conditions that affect tendon cell and matrix homeostasis (27). However, there exists a gap in understanding of not only the mechanisms that govern

tendinopathy, but also the basic biology or physiology of tendon. Virtually nothing is known about the different roles of tendon fibroblasts or what population of cells constitutes the tendon stem cell compartment, which could potentially be utilized for therapies to treat tendinopathies. The studies described in this dissertation will increase our understanding fundamental tendon biology in adulthood, and identify the populations of cells within tendon that allow this tissue to grow and adapt to mechanical stimuli.

Rotator cuff tears account for the majority of shoulder injuries, affecting roughly 4.5 million patients every year, and are accompanied by a projected annual cost of $7 billion in the United States (25). Over a quarter million rotator cuff surgeries are performed each year in the USA (7), yet the probability of re-injury after surgery can be up to 30% in moderate to severe tears, and upwards of 94% for massive, chronic tears (3). The incidence and severity of rotator cuff tears increases with age, and almost one quarter of individuals over 50 have complete rupture of the rotator cuff (32, 43). The rotator cuff is composed of four muscles: the supraspinatus, the infraspinatus, the teres minor, and the subscapularis (Figure 1.1). While not primary movers of the shoulder, these muscles play a vital role in the stabilization of the shoulder joint. The vast majority of rotator cuff tears are caused over long periods of time by repetitive micro-trauma to the rotator cuff tendon (54). Tears are associated with irreversible pathological changes to the rotator cuff muscle, and while surgical repair of the torn rotator cuff offers mild pain relief for most patients (25), the repair procedure does not protect muscle tissue from further degradation over time. Persistent muscle weakness is a major drawback in the ability to successfully treat these injuries and reduce patient recovery times (16).

Because surgical repair is unable to fully restore the function of the rotator cuff, a deeper understanding of the cellular and molecular changes within the rotator cuff following tear will likely augment current surgical repair techniques and treatment of these injuries.

Like many other unloading models of muscle injuries, tears cause atrophy and fibrosis within rotator cuff muscles. However, rotator cuff muscles also develop a substantial amount of intra- and intermuscular lipid following tear (14, 16, 19), and together with muscle atrophy and fibrosis, this phenomenon of lipid accumulation within muscle is called “myosteatosis.” Surgical repair of rotator cuff muscles does not reduce myosteatosis (15, 16), and the amount of lipid within torn rotator cuff muscles is negatively correlated with muscle function (14). Since the initial discovery of myosteatosis in 1852 (37), numerous studies have measured accumulated lipid with a variety of imaging techniques such as MRI, and while many postulate that the accumulated lipid in myosteatosis is likely pathological, the cellular and molecular mechanisms that account for the reduction in muscle function following myosteatosis is unknown. In addition to the studies on tendon biology, this dissertation will identify pathways that are involved in myosteatosis that lead to a decrease in muscle function and lead to new research directions in the field of myosteatosis.

TENDON STRUCTURE AND FUNCTION

Tendons are responsible for the transmission of force between muscle and bone to aid in movement. This tissue is primarily composed of bundles of type I collagen fibers arranged in cable like orientation along the axis of force transmission (28, 55). Other components of tendon matrix include type III collagen, elastin, and various

proteoglycans such as decorin, tenascin-C, fibromodulin, and biglycan (28). The fundamental component of tendon is the tendon fiber, which combine to form tendon fascicles, and further organized into a compartment known as the endotenon by layers of type IV and VI collagens (55). These structures are wrapped with a basement membrane-rich matrix known as the epitenon, which contains blood, nerve, and lymphatic supply for the tendon. Finally, the outermost tendon layer is the paratenon, a synovial sheath that encapsulates the epitenon and reduces friction for the tendon as it moves. Together, the paratenon and epitenon compose the peritenon.

Tendon is often exposed to a wide range of forces during movement, and the configuration of proteins within tendon allow for the proper distribution of these forces to enable movement. The biomechanics of tendon are often measured by placing loads on tendon and measuring stress as a function of tendon strain. Stress is measured as the force on the tissue normalized by tendon cross-sectional area (CSA), and strain is measured by the deformation of the tissue normalized by its resting length (33, 55). The composition of tendon makes it a viscoelastic material, such that there is a non-linear relationship between stress and strain, and load placed on the tendon to stretch it can be stored within the tendon to be released as elastic energy. A linear relationship between stress and strain is observed in springs, but for tendon, loading produces a stress-strain relationship that is marked initially by a shallow toe region, and upon more loading the stress-strain curve displays a more linear region with a steeper slope. Physiological loading typically falls within the toe region and early linear region, but upon the addition of more load, tendon reaches a “yield point,” where the tendon no longer functions within the normal elastic range. Loading tendons past the yield point

results in a “plastic range” where the tendon damage is permanent and the tendon is highly susceptible to rupture (33, 55).

The major cellular component of tendon is the fibroblast, which sits on collagen fibers and contributes to tendon matrix synthesis, degradation, and turnover (28). Physiological loading of tendons can increase tendon CSA, fibroblast density, and type I collagen levels (27, 35, 38). The cellular and molecular processes that govern tendon adaptation in adulthood are largely unknown, but in other tissues, many of the same signaling pathways and molecular networks that govern musculoskeletal tissue development also regulate the adaptation of these tissues in adults (13). One transcription factor that has been identified with a central role in tendon development is the basic helix-loop-helix (bHLH) transcription factor scleraxis (8). Scleraxis robustly marks limb tendons during development, and loss of scleraxis results in the failure to form limb tendons, which causes limb contractures and developmental disabilities (40, 49). Scleraxis continues to be widely expressed in tendon early in the postnatal stages of life, but the expression is limited to the epitenon region in adulthood (35).

In the adult tendon, scleraxis likely has many transcriptional targets important for tendon formation, including the collagen 1α1 transcript (31), and tenomodulin, a type II transmembrane glycoprotein that marks differentiated tendon cells (9, 51). During physiological loading of tendons, scleraxis levels are increased in the epitenon regions of the tendon, which also correlates with increases in the expression of tenomodulin and type I collagen transcripts (35). Not much is known about the role of scleraxis in the adaptation of adult tendon, or if scleraxis is required for the increase in tendon CSA following mechanical loading. Additionally, it is thought that tendon possesses a stem

cell compartment (59), but the location of these cells, and whether scleraxis plays a role in the differentiation of these cells into mature tenocytes is unknown.

SKELETAL MUSCLE STRUCTURE AND FUNCTION

Skeletal muscle is composed of thousands to millions of long multinucleated fibers held together by layers of ECM. Like tendon, these layers of ECM are arranged in hierarchical structure, with a layer of endomysium wrapped superficially by a perimysium, and further surrounded by an epimysium (28). The epimysium and perimysium are composed mainly of type I and III collagens, which most likely act as molecular springs to aid in protecting muscle fibers from stretch-induced injury (1). The endomysium consists of type I and III collagens that form honeycomb like structures around muscle fibers, and eventually meet to form the tendon (28). The collagens within the endomysium are important for the transmission of forces longitudinally through the muscle, and also laterally between muscle fibers (45, 46). The propagation of lateral forces is accomplished through the connection of the endomysium to the basement membranes around muscle fibers, composed of the type IV and VI collagens (28). Connecting the fibrillar collagen-rich endomysium to the network collagen-rich basement membrane is accomplished through integrin, fibronectin, and other structural proteins.

Within skeletal muscle cells, the basic structural component responsible for force generation is the sarcomere, which are tightly arranged in small, parallel myofibrils to allow the muscle fiber to contract. Individual sarcomeres are composed of three main structures- the thick filament, the thin filament, and the Z-disk (52). Thick filaments are comprised of myosin heavy chain, the main molecular driver of contraction, which binds

actin on thin filaments to contract. Thin filaments are composed of actin and other regulatory proteins, and are anchored to the Z-disk by the structural proteins, titin and nebulin (29, 52). The Z-disks are responsible for the proper transmission of forces generated both longitudinally and laterally through connections to other structures within and around the muscle cell. Longitudinal forces are carried from the Z-disks to the actin cytoskeleton of the cell, and allow forces to propagate along the muscle through the tendon. Lateral forces are produced by linkages from the Z-disk to the dystrophin-glycoprotein complex (DGC), a membrane-bound structure that is attached extracellularly to laminin and fibronectin (5, 39). The interaction of the contracting sarcomere through the Z-disk and actin cytoskeleton, the DGC, and the ECM allow for the proper function of skeletal muscles to transmit forces, reduce contraction-induced injury, and allow for proper function and locomotion.

There are three main types of contraction in skeletal muscle, each relate to the change in length of the fibers during contraction of the muscle. Isometric contractions occur when the muscle is contracting in the absence of a change in length, indicating that the force generated by the muscle is equal to the load being placed on it (12). The force that a muscle can generate is highest during isometric contraction, and this is called maximum isometric force (P_o). Normalizing P_o to the CSA of the muscle yields specific maximum tetanic force (sP_o), which is a powerful indicator of muscle function (6). Concentric, or shortening contractions, occur when the force produced by muscle is greater than the load, and a decrease in length occurs in the muscle (12). Conversely, when the load on the muscle is greater than the force being produced, a lengthening contraction occurs, and the fibers are increasing in length as they are contracting.

Contraction-induced injury occurs during lengthening contractions, where the frequency or magnitude of the force disrupts sarcomere structure, and can damage the muscle plasma membrane, called the sarcolemma (12, 34). Minor contraction-induced injuries are common during exercise or resistance training and result in positive adaptations in muscle protein synthesis and over time can yield increases in P_o (11, 17). A summary of the signaling pathways that regulate both muscle protein synthesis and degradation is outlined in Figure 1.2.

Perhaps the most widely studied activator of protein synthesis and muscle hypertrophy is IGF-1. There are alternative spliced isoforms of IGF-1, including IGF-1Ea, IGF-1Eb, and Mechano Growth Factor (MGF) (18). These isoforms appear to have various roles in the regulation of skeletal muscle growth. Transgenic mice that overexpress IGF-1 under the control of muscle-specific promoters have increased muscle mass, CSA, and P_o compared to wild-type controls (42). IGF-1 binds to its receptor and activates insulin receptor substrate-1, IRS-1, which then directs the activation if phosphatidylinositol-3-kinase (PI3K), and downstream results in Akt/mTOR signaling, causing muscle protein synthesis (48). mTOR is considered one of the most critical intracellular regulators of skeletal muscle mass. While IGF-1 activates mTOR through Akt, the alternately spliced, locally expressed isoform of IGF-1, IGF-1Ea, appears to activate mTOR independent of Akt. Downstream, mTOR signals through the activation of p70S6K, which increases protein synthesis by activating S6 and eIF4B, factors that increase mRNA translation and ribosomal biogenesis (60). Phosphorylation of 4EBP1 by mTOR releases its inhibition on eIF4E, allowing translation to proceed.

The targeted inhibition of mTOR by the drug rapamycin is an effective way to curb protein synthesis and can halt load-induced muscle growth (44).

More severe lengthening contraction-induced injuries can cause massive amount of sarcomere damage and subsequent proteolytic remodeling within sarcomeres. Damage to the sarcolemma allows an influx of extracellular Ca^{2+} into the fiber and activates of an important protease, m-calpain (24). Once active, m-calpain degrades titin, and this process likely assists in the disassembly of damaged myofibrils and subsequent physical release of sarcomeric proteins so that they can be broken down fully. Once free from the sarcomere, damaged actin, myosin, and other sarcomeric proteins are degraded in muscle fibers through induction of the E3 ubiquitin ligases, atrogin-1 and MuRF-1 (48). These ligases direct the polyubiquination of damaged proteins, and targets these proteins for breakdown in the 26S proteasome. This process likely serves as a method to recycle dysfunctional proteins into free amino acids to be used for subsequent synthesis of new proteins, and regeneration of the damaged muscle fiber.

Repair of injured muscle fibers is also facilitated by other types of cells within skeletal muscle. Outside of the muscle fibers, the other main cellular components of skeletal muscle are satellite cells and non-myogenic cells. Satellite cells are muscle stem cells that typically exist in a quiescent state between the basement membrane and sarcolemma of the muscle fiber (22). Quiescence in satellite cells is marked by the transcription factor Pax7, which is required for the specification of satellite cells to the myogenic lineage (47). Upon activation, satellite cells break from their quiescent niche, migrate to the site of injury, proliferate, and fuse to damaged muscle fibers to repair

them. The process of going from a quiescent satellite cell to a differentiated muscle fiber is a complex process that requires the activation of a group of bHLH transcription factors, called the myogenic regulatory factors (MRF) (47). The MRFs include Myf5, MyoD, myogenin, and MRF4, and each directs transcription during specific stages of skeletal muscle differentiation. Satellite cells exhibit asymmetrical division, where one daughter cell retains Pax7 expression and maintains the satellite cell pool by remaining a quiescent satellite cell, while the other daughter cell becomes a myogenic satellite cell and Pax7 directs the activation of Myf5. The myogenic cell then continues proliferating and expresses MyoD. MyoD is further upregulated quickly after differentiation, and soon thereafter myogenin is expressed. The induction of myogenin expression is associated with a decrease in Myf5 and MyoD expression, and the cell withdraws from the cell cycle. As the cell continues to differentiate, myogenin levels fall as MRF4 levels rise (47).

As a differentiated myogenic cell fuses with a damaged muscle fiber, it adds a nucleus to the fiber. Nuclei to healthy fibers are located on the periphery of the cell, but newly added nuclei are centrally located in the fiber (22). The reason behind this is unclear, but it has been proposed that the reason for a centrally located nucleus is to offer a logistically favorable location for newly synthesizing sarcomeric proteins in the muscle fiber (26). Sarcomeric proteins are very large and would require substantial cellular energy to package them in a golgi apparatus, so they are often synthesized directly at the sarcomere instead of an endoplasmic reticulum. As the cell is repaired, the nucleus then assumes the normal peripheral location.

Non-myogenic cells also contribute to the maintenance and repair of muscle fibers. Like tendons, muscles contain fibroblasts that regulate and maintain the ECM within skeletal muscle. In addition to their capacity to synthesize ECM, fibroblasts also play an important role in the direction of satellite cell activity. After skeletal muscle injury, muscle fibroblasts proliferate in response to injury in close association with satellite cells (41). The process of regeneration for muscle fibers takes significantly longer than the deposition of ECM, so the coordination of timing between satellite cells and fibroblasts is critical for the proper regeneration of skeletal muscle. After proliferating, fibroblasts synthesize matrix as a scaffold for regenerating muscle fibers, and allow satellite cells to differentiate and participate in fusion to damaged fibers. Without fibroblasts, satellite cells will prematurely differentiate, and this results in smaller muscle fibers and impaired regeneration. In the absence of satellite cells, the muscle does not regenerate at all and exhibits extreme levels of ECM deposition, which completely disrupts normal muscle architecture due to the replacement of muscle area with fibrosis, or scar tissue.

SKELETAL MUSCLE LIPID METABOLISM

Skeletal muscle uses a variety of fuel sources for generation of cellular energy in the form of ATP. There are three main cellular pathways to generate ATP. Anaerobic ATP generation can result from the hydrolysis of phosphocreatine via creatine kinase, or by anaerobic glycolysis (30). ATP is also generated in mitochondria through oxidative phosphorylation. Aerobic ATP generation in mitochondria can utilize byproducts from either glycolysis or lipids, but the pathways to metabolize lipids will be focused on here.

Lipids are transported through the blood in triglyceride-rich spheres called chylomicrons. For lipids to enter muscle cells, free fatty acids must be cleaved from triglyceride molecules by lipoprotein lipase (50), which enables long-chain free fatty acids to enter the cell via the CD36 lipid transporter (23). Once inside the cell, fatty acids stimulate the activation of the peroxisome proliferator-activated receptors (PPARs), which direct the expression of genes related to lipogenesis, lipid storage, and metabolic homeostasis (2). There are three PPAR isoforms: PPARα, PPARδ, and PPARγ, and all are expressed in skeletal muscle, though PPARδ is the most highly expressed in this tissue. Fatty acids inside the cell can either be processed for storage in triglyceride rich droplets, or be utilized for energy production in mitochondria. Storage of lipid requires the activation of several regulatory enzymes that esterify fatty acids with glycerol-3-phosphate, which is also a component of glycolysis (56). Two of the most important proteins to catalyze the formation of triglycerides from free fatty acids are glycerol-3-phosphate acyltransferease (GPAT), which directs the committed step in formation of triglyceride, and diacylglycerol acyltransferase (DGAT), which catalyzes the final step in the pathway, resulting in the formation of triglyceride.

Triglyceride-rich droplets are located within the muscle near mitochondria, and free fatty acids are cleaved from these droplets for utilization by a few key intracellular lipases, hormone sensitive lipase (HSL) and adipose triglyceride lipase (ATGL) (10, 56). Cleaved free fatty acids from lipid droplets, or fatty acids that have been imported in the cell through CD36 can then be utilized in mitochondria after first linking to coenzyme A, forming a fatty acyl-CoA (23). Fatty acyl-CoAs cannot enter the mitochondria on their own due to their polarity, so they are converted into neutral acyl-carnitine, by carnitine

palmitoyl transferase-I (CPTI). Acyl carnitine is shuttled inside the mitochondria by carnitine acyl-carnitine translocase (CAT), and in order to be oxidized in the mitochondria, must again be converted to a fatty acyl-CoA, this time by CPTII. After several rounds of beta-oxidation within mitochondria, long-chain acyl-CoAs are broken down into many two-carbon acetyl-CoA molecules, and can then be utilized for ATP production in the citric acid cycle, and electron transport chain.

In cases of lipid excess, a third fate of fatty acids can result in deleterious effects on skeletal muscle homeostasis. Over accumulation of lipid within cells increases the abundance of lipid intermediates, such as diglyceride and ceramide, which can activate inflammatory pathways such as c-Jun NH2-terminal kinase (JNK) and IκB kinase-beta (IKKβ) (56), and decrease insulin signaling. Increased intracellular lipid intermediates leads to the phosphorylation IRS-1 at multiple serine residues, which inhibits IRS-1 tyrosine phosphorylation, necessary for insulin stimulated glucose uptake (58). IRS-1 serine phosphorylation is thought to be performed by a member of the novel family of protein kinase Cs, PKCθ (20). It is not clear whether DAG activates PKCθ directly or through the activation of JNK and IKKβ (56). This pathway is considered to explain the link between insulin resistance and obesity, where excess lipid drastically reduces insulin signaling. The insulin pathway shares many of the same cellular kinases and proteins as the IGF-1 pathway, though it is unknown what effect excess lipid has on IGF-1 signaling. However, the JNK and IKKβ pathways leads to the activation of the transcription factor, NFκB, which is a major cellular mediator of inflammation and muscle atrophy through the induction of the E3 ubiquitin ligase, MuRF-1 (48).

Excess extracellular lipid can also have detrimental effects on muscle function. Large lipid droplets can be mediators of inflammation in disease through the synthesis of pro-inflammatory eicosanoids (4, 57). This occurs via the production of arachidonyl lipids within droplets, as the enzymes for arachidonic acid synthesis localize to lipid droplets. Arachidonic acid is then converted to eicosanoids though eicosanoid forming enzymes, also located on lipid droplets. Eicosanoids such as prostaglandins and leukotrienes have a wide array of cellular functions, but many have potent pro-inflammatory effects (4) and can be detrimental to the differentiation of skeletal muscle progenitor cells (36).

RATIONALE AND APPROACH

Improving the treatment of rotator cuff tears requires the proper understanding of the cellular and molecular changes that occur within rotator cuff tendons and muscles. As the pathways that govern tendon adaptation are largely unknown, studies that identify transcriptional and cellular regulators of tendon growth and adaptation will provide much needed information to enhance tendon regeneration after rotator cuff surgery. Conversely, mechanisms of muscle atrophy, growth, and regeneration following injury has been widely studied in the literature, but there is still a lack of information as to why the rotator cuff muscle develops myosteatosis. Understanding the effect of muscle lipid accumulation on muscle function will enable the development of strategies to augment muscle regeneration following these injuries.

The purpose of this dissertation is to identify several unknowns about tendon biology, scleraxis function, and myosteatosis. For studies in tendon, the main questions addressed in this dissertation include i) which populations of fibroblasts can participate

in the growth and adaptation of adult tendon, ii) whether scleraxis is required for tendon adaptation and growth in adulthood, and iii) whether scleraxis may play a central role in the differentiation of tendon progenitor cells. These questions will be addressed in Chapter II and III, using a combination of transgenic mouse models, gene expression, and a novel model of tendon growth and adaptation. For studies in myosteatosis, the main research questions that are addressed here are i) the identification of molecular pathways that can explain the increase in lipid following rotator cuff tear, and ii) measurement of the functional consequences of increased intra- and intermyocellular lipid to skeletal muscle. These questions will be addressed in Chapter IV, using a variety of omics platforms, large scale bioinformatics, muscle force measurement, and mitochondrial activity assays in a rat model. In total, the findings of these studies will add to the growing literature on tendon and muscle physiology, and hopefully lead to new treatment directions for patients with muscle and tendon injuries.

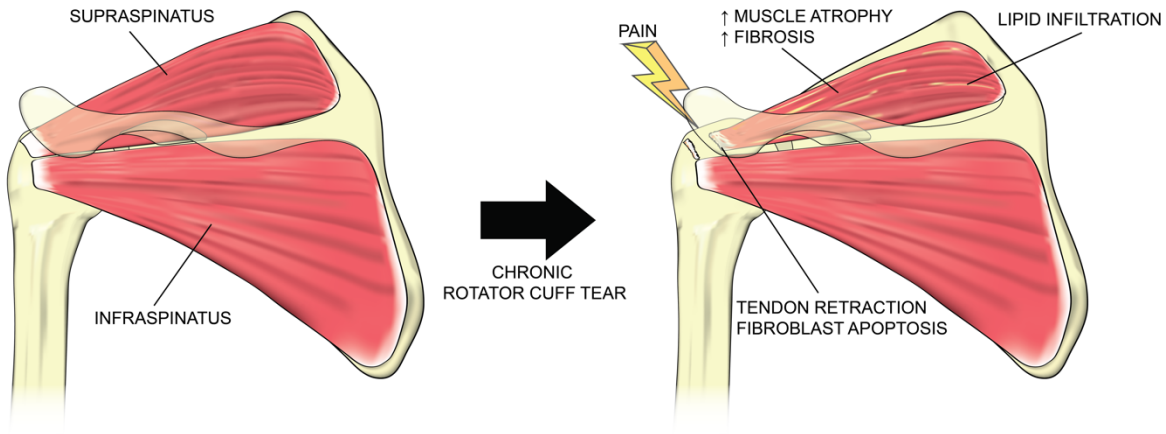

Figure 1.1. Overview of pathological changes to muscle during rotator cuff tear. The intact rotator cuff in posterior view is shown on the left, with the supraspinatus and infraspinatus visible (not shown are the teres minor and subscapularis). Following chronic rotator cuff tear, shown here for the supraspinatus, the tendon retracts, and the rotator cuff muscle undergoes dramatic atrophy, fibrosis, and lipid infiltration, collectively referred to as myosteatosis.

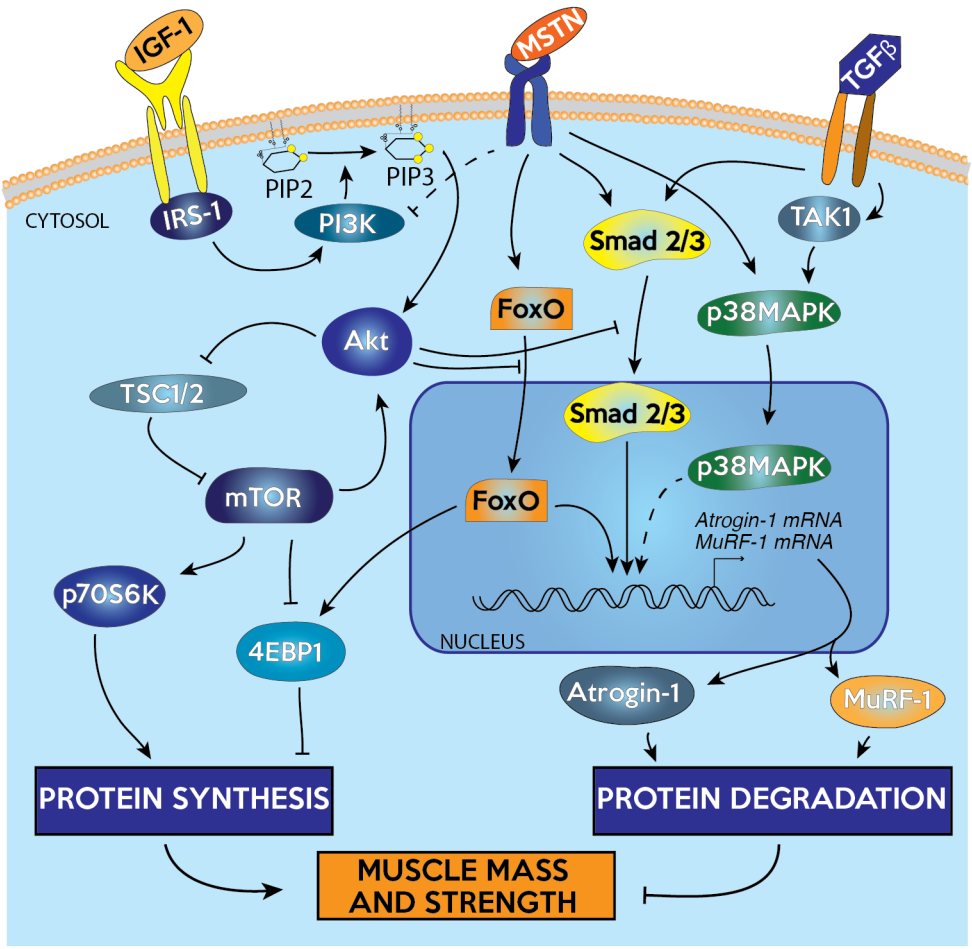

Figure 1.2. Overview of intracellular pathways within muscle that contribute to protein synthesis or protein breakdown. From Gumucio and Mendias, 2013(21)

REFERENCES

1. **Arruda EM**, **Mundy K**, **Calve S**, **Baar K**. Denervation does not change the ratio of collagen I and collagen III mRNA in the extracellular matrix of muscle. *Am J Physiol Regul Integr Comp Physiol* 292: R983–R987, 2007.

2. **Barish GD**, **Narkar VA**, **Evans RM**. PPAR delta: a dagger in the heart of the metabolic syndrome. *J Clin Invest* 116: 590–597, 2006.

3. **Bedi A**, **Dines J**, **Warren RF**, **Dines DM**. Massive tears of the rotator cuff. *The Journal of Bone and Joint Surgery* 92: 1894–1908, 2010.

4. **Bozza PT**, **Viola JPB**. Lipid droplets in inflammation and cancer. *Prostaglandins Leukot Essent Fatty Acids* 82: 243–250, 2010.

5. **Capetanaki Y**, **Bloch RJ**, **Kouloumenta A**, **Mavroidis M**, **Psarras S**. Muscle intermediate filaments and their links to membranes and membranous organelles. *Experimental Cell Research* 313: 2063–2076, 2007.

6. **Claflin DR**, **Larkin LM**, **Cederna PS**, **Horowitz JF**, **Alexander NB**, **Cole NM**, **Galecki AT**, **Chen S**, **Nyquist LV**, **Carlson BM**, **Faulkner JA**, **Ashton-Miller JA**. Effects of high- and low-velocity resistance training on the contractile properties of skeletal muscle fibers from young and older humans. *J Appl Physiol* 111: 1021–1030, 2011.

7. **Colvin AC**, **Egorova N**, **Harrison AK**, **Moskowitz A**, **Flatow EL**. National trends in rotator cuff repair. *The Journal of Bone and Joint Surgery* 94: 227–233, 2012.

8. **Cserjesi P**, **Brown D**, **Ligon KL**, **Lyons GE**, **Copeland NG**, **Gilbert DJ**, **Jenkins NA**, **Olson EN**. Scleraxis: a basic helix-loop-helix protein that prefigures skeletal formation during mouse embryogenesis. *Development* 121: 1099–1110, 1995.

9. **Docheva D**, **Hunziker EB**, **Fässler R**, **Brandau O**. Tenomodulin is necessary for tenocyte proliferation and tendon maturation. *Mol Cell Biol* 25: 699–705, 2005.

10. **Ducharme NA**, **Bickel PE**. Lipid droplets in lipogenesis and lipolysis. *Endocrinology* 149: 942–949, 2008.

11. **Evans WJ**. Protein Nutrition and Resistance Exercise. *Can J Appl Physiol* 26: S141–S152, 2001.

12. **Faulkner JA**, **Brooks SV**, **Opiteck JA**. Injury to Skeletal Muscle Fibers During Contractions: Conditions of Occurrence and Prevention. *Physical Therapy* 73: 911–921, 1993.

13. **Gayraud-Morel B**, **Chrétien F**, **Tajbakhsh S**. Skeletal muscle as a paradigm for regenerative biology and medicine. *http://dxdoiorg/102217/1746075142293* 4: 293–319, 2009.

14. **Gerber C**, **Schneeberger AG**, **Hoppeler H**, **Meyer DC**. Correlation of atrophy and fatty infiltration on strength and integrity of rotator cuff repairs: a study in thirteen patients. *J Shoulder Elbow Surg* 16: 691–696, 2007.

15. **Gerber C**, **Wirth SH**, **Farshad M**. Treatment options for massive rotator cuff tears. *J Shoulder Elbow Surg* 20: S20–9, 2011.

16. **Gladstone JN**, **Bishop JY**, **Lo IKY**, **Flatow EL**. Fatty infiltration and atrophy of the rotator cuff do not improve after rotator cuff repair and correlate with poor functional outcome. *American Journal of Sports Medicine* 35: 719–728, 2007.

17. **Glass DJ**. Molecular mechanisms modulating muscle mass. *Trends in Molecular Medicine* 9: 344–350, 2003.

18. **Goldspink G**. Mechanical signals, IGF-I gene splicing, and muscle adaptation. *Physiology (Bethesda)* 20: 232–238, 2005.

19. **Goutallier D**, **Postel JM**, **Bernageau J**, **Lavau L**, **Voisin MC**. Fatty muscle degeneration in cuff ruptures. Pre- and postoperative evaluation by CT scan. *Clin Orthop Relat Res* : 78–83, 1994.

20. **Griffin ME**, **Marcucci MJ**, **Cline GW**, **Bell K**, **Barucci N**, **Lee D**, **Goodyear LJ**, **Kraegen EW**, **White MF**, **Shulman GI**. Free fatty acid-induced insulin resistance is associated with activation of protein kinase C theta and alterations in the insulin signaling cascade. *Diabetes* 48: 1270–1274, 1999.

21. **Gumucio JP**, **Mendias CL**. Atrogin-1, MuRF-1, and sarcopenia. *Endocrine* 43: 12–21, 2013.

22. **Hawke TJ**, **Garry DJ**. Myogenic satellite cells: physiology to molecular biology. *J Appl Physiol* 91: 534–551, 2001.

23. **Holloway GP**, **Luiken JJFP**, **Glatz JFC**, **Spriet LL**, **Bonen A**. Contribution of FAT/CD36 to the regulation of skeletal muscle fatty acid oxidation: an overview. *Acta Physiologica* 194: 293–309, 2008.

24. **Jackman RW**, **Kandarian SC**. The molecular basis of skeletal muscle atrophy. *Am J Physiol, Cell Physiol* 287: C834–43, 2004.

25. **Jain NB**, **Wilcox RB**, **Katz JN**, **Higgins LD**. Clinical examination of the rotator cuff. *PM R* 5: 45–56, 2013.

26. **Kiri A**, **Goldspink G**. RNA–protein interactions of the 3′ untranslated regions of myosin heavy chain transcripts. *J Muscle Res Cell Motil* 23: 119–129, 2002.

27. **Kjaer M**, **Langberg H**, **Heinemeier K**, **Bayer ML**, **Hansen M**, **Holm L**, **Doessing S**, **Kongsgaard M**, **Krogsgaard MR**, **Magnusson SP**. From mechanical loading to collagen synthesis, structural changes and function in human tendon. *Scand J*

Med Sci Sports 19: 500–510, 2009.

28. **Kjaer M**. Role of extracellular matrix in adaptation of tendon and skeletal muscle to mechanical loading. *Physiol Rev* 84: 649–698, 2004.

29. **Knupp C**, **Luther PK**, **Squire JM**. Titin Organisation and the 3D Architecture of the Vertebrate-striated Muscle I-band. *Journal of Molecular Biology* 322: 731–739, 2002.

30. **Lanza IR**, **Befroy DE**, **Kent-Braun JA**. Age-related changes in ATP-producing pathways in human skeletal muscle in vivo. *J Appl Physiol* 99: 1736–1744, 2005.

31. **Léjard V**, **Brideau G**, **Blais F**, **Salingcarnboriboon R**, **Wagner G**, **Roehrl MHA**, **Noda M**, **Duprez D**, **Houillier P**, **Rossert J**. Scleraxis and NFATc Regulate the Expression of the Pro-α1(I) Collagen Gene in Tendon Fibroblasts. *Journal of Biological Chemistry* 282: 17665–17675, 2007.

32. **Lin J**, **Weintraub N**, **Aragaki D**. Nonsurgical Treatment for Rotator Cuff Injury in the Elderly. *Journal of the American Medical Directors Association* 9: 626–632, 2008.

33. **Magnusson SP**, **Hansen P**, **Kjaer M**. Tendon properties in relation to muscular activity and physical training. *Scand J Med Sci Sports* 13: 211–223, 2003.

34. **McCully KK**, **Faulkner JA**. Injury to skeletal muscle fibers of mice following lengthening contractions. *J Appl Physiol* 59: 119–126, 1985.

35. **Mendias CL**, **Gumucio JP**, **Bakhurin KI**, **Lynch EB**, **Brooks SV**. Physiological loading of tendons induces scleraxis expression in epitenon fibroblasts. *J Orthop Res* 30: 606–612, 2012.

36. **Mendias CL**, **Tatsumi R**, **Allen RE**. Role of cyclooxygenase-1 and -2 in satellite cell proliferation, differentiation, and fusion. *Muscle Nerve* 30: 497–500, 2004.

37. **Meryon E**. On Granular and Fatty Degeneration of the Voluntary Muscles. *Med Chir Trans* 35: 73–84.1, 1852.

38. **Michna H**, **Hartmann G**. Adaptation of tendon collagen to exercise. *International Orthopaedics (SICOT)* 13: 161–165, 1989.

39. **Monti RJ**, **Roy RR**, **Hodgson JA**, **Edgerton VR**. Transmission of forces within mammalian skeletal muscles. *J Biomech* 32: 371–380, 1999.

40. **Murchison ND**, **Price BA**, **Conner DA**, **Keene DR**, **Olson EN**, **Tabin CJ**, **Schweitzer R**. Regulation of tendon differentiation by scleraxis distinguishes force-transmitting tendons from muscle-anchoring tendons. *Development* 134: 2697–2708, 2007.

41. **Murphy MM**, **Lawson JA**, **Mathew SJ**, **Hutcheson DA**, **Kardon G**. Satellite cells, connective tissue fibroblasts and their interactions are crucial for muscle regeneration. *Development* 138: 3625–3637, 2011.

42. **Musaro A**, **McCullagh K**, **Paul A**, **Houghton L**, **Dobrowolny G**, **Molinaro M**, **Barton ER**, **Sweeney HL**, **Rosenthal N**. Localized Igf-1 transgene expression sustains hypertrophy and regeneration in senescent skeletal muscle. *Nat Genet* 27: 195–200, 2001.

43. **Nho SJ**, **Yadav H**, **Shindle MK**, **MacGillivray JD**. Rotator Cuff Degeneration: Etiology and Pathogenesis. *American Journal of Sports Medicine* 36: 987–993, 2008.

44. **Pallafacchina G**, **Calabria E**, **Serrano AL**, **Kalhovde JM**, **Schiaffino S**. A protein kinase B-dependent and rapamycin-sensitive pathway controls skeletal muscle growth but not fiber type specification. *Proc Natl Acad Sci USA* 99: 9213, 2002.

45. **Purslow PP**, **Trotter JA**. The morphology and mechanical properties of endomysium in series-fibred muscles: variations with muscle length. *J Muscle Res Cell Motil* 15: 299–308, 1994.

46. **Purslow PP**. Muscle fascia and force transmission. *J Bodyw Mov Ther* 14: 411–417, 2010.

47. **Rudnicki MA**, **Le Grand F**, **McKinnell I**, **Kuang S**. The Molecular Regulation of Muscle Stem Cell Function. *Cold Spring Harb Symp Quant Biol* 73: 323–331, 2008.

48. **Sandri M**. Signaling in muscle atrophy and hypertrophy. *Physiology (Bethesda)* 23: 160–170, 2008.

49. **Schweitzer R**, **Chyung JH**, **Murtaugh LC**, **Brent AE**, **Rosen V**, **Olson EN**, **Lassar A**, **Tabin CJ**. Analysis of the tendon cell fate using Scleraxis, a specific marker for tendons and ligaments. *Development* 128: 3855–3866, 2001.

50. **Seip RL**, **Semenkovich CF**. Skeletal muscle lipoprotein lipase: molecular regulation and physiological effects in relation to exercise. *Exerc Sport Sci Rev* 26: 191–218, 1998.

51. **Shukunami C**, **Takimoto A**, **Oro M**, **Hiraki Y**. Scleraxis positively regulates the expression of tenomodulin, a differentiation marker of tenocytes. *Dev Biol* 298: 234–247, 2006.

52. **Squire JM**. Architecture and function in the muscle sarcomere. *Current Opinion in Structural Biology* 7: 247–257, 1997.

53. **United States Bone and Joint Initiative:** *The Burden of Musculoskeletal*

Diseases in the United States (BMUS), Second Edition, 2011. Rosemont, IL

54. **Walsworth MK**, **Doukas WC**, **Murphy KP**, **Bimson W**, **Mielcarek BJ**, **Michener LA**. Descriptive analysis of patients undergoing shoulder surgery at a tertiary care military medical center. *Mil Med* 174: 642–644, 2009.

55. **Wang JH-C**. Mechanobiology of tendon. *J Biomech* 39: 1563–1582, 2006.

56. **Watt MJ**. Storing up trouble: does accumulation of intramyocellular triglyceride protect skeletal muscle from insulin resistance? *Clin Exp Pharmacol Physiol* 36: 5–11, 2009.

57. **Yaqoob P**. Fatty acids as gatekeepers of immune cell regulation. *Trends Immunol* 24: 639–645, 2003.

58. **Yu C**, **Chen Y**, **Cline GW**, **Zhang D**, **Zong H**, **Wang Y**, **Bergeron R**, **Kim JK**, **Cushman SW**, **Cooney GJ**, **Atcheson B**, **White MF**, **Kraegen EW**, **Shulman GI**. Mechanism by which fatty acids inhibit insulin activation of insulin receptor substrate-1 (IRS-1)-associated phosphatidylinositol 3-kinase activity in muscle. *Journal of Biological Chemistry* 277: 50230–50236, 2002.

59. **Zhang J**, **Wang JH-C**. Mechanobiological response of tendon stem cells: implications of tendon homeostasis and pathogenesis of tendinopathy. *J Orthop Res* 28: 639–643, 2010.

60. **Zoncu R**, **Efeyan A**, **Sabatini DM**. mTOR: from growth signal integration to cancer, diabetes and ageing. *Nat Rev Mol Cell Biol* 12: 21–35, 2010.

CHAPTER II

Synergist Ablation Induces Rapid Tendon Growth Through the Synthesis of a Neotendon Matrix

ABSTRACT

Mechanical loading can increase tendon cross-sectional area (CSA), but the mechanisms by which this occurs are largely unknown. To gain a greater understanding of the cellular mechanisms of adult tendon growth in response to mechanical loading, we used a synergist ablation model whereby a tenectomy of the Achilles tendon was performed to induce growth of the synergist plantaris tendon. We hypothesized that, following synergist ablation, progenitor cells in the epitenon would proliferate and increase the size of the existing tendon matrix. Adult male mice were subjected to a bilateral Achilles tenectomy, and plantaris tendons were isolated from mice at 0, 2, 7, 14, and 28 days after surgery. Tendons were sectioned stained with either fast green and hematoxylin, prepared for fluorescent microscopy, or prepared for gene expression of scleraxis and type I collagen. Following overload, there was a dramatic increase in total CSA of tendons, while the size of the original tendon matrix was not changed. Growth primarily occurred through the formation of a neotendon matrix between the original tendon and the epitenon, and contained cells that were proliferative and scleraxis positive. Additionally, an initial expansion of fibroblast cells occurred prior to the synthesis of new extracellular matrix. Fibroblasts in the original tendon did not re-enter the cell cycle. The results from this study provide new insight into the mechanisms

of tendon growth, indicate tendon consists mostly of post-mitotic cells, and that growth of tendon primarily occurs from the most superficial layers outward.

INTRODUCTION

Tendons are organized into functional cable like units of primarily type I collagen and a surrounding matrix of network collagens, elastin, and various proteoglycans (2). Collagen fibers are arranged into fascicles in hierarchical order, which make up the tendon proper. Surrounding this is a basement membrane called the epitenon, and loose peritendinous connective tissue, which contains the principal blood and nerve supply to the tendon. In sedentary mice, tendons continue to grow in size and length until approximately 10 weeks of age (15), and for humans the majority of tendon growth occurs in the first two decades of life (5). Mechanical loading can be a stimulus for tendon growth after adolescence, with vigorous exercise programs resulting in increases in cross-sectional area (CSA) of approximately 30% in both mice (13) and humans (19).

While the phenomenon of gross tendon growth in adult animals has been reported, the cellular mechanisms that are responsible for this growth remain largely unknown. There is, however, much more known about the initial formation and growth of tendons during embryonic development and early post-natal stages of life. Scleraxis is a basic helix-loop-helix transcription factor required for the formation of limb tendons in embryonic development, with genetic inactivation of scleraxis resulting in a severe disruption in tendon formation (16). Scleraxis is highly regulated by both mechanical loading, and also the TGF-β/BMP superfamily (10, 14). Mice with a genetic inactivation of TGF-β signaling (*Tgfbr2*$^{-/-}$) fail to form limb tendons and have severely disrupted

scleraxis expression (18), and administration of TGF-β to cultured tendon fibroblasts results in increases scleraxis expression (10, 14). In Achilles tendons, scleraxis is expressed in the majority of fibroblasts throughout the tendon up through 2 months of age, but past this point, scleraxis expression is confined to the epitenon region (13). While chronic mechanical loading can increase tendon mass, CSA and fibroblast density (13), it is not known whether the increase in CSA and fibroblast density occurs due to proliferation and expansion of existing tendon fibroblast cells throughout the tendon, or whether growth occurs in distinct regions within the tendon.

To gain a greater understanding into the mechanism by which adult tendon adapts to mechanical loading, and the role of scleraxis in adult tendon adaptation, we subjected adult mice to bilateral synergist ablation surgery. By removing the Achilles tendon, the synergist plantaris tendon receives a robust, supraphysiological increase in load and is solely responsible for all plantarflexion in the hindlimb (1, 11). We hypothesized that, following synergist ablation, progenitor cells in the epitenon would proliferate and increase the size of the existing tendon matrix. Additionally, we hypothesized that synergist ablation would increase scleraxis expression throughout the period of rapid cell expansion, and precede the synthesis of type I collagen.

METHODS

Animals. All experiments were approved by the University of Michigan Committee on the Use and Care of Animals, and all procedures followed the ethical guidelines of the US Public Health Service and American Physiological Society. Approximately six month old male mice that express green fluorescent protein (GFP) under the control of the scleraxis promoter (ScxGFP mice, N=6 per group), kindly

provided by Dr. Ronen Schweitzer (17), were used in this study. To induce a supraphysiological load on plantaris tendons, mice were anesthetized with isoflurane, and bilateral Achilles tenectomies were performed as previously described (1). A representative image of this surgical procedure is displayed in Figure 2.1. After tenectomy, mice were allowed to recover and ambulate freely about their cages, with no post-operative analgesia given. At 2, 7, 14 or 28 days after the surgery, plantaris tendons were harvested from both limbs. Age-matched mice that did not undergo surgery were used as controls. We chose these time points based on previous studies using the synergist ablation model (1). At 24 and 48 hours prior to harvest, mice received an intraperitoneal injection of 100μg of the thymidine analog 5-ethynyl-2'-deoxyuridine (EdU, Invitrogen) to mark proliferative cells. At the time of harvest, animals were anesthetized with sodium pentobarbital, and plantaris tendons were removed. The right tendon was then prepared for histology while RNA was isolated from the left tendon. Animals were then humanely euthanized with overdose of sodium pentobarbital.

Histology. Plantaris tendons were placed in TissueTek (Sakura) and snap frozen in isopentane cooled in liquid nitrogen, and stored at -80ºC until use. Tendons were sectioned at a thickness of 10 μm on a cryostat, and either stained with fast green and hematoxylin, or treated with DAPI (Sigma Aldrich) and a Click-iT kit with AlexaFluor 546 Azide (Invitrogen) to label EdU. Slides were imaged using a Axiovert 200M microscope (Zeiss) outfitted with the ApoTome system and an 8MP digital camera. Total CSA was measured by pixel area in imaged fast green and hematoxylin sections, and converted to square microns using a known scale. The original tendon CSA in treated samples

and subtracted from the total tendon area to obtain neotendon CSA. Fibroblast density for each region of the tendon was calculated by dividing the number of nuclei within a specific tendon area by the CSA. All histomorphometric analyses were performed in ImageJ (NIH).

Gene expression. Tendons were finely minced and homogenized in QIAzol (Qiagen), and RNA was extracted using a miRNeasy Mini kit (Qiagen). Total RNA was quantified using a NanoDrop (ThermoFisher), and RNA was reversed transcribed with an iScript cDNA synthesis kit (Bio-Rad). Quantitative PCR was performed using SsoFast EvaGreen reagents (Bio-Rad) in a CFX96 real time thermal cycler (Bio-Rad), and primers to detect scleraxis (*SCX*) and type 1α2 collagen (*COL1A2*), and normalized to the stable housekeeping gene, β2-microglobulin (*B2M*). Primer sequences and cycling parameters have been previously described (3). Differences in gene expression between time points were quantified using the $2^{-\Delta Ct}$ method (20).

Statistical Analyses. One-way ANOVAs (α=0.05), followed by Holm-Sidak post-hoc sorting, were used to assess differences between time points. Analysis was performed using Prism 6.0 (GraphPad). Values are presented as mean±SE.

RESULTS

Supraphysiological overload of the plantaris tendon resulted in the generation of an immature tendon matrix, or neotendon, between the epitenon and the original tendon matrix (Figure 2.2). The initial formation of the neotendon matrix could be seen as early as 2 days post overload, and this growth continued through 28 days (Figure 2.2) to fully surround the original tendon. Compared to controls, no significant differences in total tendon CSA were observed at 2 days, while there was a dramatic 2.5-fold increase in

tendon CSA at 7 days, which increased to 3-fold at 14 days and 3.5-fold at 28 days (Figure 2.3A). Throughout the overload period, the CSA of the original tendon matrix did not change compared to controls (Figure 2.3B). The increase in the CSA of the neotendon was responsible for the overall increase in the total tendon CSA. While no significant changes in neotendon CSA were observed at 2 and 7 days after overload, compared to the value at 2 days, the neotendon increased by 4-fold at 14 days and by nearly 5-fold at 28 days (Figure 2.3C). While widespread changes in CSA were observed throughout the overload period, the cell density in the tendon overall (Figure 2.3D), as well as in the original tendon (Figure 2.3E) and neotendon (Figure 2.3F) regions, remained largely unchanged, with a nearly 2-fold decrease in cell density in the neotendon at 7 days compared to 2 days.

We next sought to determine which cells in the tendons were actively undergoing mitosis by labeling proliferating cells with EdU. As shown in Figure 2.4A, the only EdU+ cells were observed in the neotendon region, and at no time did we detect EdU+ cells in the original tendon. Additionally, EdU was detected only in scleraxis-expressing fibroblasts in the neotendon, although not every scleraxis expressing fibroblast was EdU+. In the original tendon, while scleraxis was not detected in fibroblasts in unloaded tendons, mechanical overload caused fibroblasts to induce scleraxis expression.

Finally, we performed quantitative measures of scleraxis and type I collagen gene expression with qPCR. Compared to control tendons, scleraxis expression increased nearly 3-fold at 2 days, 5.5-fold at 7 days, 4-fold at 14 days, and 2.5-fold at 28 days (Figure 2.5A). For type I collagen expression, compared to control tendons, no

change was observed at 2 days, but expression increased 4-fold at 7 days, 7-fold at 14 days, and back down to 5-fold through 28 days (Figure 2.5B).

DISCUSSION

The results from this study provide novel insight into the cellular mechanisms of tendon growth. The synergist ablation procedure is a commonly used technique used to study skeletal muscle growth (1, 11), and we postulated this approach could also be used to study rapid tendon growth. While many previous studies have used chronic exercise training as a model to study tendon growth (4), the current study was the first, to our knowledge, that reported synergist ablation as a model to study the rapid growth of mechanically overloaded tendon tissue. Additionally, we report novel findings regarding the proliferation capacities of cells in different regions of the tendon. The combined findings from the current study suggest that synergist ablation is a useful model to study tendon growth, and that the fibroblasts within the core of the tendon do not re-enter the cell cycle to contribute to tendon growth.

Based on morphological appearance, Ippolito (7) postulated that the fibroblasts within tendon could be divided into two distinct categories – tenoblasts, which are proliferative fibroblasts that decline as organisms progress into adulthood, and tenocytes, which are terminally differentiated fibroblasts that are responsible for synthesizing and remodeling the tendon ECM. Although the terms tenoblast and tenocyte are often used in the adult tendon literature, there is little molecular evidence to support these cells as having the role ascribed to them by their suffix. However, during early and adolescent development, using the thymidine analog IdU, Tan and colleagues (21) demonstrated that tendon contains approximately 10% IdU+ cells at 4

weeks of age, and this number decreases to approximately 2% by 8 weeks of age. Additionally, there is a gradient to this distribution, with the outer most layers of the tendon showing more IdU+ cells than the midsubstance. The work of Tan and colleagues (21) is in agreement with Michna (15) who reported a cessation of growth in rodent tendons at around 10 weeks of age. In adult humans, Heinemeier and colleagues (5) used the global increase in atmospheric ^{14}C that came about due to above ground nuclear bomb testing to measure tissue growth rates in Achilles tendons, and found that the core of tendon tissue appears to form and stop growing by 17 years of age, with no appreciable changes in ^{14}C content observed after this time point. In this study, we demonstrate that in response to a mechanical growth stimulus, the existing fibroblasts within the midsubstance of tendons do not proliferate to contribute to tendon growth. Rather, there appears to be an expansion of fibroblasts in the outermost layers of tendon that likely arise from a progenitor cell population in or around the epitenon/peritenon region. Combined, the data from the current study, along with the work of Tan (21) and Heinemeier (5) suggest that the majority of fibroblasts within adult tendons are likely terminally differentiated, and support the use of the term tenocyte to describe this cell population.

In addition to identifying populations of proliferative cells within tendon, this study also provided insight into the mechanisms of tendon ECM synthesis in the context of whole tendon growth. In Achilles tendons, scleraxis is expressed in nearly every fibroblast at 2 months of age (13). By 3 to 4 months of age, scleraxis expression declines in most cells throughout the tendon, but persists in a population of cells in the epitenon (13). After supraphysiological overload, there was an increase in scleraxis

positive cells in the neotendon, some of which also were positive for EdU. Interestingly, although scleraxis was detected in the cells in the original tendon in response to overload, these cells did not appear to be proliferative. Further, cell density in the neotendon was higher at 2 days compared to 7 days, and scleraxis expression was increased at 2 days, which preceded the increase in type I collagen expression at 7 days. This early expansion of cells, coupled with increased scleraxis expression, also occurred before the increase in CSA at 7, 14, and 28 days. Previous studies in cultured tendon fibroblasts have shown that scleraxis expression is correlated with increased cell proliferation and a reduction in scleraxis is correlated with hypocellular tendons (12), and that scleraxis directly regulates the expression of type I collagen (9). These results suggest that tendon growth likely occurs initially through an expansion of fibroblasts and is subsequently followed by an increase in ECM production. Based on in vitro studies of tendon fibroblasts and findings of the current study, scleraxis likely plays an important role in both of these processes.

While we provided important insight into the changes in scleraxis expression following supraphysiological overload, there are several limitations to this study. First, while we show proliferating cells in the neotendon, we did not track cells over time using lineage tracing or dye. We also did not measure TGF-β superfamily signaling following plantaris overload. We focused on the plantaris tendon, due to the fact that this is a highly established and simple synergist ablation model, but other tendons may behave very differently. We visualized an abundance of scleraxis positive cells in the neotendon regions following overload, but did not stain for other cell types inside the neotendon. Finally, a specific marker that identifies undifferentiated tendon progenitor cells in vivo is

not yet known, and we did not identify one in this study. However, these progenitor cells are likely to be a type of mesenchymal stem cell, as injection of these cells into injured mouse Achilles tendon resulted in pockets of immature tendon matrix formation (6).

Tendons play an important role in transmitting and storing force in the musculoskeletal system, and are among the most frequently injured and difficult to treat soft tissue injuries (8). Despite the importance of tendons in animal locomotion, relatively little is known about the fundamental cellular and molecular pathways that regulate tendon growth. The results from this study indicate that there appear to be at least two populations of cells that exist within tendon, and these different populations have altered responses following tendon mechanical loading. Although inducing a substantial growth stimulus caused an overall increase in tendon CSA, the existing fibroblasts within the tendon remained in a terminally differentiated state, and the growth occurred entirely by the addition of new cells and matrix in the outer-most layers of the tendon. Along with the work of Tan (21) and Heinemeier (5), the results from the current study suggest that tendons in adult animals grow from the most superficial layers out, in a fashion similar to the growth patterns of tree trunks. Additionally, gaining further understanding of the fundamental biology of tendon cell specification, proliferation and migration will likely enhance our understanding of adult tendon mechanobiology, and potentially inform future treatments for tendon injuries and diseases.

ACKNOWLEDGEMENTS

The ScxGFP mice were a kind gift of Dr. Ronen Schewitzer. This work was supported by NIH/NIAMS grants R01-AR063649 and F31-AR065931.

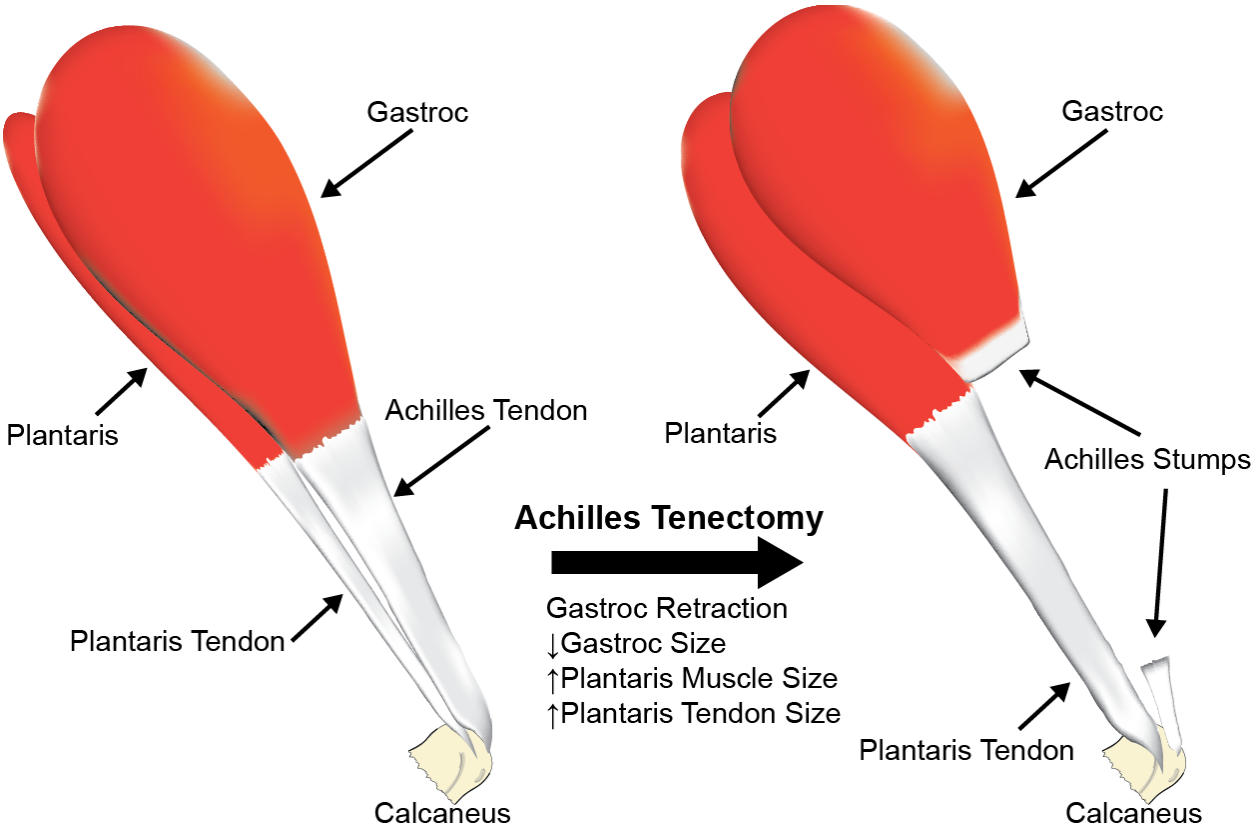

Figure 2.1. Representative image demonstrating the synergist ablation model. The Achilles tendon is removed, leaving the plantaris as the sole plantarflexor group. Over a short period of time, both the plantaris muscle and tendon increase in size.

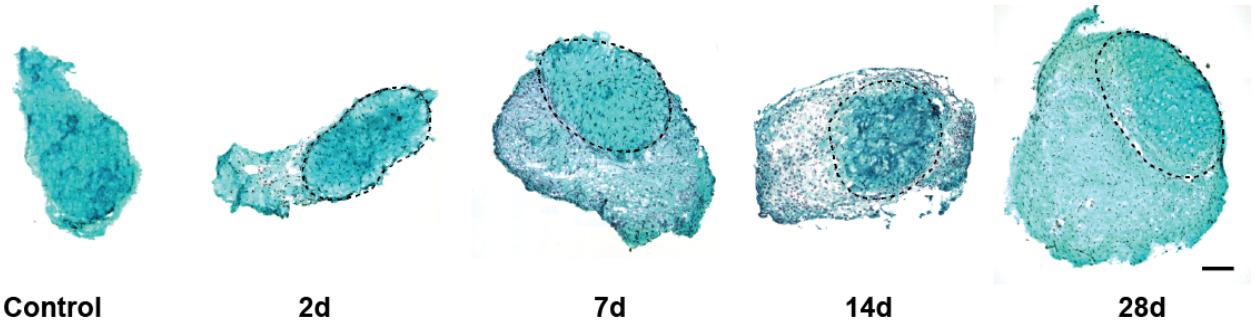

Figure 2.2. Representative cross-sections of plantaris tendons from control and synergist ablation groups. Sections stained with fast green and hematoxylin. The original tendon in all groups subjected to synergist ablation is circled in a dashed line, and the neotendon matrix is located superficial to this line. Scale bar for all panels = 100μm.

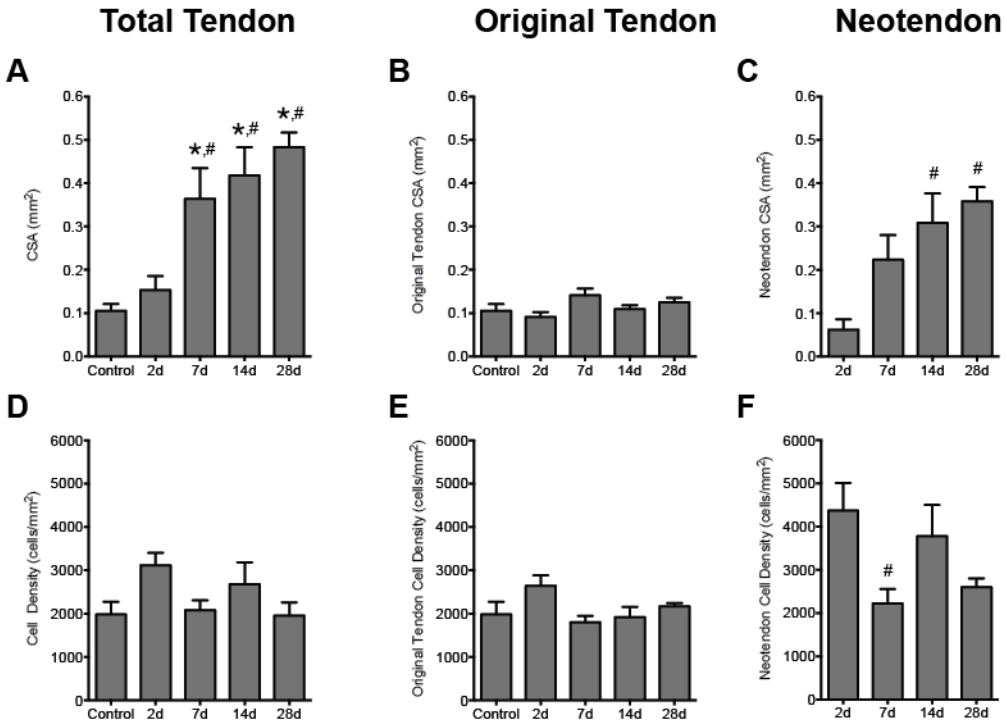

Figure 2.3. Quantitative histomorphometry of plantaris tendons from control and synergist ablation groups. CSA of the (A) total tendon, (B) original tendon, and (C) neotendon. Cell density of the (D) total tendon, (E) original tendon, and (F) neotendon. Values are mean±SEM. Differences were tested with a one-way ANOVA and Holm-Sidak post-hoc sorting ($P<0.05$). Differences: *, from control; #, from 2d.

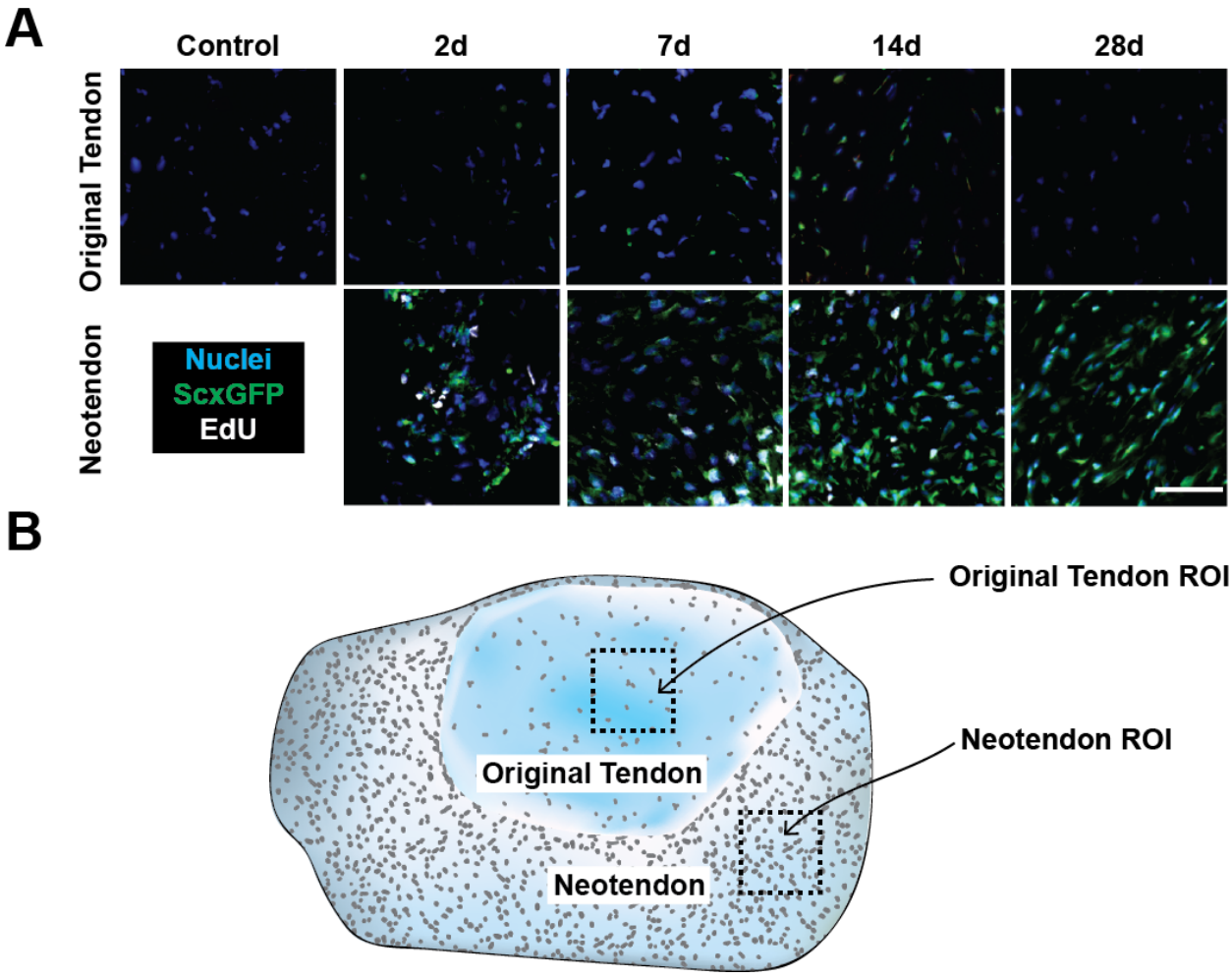

Figure 2.4. Representative immunohistochemistry of plantaris tendons from control and synergist ablation groups. (A) High magnification views of cells in the original tendon and neotendon. Blue, nuclei (DAPI); Green, scleraxis-GFP; White, EdU. Scale bar for all panels = 50μm. An illustration showing the regions of interest is shown in (B).

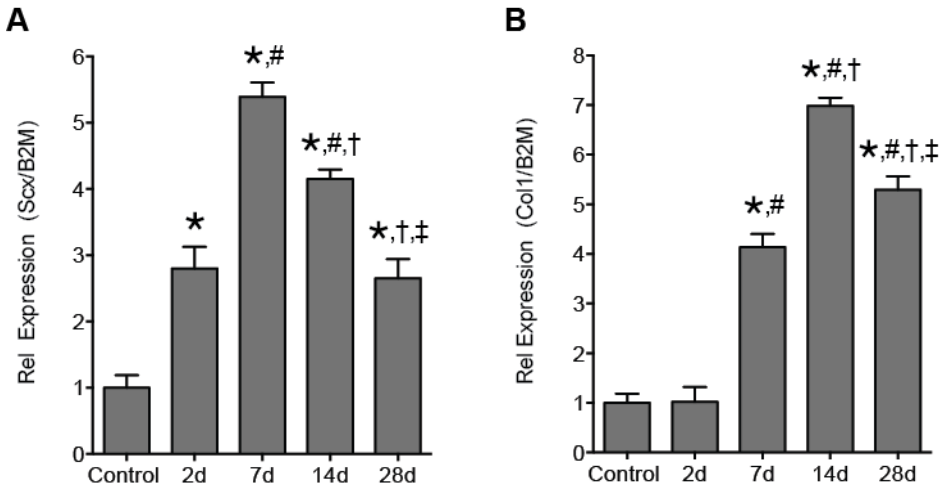

Figure 2.5. Gene expression of plantaris tendons from control and synergist ablation groups. (A) Scleraxis expression and (B) Collagen type Iα2 expression. Target gene expression was normalized to the stable housekeeping gene β2-microglobulin. Values are mean±SEM. Differences were tested with a one-way ANOVA and Holm-Sidak post-hoc sorting ($P<0.05$). Differences: *, from control; #, from 2d; †, from 7d; ‡ from 14d.

References

1. **Calve S**, **Isaac J**, **Gumucio JP**, **Mendias CL**. Hyaluronic acid, HAS1, and HAS2 are significantly upregulated during muscle hypertrophy. *AJP: Cell Physiology* 303: C577–88, 2012.

2. **Davis ME**, **Gumucio JP**, **Sugg KB**, **Bedi A**, **Mendias CL**. MMP inhibition as a potential method to augment the healing of skeletal muscle and tendon extracellular matrix. *Journal of Applied Physiology* 115: 884–891, 2013.

3. **Gumucio JP**, **Flood MD**, **Phan AC**, **Brooks SV**, **Mendias CL**. Targeted inhibition of TGF-β results in an initial improvement but long-term deficit in force production after contraction-induced skeletal muscle injury. *Journal of Applied Physiology* 115: 539–545, 2013.

4. **Heinemeier KM**, **Kjaer M**. In vivo investigation of tendon responses to mechanical loading. *J Musculoskelet Neuronal Interact* 11: 115–123, 2011.

5. **Heinemeier KM**, **Schjerling P**, **Heinemeier J**, **Magnusson SP**, **Kjaer M**. Lack of tissue renewal in human adult Achilles tendon is revealed by nuclear bomb (14)C. *The FASEB Journal* 27: 2074–2079, 2013.

6. **Hoffmann A**, **Pelled G**, **Turgeman G**, **Eberle P**, **Zilberman Y**, **Shinar H**, **Keinan-Adamsky K**, **Winkel A**, **Shahab S**, **Navon G**, **Gross G**, **Gazit D**. Neotendon formation induced by manipulation of the Smad8 signalling pathway in mesenchymal stem cells. *J Clin Invest* 116: 940–952, 2006.

7. **Ippolito E**, **Natali PG**, **Postacchini F**, **Accinni L**, **De Martino C**. Morphological, immunochemical, and biochemical study of rabbit achilles tendon at various ages. *J Bone Joint Surg Am* 62: 583–598, 1980.

8. **Kjaer M**, **Bayer ML**, **Eliasson P**, **Heinemeier KM**. What is the impact of inflammation on the critical interplay between mechanical signaling and biochemical changes in tendon matrix? *Journal of Applied Physiology* 115: 879–883, 2013.

9. **Léjard V**, **Brideau G**, **Blais F**, **Salingcarnboriboon R**, **Wagner G**, **Roehrl MHA**, **Noda M**, **Duprez D**, **Houillier P**, **Rossert J**. Scleraxis and NFATc Regulate the Expression of the Pro-α1(I) Collagen Gene in Tendon Fibroblasts. *Journal of Biological Chemistry* 282: 17665–17675, 2007.

10. **Maeda T**, **Sakabe T**, **Sunaga A**, **Sakai K**, **Rivera AL**, **Keene DR**, **Sasaki T**, **Stavnezer E**, **Iannotti J**, **Schweitzer R**, **Ilic D**, **Baskaran H**, **Sakai T**. Conversion of mechanical force into TGF-β-mediated biochemical signals. *Curr. Biol.* 21: 933–941, 2011.

11. **McCarthy JJ**, **Mula J**, **Miyazaki M**, **Erfani R**, **Garrison K**, **Farooqui AB**, **Srikuea R**, **Lawson BA**, **Grimes B**, **Keller C**, **Van Zant G**, **Campbell KS**, **Esser KA**,

Dupont-Versteegden EE, **Peterson CA**. Effective fiber hypertrophy in satellite cell-depleted skeletal muscle. *Development* 138: 3657–3666, 2011.

12. **Mendias CL**, **Bakhurin KI**, **Faulkner JA**. Tendons of myostatin-deficient mice are small, brittle, and hypocellular. *Proc. Natl. Acad. Sci. U.S.A.* 105: 388–393, 2008.

13. **Mendias CL**, **Gumucio JP**, **Bakhurin KI**, **Lynch EB**, **Brooks SV**. Physiological loading of tendons induces scleraxis expression in epitenon fibroblasts. *J. Orthop. Res.* 30: 606–612, 2012.

14. **Mendias CL**, **Gumucio JP**, **Lynch EB**. Mechanical loading and TGF-β change the expression of multiple miRNAs in tendon fibroblasts. *J Appl Physiol* 113: 56–62, 2012.

15. **Michna H**. Morphometric analysis of loading-induced changes in collagen-fibril populations in young tendons. *Cell Tissue Res* 236: 465–470, 1984.

16. **Murchison ND**, **Price BA**, **Conner DA**, **Keene DR**, **Olson EN**, **Tabin CJ**, **Schweitzer R**. Regulation of tendon differentiation by scleraxis distinguishes force-transmitting tendons from muscle-anchoring tendons. *Development* 134: 2697–2708, 2007.

17. **Pryce BA**, **Brent AE**, **Murchison ND**, **Tabin CJ**, **Schweitzer R**. Generation of transgenic tendon reporters, ScxGFP and ScxAP, using regulatory elements of the scleraxis gene. *Dev. Dyn.* 236: 1677–1682, 2007.

18. **Pryce BA**, **Watson SS**, **Murchison ND**, **Staverosky JA**, **Dünker N**, **Schweitzer R**. Recruitment and maintenance of tendon progenitors by TGFbeta signaling are essential for tendon formation. *Development* 136: 1351–1361, 2009.

19. **Rosager S**, **Aagaard P**, **Dyhre-Poulsen P**, **Neergaard K**, **Kjaer M**, **Magnusson SP**. Load-displacement properties of the human triceps surae aponeurosis and tendon in runners and non-runners. *Scand J Med Sci Sports* 12: 90–98, 2002.

20. **Schmittgen TD**, **Livak KJ**. Analyzing real-time PCR data by the comparative CT method. *Nature protocols* 3:1101–1108, 2008

21. **Tan Q**, **Lui PPY**, **Lee YW**. In vivo identity of tendon stem cells and the roles of stem cells in tendon healing. *Stem Cells and Development* 22: 3128–3140, 2013.

CHAPTER III

Scleraxis is Required for the Growth and Adaptation of Tendon Following Mechanical Loading

ABSTRACT

Tendon is organized into functional cable-like units of primarily type I collagen and transmits forces from muscle to bone. Mechanical loading can increase tendon cross-sectional area (CSA), but the mechanisms by which this occurs are largely undetermined. Scleraxis is a basic helix-loop-helix transcription factor that plays a central role in the embryonic development of tendons. Mice with a targeted inactivation of scleraxis fail to properly form limb tendons, but the role that scleraxis has in regulating the growth and adaptation of tendons from adult organisms is unknown. Our lab has previously used a supraphysiological plantaris overload model in mice, by which the Achilles tendon is removed and the plantaris is solely responsible for all plantarflexion. This causes rapid and robust growth of the plantaris tendon and is a useful model for the study of post-natal tendon growth. Using this model, our lab has previously demonstrated that adult tendon grows from the most superficial layers-outwards, similar to the rings of a tree. Early after plantaris overload, the tendon forms an immature matrix, or “neotendon,” surrounding the original tendon matrix. This expansion of tendon matrix corresponds to an increase in scleraxis expression, and most cells within the neotendon are proliferative, while cells in the original tendon matrix

do not re-enter the cell cycle. Additionally, the neotendon contains CD146+ pericytes, a class of cells that surround blood vessels and are able to become mesenchymal progenitor cells in a variety of tissues. To further determine the role of scleraxis in adult tendon adaptation to mechanical loading, we used a line of mice that allowed for a tamoxifen-inducible inactivation of scleraxis ($Scx^{\Delta/\Delta}$), and performed a plantaris overload procedure. After 7 or 14 days, mice were euthanized and tendons were isolated for histological and biochemical measures. Both $Scx^{+/+}$ mice, and $Scx^{\Delta/\Delta}$ mice form neotendon matrices, however, compared to $Scx^{+/+}$ mice, tendons from $Scx^{\Delta/\Delta}$ mice have a much smaller neotendon CSA, and reduced expression of many genes involved in matrix synthesis and remodeling, suggesting the accumulation of tendon matrix is blunted in $Scx^{\Delta/\Delta}$ mice. The neotendon of $Scx^{\Delta/\Delta}$ mice have increased density of CD146+ cells compared to controls, and $Scx^{\Delta/\Delta}$ tendons have decreased expression of the mature tendon marker, tenomodulin, suggesting a failure in differentiation of perivascular progenitor cells. While further study is necessary, these results suggest that scleraxis plays a pivotal role in the expansion of tendon matrix and differentiation of perivascular progenitor cells towards the tendon lineage following mechanical loading in adult tendons.

INTRODUCTION

Tendons are made up of an extracellular matrix (ECM) containing primarily type I collagen, and a surrounding matrix of other collagens, elastin, and various proteoglycans (4). The adult tendon is arranged in hierarchical order, with densely packed collagen fibers wrapped by layers of basement membrane, making up the tendon proper. Further wrapping the tendon proper is the outermost basement

membrane called the epitenon, which provides blood and nerve supply to the tendon. The organization of the ECM allows the tendon to properly transmit forces from muscle to bone and allow for locomotion, and respond to mechanical stimuli. Mechanical loading can increase tendon cross sectional area (CSA) up to 30% (17) and improve tendon mechanical properties (13), but the cellular and molecular mechanisms that allow this to occur are largely unknown. Work in recent years has identified many factors that may play a role in the embryonic development of tendon, which have been useful to identify those that may be important for the adaptation of tendon in adult animals (10).

Scleraxis (Scx) is a basic helix-loop-helix (bHLH) transcription factor that was first discovered in the early stages of tendon development, and robustly marked tendon cells in the embryo (24). Currently, scleraxis is the earliest detectible marker for differentiated tendon cells, (9) and activates downstream tendon differentiation genes such as Collagen 1α1 (*Col1a1*) and Tenomodulin (*Tmnd*) through its interaction with the bHLH transcription factor, E47 (3, 15, 26). Loss of scleraxis results in the loss or severe disruption of long tendons throughout the body (19), and leads to the absence of bone ridges that allow for the attachment of tendons to bone (29). Additionally, the expression of later stage tendon markers is dramatically reduced, including tenomodulin (Tnmd) which, to date, is perhaps the best late stage differentiation marker of tendon. Scleraxis is robustly expressed through birth and early postnatal period, but scleraxis expression is limited to the epitenon in adult animals (17). Mechanical loading increases scleraxis expression and promotes the proliferation of scleraxis+ cells in the epitenon, which

correlates to increased type I collagen expression and increased CSA of the tendon (7, 17).

Previously, our group utilized a new model of tendon growth, whereby the Achilles tendon is removed, causing the synergist plantaris tendon to undergo a robust increase in CSA (7, 20). This loading model causes expansion of the tendon matrix outward, through the development of a newly synthesized immature tendon matrix, or neotendon. The neotendon contained a large population of proliferative scleraxis+ cells, which corresponded to elevations in scleraxis transcript in the whole tendon. In a rat model of synergist ablation, the neotendon also contains a population of CD146+ cells (23). Pericytes, or perivascular stem cells, are a population of multipotent stem cells surrounding small vessels and are capable of differentiation into many types of mesenchymal cells, including fibroblasts. CD146+ pericytes have been observed within tendon, and these cells appear to participate in tendon ECM regeneration (14, 28), and the mechanisms by which pericytes may participate in tenogenic differentiation and subsequent matrix production is unknown.

Despite the load applied on the plantaris tendon in the synergist ablation model, cells within the original tendon matrix do not re-enter the cell cycle, suggesting the original tendon area does not turn over much, if at all. This is in agreement with human studies, where the core tendon matrix does not turn over past roughly 17 years of age (8). Consistent with this, in mice, scleraxis is robustly expressed in the original tendon matrix until early adulthood, but is undetectable following this time (17). Scleraxis therefore may be critically important for proper tendon tissue turnover and maintenance in the early stages of life, and the lack of scleraxis in the tendon proper contributes to

decreased tendon turnover during adulthood. Given that scleraxis is dramatically elevated following synergist ablation in adult animals (7), we sought to investigate whether scleraxis was required for the growth and adaptation of adult tendons during this process. We generated a line of mice that allow for the conditional inactivation of scleraxis ($Scx^{flox/flox}$:$Rosa26^{CreERT2}$, or $Scx^{\Delta/\Delta}$) to test the hypothesis that scleraxis was required for adult tendon growth following synergist ablation.

METHODS

Animals. This study was approved by the University of Michigan IACUC. Four to six-month-old mice (N=10 per group) were used in this study. A line of transgenic mice containing loxP sites flanking exon 1 of scleraxis ($Scx^{flox/flox}$) were kindly provided by Dr. Ronen Schweitzer and crossed to a line of mice that expressed CreERT2 under the control of the Rosa26 promoter ($R26^{CreERT2/CreERT2}$, The Jackson Laboratory, Farmington, CT), generating mice that allowed for the conditional inactivation of scleraxis by tamoxifen ($Scx^{\Delta/\Delta}$, Figure 3.1A). Mice were given tamoxifen (2mg/day, Sigma-Aldrich, St. Louis, MO) via intraperitoneal injection 5 days prior to synergist ablation, and daily until sacrifice. Synergist ablation surgery was performed as described previously (7). Briefly, an approximately 3-4mm piece of the Achilles tendon was removed from each hindlimb to overload the synergist plantaris tendon. After recovery, mice were given post-operative buprenorphine (0.05mg/kg) and returned to their cages. Mice were allowed to ambulate freely for 7 or 14 days following synergist ablation. We chose these time points because scleraxis expression was highest at this time in a previous study (7). Plantaris tendons were removed and prepared for either DNA isolation, histology, electron microscopy, or RNA isolation. A separate cohort of

animals was used for in vitro studies. Age-matched wild type mice were used as controls ($Scx^{+/+}$), and received the same doses of tamoxifen to control for the effect of the treatment on normal tendon function.

DNA isolation. Portions of proximal plantaris tendons were isolated and prepared for DNA isolation using the DNeasy Blood & Tissue Kit (Qiagen, Valencia, CA). DNA was amplified via qPCR with custom primers for Scx exon 1 (*Fwd:*5'GACCGCAAGCTCTCCAAGAT3'; *Rev:*5'ACGACCGCTGTGGAAGAAAG3') and exon 2 (*Fwd:*5'CGCAGGTCCCCAAGAGCACG3'; *Rev:*5'GGCCTGGGTCAGTGTTCGGC3'). Knockdown efficiency was calculated by measuring the change in exon 1 genomic DNA relative to exon 2 gDNA using the $2^{-\Delta Cq}$ method (22). $Scx^{\Delta/\Delta}$ tendons exhibited approximately a 96% reduction in exon 1 gDNA compared to controls (Figure 3.1B).

Histology. Distal plantaris tendons were snap frozen in liquid nitrogen cooled isopentane and stored at -80ºC until use. Tendons were sectioned and stained with fast green and hematoxylin as described previously (7). Fast Green and hematoxylin sections were imaged on a Olympus BX microscope (Olympus, Center Valley, PA). For immunohistochemistry, tendons were sectioned and permeabilized in Triton-X-100 (0.02%) and blocked with 5% goat serum. Sections were incubated overnight in primary antibody against CD146 (AbCam, San Francisco, CA) and then incubated in secondary antibody conjugated to Alexa Fluor 555. Samples were also stained with DAPI and wheat germ agglutinin conjugated to Alexa Fluor 488. Images were taken on a Nikon A-1 confocal microscope equipped with a high-resolution camera (Nikon, Tokyo, Japan). Images were imported into ImageJ for histomorphametric measures. Cell density was

calculated by the number of nuclei per unit area of the tendon. The percentage of CD146+ cells was measured by the total number of CD146+/DAPI+ cells in the neotendon normalized by the number of CD146-/DAPI+ cells.

Transmission Electron Microscopy. Proximal tendon portions were fixed in 1% tannic acid, 1% glutaraldehyde in Sorenson's buffer, followed by post-fixation in 2% osmium tetroxide (Electron Microscopy Sciences, Hatfield, PA). Samples were then dehydrated using a graded ethanol series and embedded in EMBed 812 resin using a graded resin and propylene oxide series. One micron transverse sections were cut with a diamond knife ultramicrotome, and imaged using a JEOL 1400-plus transmission electron microscope with a high-resolution AMT digital camera (JEOL USA, Peabody, MA).

Tendon RNA Isolation. Plantaris tendons were isolated, snap frozen, and stored at -80ºC until use. On the day of RNA isolation, tendons were homogenized immediately in QIAzol and isolated using a micro RNeasy kit (Qiagen). RNA concentration was determined using a NanoDrop 2000 (Thermo Fisher Scientific, Waltham, MA).

RNA Sequencing (RNASeq). Approximately 200-400ng total RNA per sample was delivered to the University of Michigan Sequencing Core for RNA sequencing. Sample concentrations were normalized and cDNA pools were created for each sample, and then subsequently tagged with a barcoded oligo adapter to allow for sample specific resolution. Sequencing was carried out using an Illumina-HiSeq platform (Illumina, San Diego, CA) and 50bp single end reads. Raw RNASeq data was uploaded into BaseSpace (Illumina) for adapter trimming, quality control, and alignment. Reads were mapped to the mm10 genome assembly (UCSC, Santa Cruz, CA) using

the STAR aligner (Illumina) and differential expression analysis was performed using the DESeq2 application (Illumina).

Tendon fibroblast culture. Tail tendons were isolated from $Scx^{flox/flox}$:$R26^{CreERT2}$ mice and cultured as described previously (16). Tendon fascicles were carefully isolated from tail tendons, minced, and placed in DMEM with 0.2% type II collagenase (Invitrogen, Carlsbad, CA) for 1h at 37°C with agitation. After dissociation, samples were centrifuged and resuspended in media containing 10% FBS and 1% antibiotic-antimycotic (ABAM, Invitrogen) and plated on 100-mm type I collagen coated dishes (BD Biosciences, San Jose, CA). Fibroblasts were passaged upon reaching 70% confluence onto 6-well dishes coated with type I collagen (BD Biosciences), and media was switched to DMEM containing 2% horse serum and 1% ABAM. Cells were split into two groups, a group that received 10μM 4-hydroxytamoxifen (4HT, Sigma), and a group that received an equivalent volume of DPBS (Thermo Fisher). Upon reaching 70% confluence, each group (-4HT or +4HT) was either supplemented with 2 ng/ml of recombinant human Transforming Growth Factor beta 1 (TGF-β1 or TGFβ, R&D Systems), or in equivalent volumes of DPBS (Thermo Fisher) for 2 h. Following treatment, cells were scraped from their dishes and prepared for total RNA isolation using the RNeasy micro kit (Qiagen). A separate cohort of cells were isolated, grown to 70% confluence, and treated with or without 4HT for Scx gDNA content. Cells treated with 4HT had dramatically decreased Scx exon 1 gDNA content compared to cells not treated with 4HT (Figure 3.1C).

Statistics. Differences between groups were measured using Two-way ANOVAs (α=0.05), followed by Fishers LSD post hoc sorting, except for knockdown efficiency

calculations, which were tested using t-tests (α=0.05). Analyses were performed using Prism 6.0 (GraphPad Software, La Jolla, CA). Values are presented as mean+SD.

RESULTS

Following synergist ablation, there was a dramatic increase in the size of the plantaris tendon in $Scx^{+/+}$ animals, through the induction of a neotendon matrix (Figure 3.2A,B). The original tendon area did not change between groups (Figure 3.2B), but total tendon CSA was decreased in mutant animals, due to a dramatically blunted neotendon compared to controls (Figure 3.2A,B). There were modest differences in total tendon cell density between genotypes at 7D, with a slightly reduced cell density in the $Scx^{\Delta/\Delta}$ animals compared to controls (Figure 3.2C). There was a slight increase in cell density of the neotendon at 14D in $Scx^{\Delta/\Delta}$ animals compared to controls (Figure 3.2C).

Electron micrographs were used to examine the structural differences in tendon between genotypes. There were no appreciable differences in fibril CSA or distribution between genotyped for fibrils within the original tendon matrix (Figure 3.3A). In $Scx^{+/+}$ animals, there was evidence of collagen fibril formation within neotendon tissue, and the fibrils were arranged along the axis of force transmission (Figure 3.3B). Conversely, neotendons from $Scx^{\Delta/\Delta}$ mice exhibited disrupted collagen alignment, where many fibrils were assembled perpendicular to the axis of force transmission (Figure 3.3B). There were still pockets of aligned collagen fibrils in $Scx^{\Delta/\Delta}$ mice, but not to the level of controls (Figure 3.3B).

We measured the expression of several transcripts related to ECM production, ECM turnover, and cellular differentiation with RNASeq. The expression of type I (*Col1a1*, *Col1a2*) and type XII collagen (*Col12a1*) was decreased between genotypes at

each time point, but there were no changes in the expression of type III collagen (*Col3a1*) with time or between groups (Figure 3.4A). There was a dramatic decrease of matrix metalloproteinase (MMP) -9 (*Mmp9*), and a decrease of MMP14 (*Mmp14*) at 7D in $Scx^{\Delta/\Delta}$ mice compared to controls, despite a decrease in tissue inhibitor of metalloproteinases-1 (TIMP1, *Timp1*) in mutant animals at 7D and decreases in TIMP2 (*Timp2*) expression at 14D in $Scx^{\Delta/\Delta}$ mice compared to controls (Figure 3.4B). There were decreases in MMP9 and MMP14 across genotypes at 14D compared to 7D (Figure 3.4B). The expression of other ECM proteins were altered with the loss of scleraxis, including hyaluronic acid synthase 2 (*Has2*), which was decreased in $Scx^{\Delta/\Delta}$ mice compared to controls at 7D, and fibromodulin (*Fmod*), which was decreased in $Scx^{\Delta/\Delta}$ mice across both time points compared to $Scx^{+/+}$ mice (Figure 3.4C). Additionally, the expression of thrombospondin-1 (*Thbs1*) was decreased in mutant animals compared to controls at each time point, and fibronectin (*Fn1*) was decreased in $Scx^{\Delta/\Delta}$ mice compared to controls at 14D (Figure 3.4C). As expected, there was a dramatic decrease in *Scx* transcript in mutant mice compared to controls, and the expression of *Scx* decreased at 14D compared to 7D in control animals (Figure 3.4D). *Tnmd* was decreased in mutant animals compared to controls in both time points, and there was no change in *Sox9* expression between genotypes at either time point (Figure 3.4D). The expression of apolipoprotein-E (*Apoe*) was increased in $Scx^{\Delta/\Delta}$ mice compared to $Scx^{+/+}$ mice at 7D (Figure 3.4D).

The role of scleraxis on tendon fibroblast activity was also tested in vitro. Loss of scleraxis did not affect the proliferative capacity of tendon fibroblasts (Figure 3.5A). TGFβ is a known activator of scleraxis (18), and treatment of tendon fibroblasts resulted

in the increase in many genes related to tendon cell differentiation and matrix production, including *Scx*, *Tnmd*, *Col1a2*, and *Eln* (Figure 3.5B). Loss of scleraxis resulted in decreased expression of all transcripts with addition of TGFβ (Figure 3.5B).

Using immunohistochemistry, we measured the abundance of CD146+ cells within the neotendon of overloaded plantaris tendons. There was an abundance of CD146+ cells in the neotendon in both genotypes (Figure 3.6A). Compared to $Scx^{+/+}$ mice, there was a dramatic increase in the percentage of CD146+ cells in the neotendons of $Scx^{\Delta/\Delta}$ mice across each time point (Figure 3.6B). No differences between time points were observed for either genotype.

DISCUSSION

Unlike other neighboring mesenchymal tissues, the mechanisms behind post-natal tendon growth is poorly understood. Previously, using the synergist ablation model, we identified the formation of a neotendon matrix that develops around the original tendon matrix, and this new matrix was populated with proliferative, scleraxis expressing cells (7). The aim of this study was to identify whether scleraxis was required for the adaptation of tendon to mechanical loading. The results indicate that not only is scleraxis required for the proper expansion, formation, and remodeling of tendon ECM during mechanical loading, but scleraxis may also possess a previously unknown role in the fate determination of a population of perivascular tendon stem cells. While further study is needed to fully elucidate the role of scleraxis in differentiating stem cells, this study provided substantial insight into the role of scleraxis in tendon growth and remodeling.

It has long been suggested that tendon possessed a compartment of stem-like cells that could participate in tendon regeneration (5, 12), but the location of these cells was unknown. Recent work describes a compartment of perivascular stem cells expressing CD146 located in tendon, which may be involved in the regeneration of tendon following injury or mechanical loading (14, 23, 28). In a rat model of patellar tendon injury and repair, these cells participate in tenogenic differentiation when stimulated with connective tissue growth factor (CTGF) (14). In the patellar tendon, approximately 0.8% of cells are CD146+, which is consistent with the relatively low amount of vasculature within resting tendon (14). Previous studies in our laboratory using the synergist ablation model in rats showed that these cells appear to migrate from their niche in the vasculature and proliferate within the neotendon (23). In the current study, in wild type animals, the percentage of CD146+ cells can reach almost 30% in the newly developing neotendon region, and reaches almost double this value with the loss of scleraxis. The gain in CD146+ cells in the absence of scleraxis raises a very intriguing new role for scleraxis biology, as a lack of differentiated cells in the neotendons of $Scx^{\Delta/\Delta}$ mice can indicate an inability of these cells to fully differentiate into mature tendon cells. Consistent with this was a dramatic decrease in tenomodulin transcript. Tenomodulin is to date the best marker of a differentiated tendon cell (6, 10), and is regulated, at least in part, by scleraxis (27). Like scleraxis, TGFβ may also regulate tenomodulin, as both tenomodulin and scleraxis transcripts are completely lost in $Tgfbr2^{-/-}$ and $Tgfbr3^{-/-}$ mice (21). $Scx^{\Delta/\Delta}$ cells in the current study had blunted tenomodulin expression when stimulated with TGFβ in culture, indicating that scleraxis also plays a role in the TGFβ-induced expression of tenomodulin. Animals deficient in

tenomodulin have disrupted tendon fibril maturation (6), which is apparent in the disordered fibrils within the neotendon of mutant mice in the current study. There were no changes between groups in Sox9 expression, a chondrogenic marker, suggesting no increase in chondrogenesis with the loss of scleraxis. However, there was a substantial increase in the expression of ApoE in mutant mice at 7D, which could increase cholesterol deposition in the tendon, making tendon more susceptible to injuries and tendinopathy (2, 25). The results from this study have led to a new model of tendon adaptation and regeneration that involves the activation and differentiation of resident CD146+ stem cells, which can migrate from their niche to participate in tendon remodeling through the activation of scleraxis (Figure 3.7A). Removal of scleraxis renders a buildup of stem cells that have diminished tenogenic differentiation capacity (Figure 3.7B).

Scleraxis has a very well defined role in the development of tendon in the embryo, and $Scx^{-/-}$ mice have a severely disrupted tendon phenotype (19). Scleraxis has been shown to activate the expression of type I collagen (15), tenomodulin (6, 27, 30), and fibronectin (1). Mechanical loading increases the expression of scleraxis, type I collagen, and tenomodulin in tendon (7, 18), and transcriptomic analysis identified a decrease in collagen1α1, collagen1α2, tenomodulin, and fibronectin, among others in $Scx^{\Delta/\Delta}$ mice following synergist ablation. Additionally, TGFβ is a potent activator of scleraxis, type I collagen, and tenomodulin *in vitro* (18), and the loss of scleraxis decreases the effect of TGFβ on all of these transcripts in the current study. These results clearly show that the effects of both mechanical loading as well as TGFβ on the expression of downstream tendon fibroblast markers are regulated by scleraxis.

Within the developmental literature, it is thought that scleraxis may not be the master regulator of the tendon cell fate (10), and this seems to be conserved in adulthood. Despite decreases in many downstream tendon markers in $Scx^{\Delta/\Delta}$ mice, their expression was not completely ablated, and the expression of other ECM components were unchanged, such as type III collagen. Additionally, while blunted, $Scx^{\Delta/\Delta}$ mice still developed a small neotendon with some tendon fibrils in alignment among the many in disarray. There are several possible mechanisms to account for this, including a compensatory mechanism that accounts for the loss in scleraxis, or likely an upstream tenogenic differentiation factor which, prior to the induction of scleraxis, activates an initial expansion of matrix following mechanical loading.

Despite providing substantial new insight into the role of scleraxis in adult tendon adaptation, this study is not without limitation. We only used two time points following overload to study scleraxis function. We chose these time points as they were the highest in scleraxis expression in a previous study using the same tendon growth model (7). It would be useful to assess the effects of a loss in scleraxis before and after these time points. While we showed that CD146+ stem cells are likely activated by scleraxis for tenogenic differentiation, we did not test this with lineage tracing. We also did not measure the direct activation of the TGFβ signaling pathway following synergist ablation in mutant animals. Lastly, while this model is an extremely useful one to study mechanical load-induced tendon growth, the model only assesses changes in the plantaris tendon, where other tendons in the body may behave differently.

Tendons connect muscle to bone, and are often overlooked in the literature due to their relative hypocellularity and difficulty as a tissue to work with. However, tendon

injuries and painful tendinopathies are a significant healthcare problem, and treatment options are limited to many conservative therapies, or painful surgeries. Tendinosis is a painful, chronic condition which is thought to occur due to the failure of fibroblasts to maintain and synthesize ECM (11). Understanding the basic mechanisms of tendon adaptation to injury or mechanical loading will undoubtedly inform future treatments towards tendinopathy. The lack of scleraxis in mice results in an inability to produce a proper increase in ECM to respond to increased loads. If the function of scleraxis also translates to humans, it is conceivable that a lack of scleraxis in patients would result in the inability of fibroblasts to sense loads and maintain matrix homeostasis, leading to painful tendinopathy. In addition to the expansion of knowledge in fundamental scleraxis biology, the results from this study offer a new and unique perspective to the function of scleraxis in tendon progenitor cells, which also requires further study in human tendon tissue. While more study is needed, these results indicate that scleraxis may be an attractive therapeutic target for individuals with painful tendinopathies to rescue ECM production in tendinopathic tendons and improve quality of life.

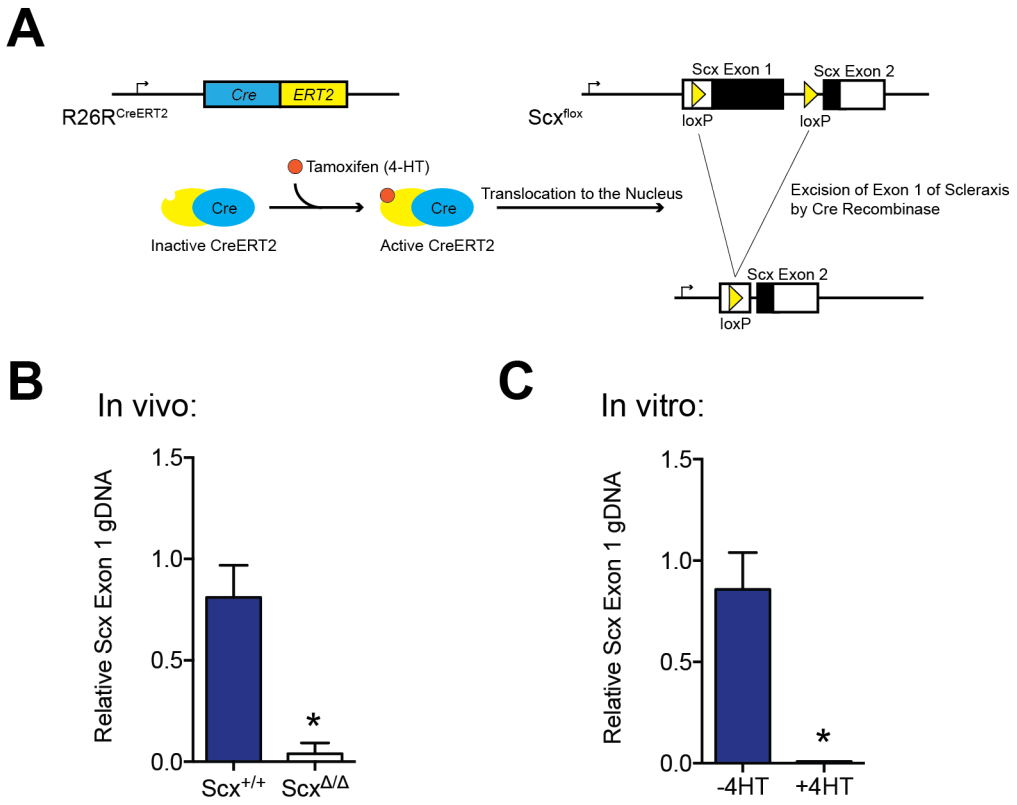

Figure 3.1. Overview of model to generate $Scx^{\Delta/\Delta}$ mice. (A) $Scx^{\Delta/\Delta}$ mouse model used that allowed for the conditional inactivation of scleraxis in this study. (B) Relative abundance of scleraxis exon 1 genomic DNA in wild type or $Scx^{\Delta/\Delta}$ mice. Data are presented mean+SD. *, Different from $Scx^{+/+}$ ($P < 0.05$) (C) Relative abundance of scleraxis exon 1 genomic DNA in tendon fibroblasts from R26RCreERT2:Scxflox/flox mice treated with or without 4-hydroxy-tamoxifen (4HT). Data are presented mean+SD. *, Different from -4HT ($P < 0.05$).

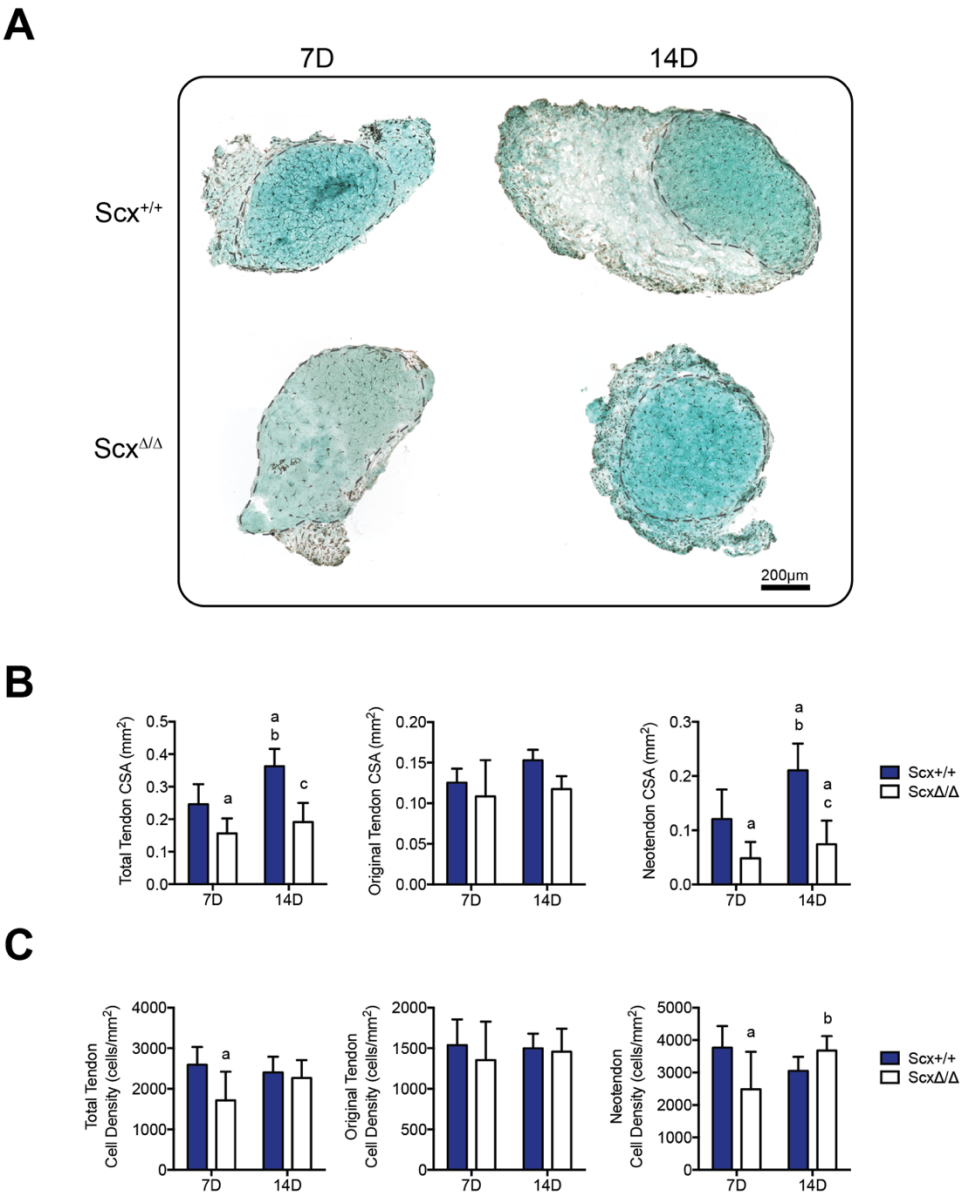

Figure 3.2. Histology and histomorphometric measures of $Scx^{+/+}$ and $Scx^{\Delta/\Delta}$ mice after plantaris overload. (A) Representative fast green stained plantaris tendons from $Scx^{+/+}$ and $Scx^{\Delta/\Delta}$ mice following 7 or 14 days plantaris overload. Black outline indicates original tendon area (B) Quantification of cross sectional area (CSA) in the whole tendon, original tendon, or neotendon of $Scx^{+/+}$ and $Scx^{\Delta/\Delta}$ mice following 7 or 14 days plantaris overload. (C) Quantification of cell density in the whole tendon, original tendon, or neotendon of $Scx^{+/+}$ and $Scx^{\Delta/\Delta}$ mice following 7 or 14 days plantaris overload. Data are presented mean+SD. a, Different from 7D $Scx^{+/+}$; b, Different from 7D $Scx^{\Delta/\Delta}$; c, Different from 14D $Scx^{+/+}$ ($P < 0.05$).

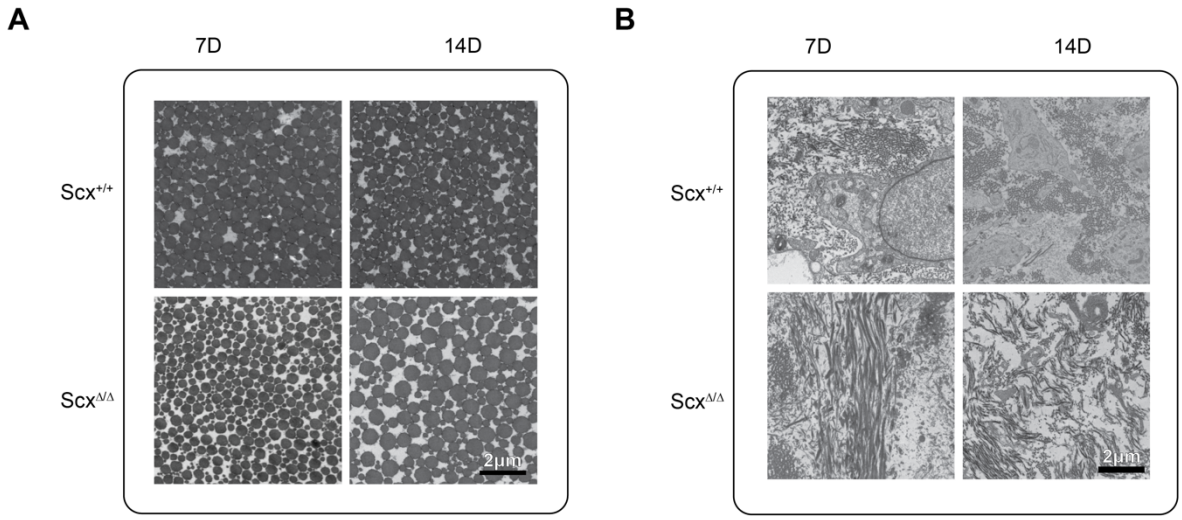

Figure 3.3. Electron micrographs of $Scx^{+/+}$ and $Scx^{\Delta/\Delta}$ mice after plantaris overload. (A) Representative electron microscopy (EM) images of tendon fibrils within the original tendon of $Scx^{+/+}$ and $Scx^{\Delta/\Delta}$ mice following 7 or 14 days plantaris overload. (B) Representative electron microscopy (EM) images of collagen fibrils in the neotendon of $Scx^{+/+}$ and $Scx^{\Delta/\Delta}$ mice following 7 or 14 days plantaris overload.

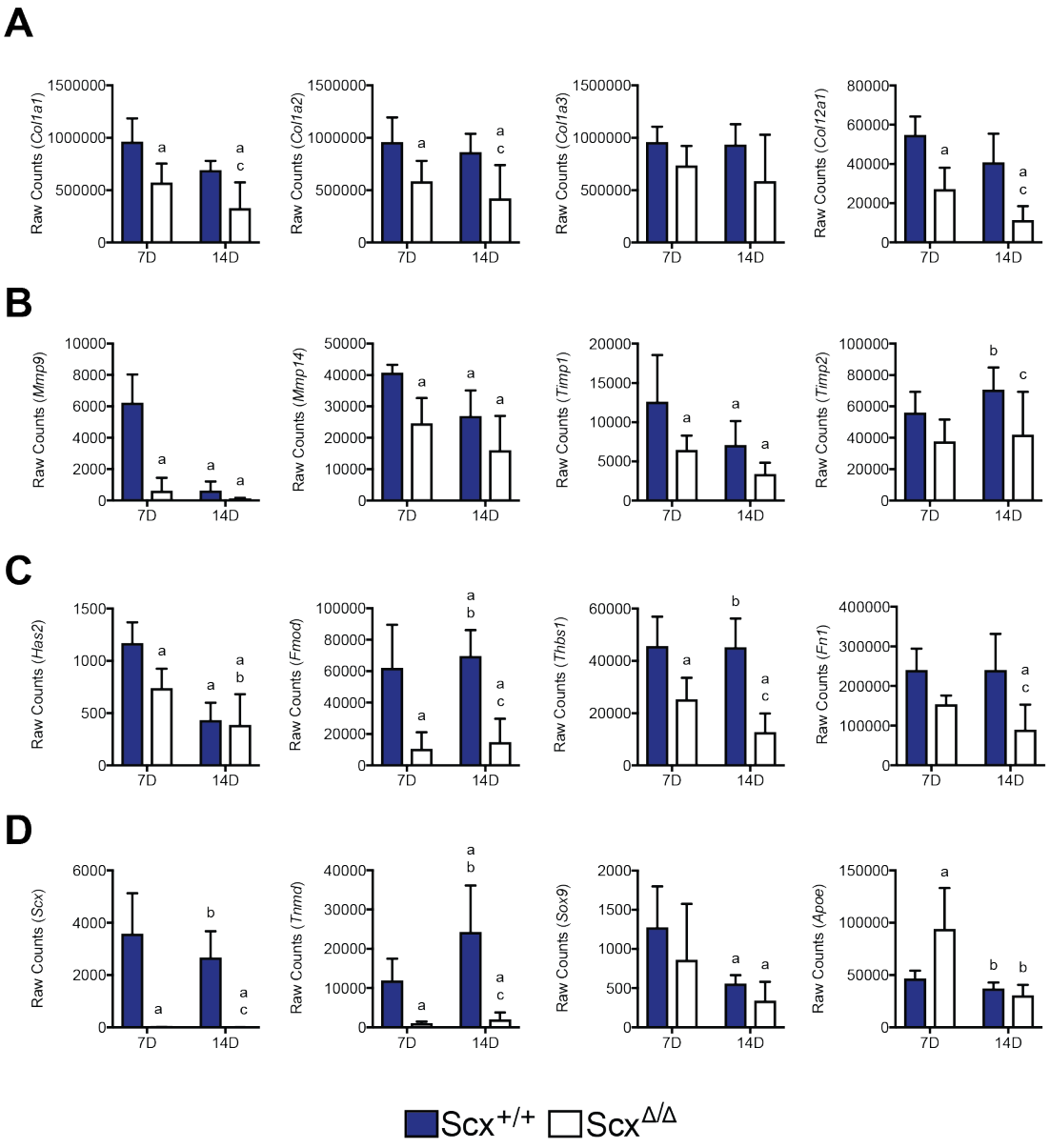

Figure 3.4. Expression of transcripts measured by RNA Sequencing in $Scx^{+/+}$ and $Scx^{\Delta/\Delta}$ mice after plantaris overload. Transcripts related to (A) collagen synthesis, (B) matrix metalloproteinase and tissue inhibitor of metalloproteinase, (C) other ECM components such as SLRP, glycoprotein, and glycosaminoglycan synthesis, and (D) cellular differentiation. Data are presented mean+SD. a, Different from 7D $Scx^{+/+}$; b, Different from 7D $Scx^{\Delta/\Delta}$; c, Different from 14D $Scx^{+/+}$ ($P < 0.05$).

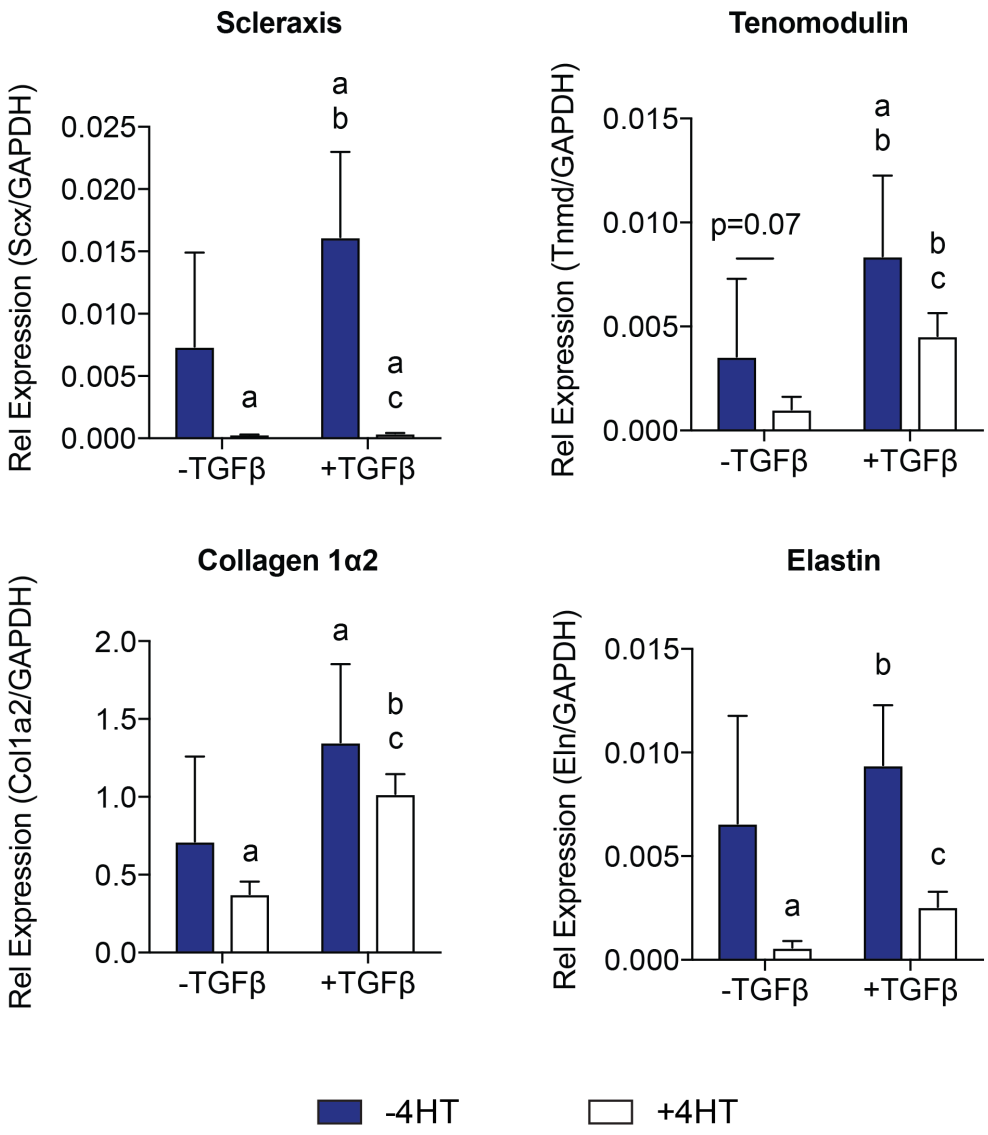

Figure 3.5. Expression of genes related to tendon fibroblast differentiation and ECM synthesis in isolated tendon fibroblasts from R26RCreERT2:Scxflox/flox mice treated with or without 4-hydroxy-tamoxifen (4HT) and in response to TGFβ treatment. Data are presented mean+SD. a, Different from -4HT/-TGFβ; b, Different from +4HT/-TGFβ; c, Different from -4HT/+TGFβ ($P < 0.05$).

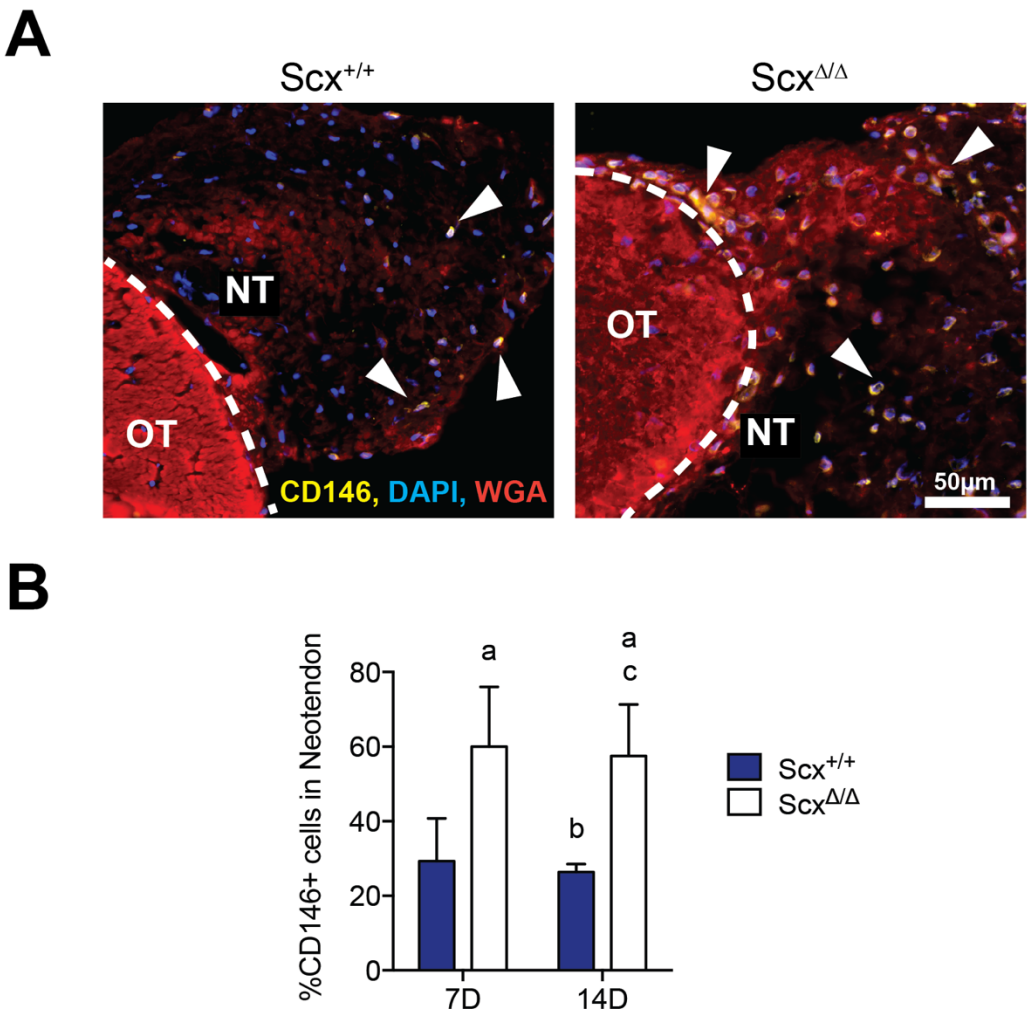

Figure 3.6. Quantification of CD146+ cells in the neotendon of $Scx^{+/+}$ and $Scx^{\Delta/\Delta}$ mice following plantaris overload. (A) Representative immunohistochemistry image from $Scx^{+/+}$ and $Scx^{\Delta/\Delta}$ mice showing the location of CD146+ cells in the neotendon. OT, original tendon; NT, neotendon. Nuclei (blue), ECM (red), CD146+ cells (yellow). White outline indicates border of original tendon and neotendon. White arrows indicate CD146+ cell in the neotendon. (B) Quantification of CD146+ cells in the neotendon. Data are presented mean+SD. a, Different from 7D $Scx^{+/+}$; b, Different from 7D $Scx^{\Delta/\Delta}$; c, Different from 14D $Scx^{+/+}$ ($P < 0.05$).

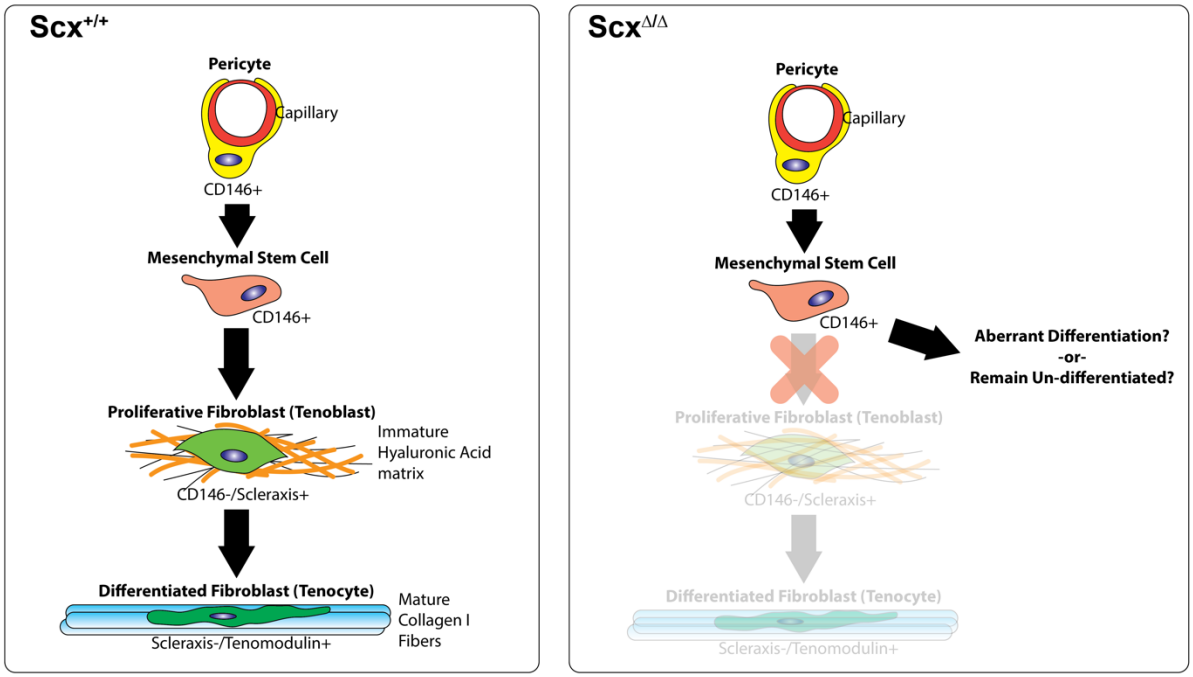

Figure 3.7. Proposed model of scleraxis function in CD146+ perivascular stem cells. In wild-type mice (left), scleraxis helps direct the differentiation of CD146+ cells into a tenogenic lineage. When scleraxis is lost (right), CD146+ cells buildup in an un-differentiated state which may undergo aberrant differentiation or remain un-differentiated, rendering the cell unable to participate in normal ECM maintenance and synthesis.

REFERENCES

1. **Bagchi RA**, **Lin J**, **Wang R**, **Czubryt MP**. Regulation of fibronectin gene expression in cardiac fibroblasts by scleraxis. *Cell Tissue Res* 366: 381–391, 2016.

2. **Beason DP**, **Abboud JA**, **Kuntz AF**, **Bassora R**, **Soslowsky LJ**. Cumulative effects of hypercholesterolemia on tendon biomechanics in a mouse model. *J Orthop Res* 29: 380–383, 2011.

3. **Carlberg AL**, **Tuan RS**, **Hall DJ**. Regulation of scleraxis function by interaction with the bHLH protein E47. *Mol Cell Biol Res Commun* 3: 82–86, 2000.

4. **Davis ME**, **Gumucio JP**, **Sugg KB**, **Bedi A**, **Mendias CL**. MMP inhibition as a potential method to augment the healing of skeletal muscle and tendon extracellular matrix. 115: 884–891, 2013.

5. **de Mos M**, **Koevoet WJLM**, **Jahr H**, **Verstegen MMA**, **Heijboer MP**, **Kops N**, **van Leeuwen JPTM**, **Weinans H**, **Verhaar JAN**, **van Osch GJVM**. Intrinsic differentiation potential of adolescent human tendon tissue: an in-vitro cell differentiation study. *BMC Musculoskelet Disord* 8: 16, 2007.

6. **Docheva D**, **Hunziker EB**, **Fässler R**, **Brandau O**. Tenomodulin is necessary for tenocyte proliferation and tendon maturation. *Mol Cell Biol* 25: 699–705, 2005.

7. **Gumucio JP**, **Phan AC**, **Ruehlmann DG**, **Noah AC**, **Mendias CL**. Synergist ablation induces rapid tendon growth through the synthesis of a neotendon matrix. *J Appl Physiol* 117: 1287–1291, 2014.

8. **Heinemeier KM**, **Schjerling P**, **Heinemeier J**, **Magnusson SP**, **Kjaer M**. Lack of tissue renewal in human adult Achilles tendon is revealed by nuclear bomb (14)C. *The FASEB Journal* 27: 2074–2079, 2013.

9. **Huang AH**, **Lu HH**, **Schweitzer R**. Molecular regulation of tendon cell fate during development. *J. Orthop. Res.* (March 18, 2015). doi: 10.1002/jor.22834.

10. **Huang AH**, **Lu HH**, **Schweitzer R**. Molecular regulation of tendon cell fate during development. *J Orthop Res* 33: 800–812, 2015.

11. **Khan K**, **Cook J**. The painful nonruptured tendon: clinical aspects. Clin Sports Med 22:711-725, 2003.

12. **Kjaer M**, **Langberg H**, **Bojsen-Møller J**. Novel methods for tendon investigations. *Disability and …* 30: 1514–1522, 2008.

13. **Kjaer M**, **Magnusson P**, **Krogsgaard M**, **Boysen Møller J**, **Olesen J**, **Heinemeier K**, **Hansen M**, **Haraldsson B**, **Koskinen S**, **Esmarck B**, **Langberg H**. Extracellular matrix adaptation of tendon and skeletal muscle to exercise. *J*

Anat 208: 445–450, 2006.

14. **Lee CH**, **Lee FY**, **Tarafder S**, **Kao K**, **Jun Y**, **Yang G**, **Mao JJ**. Harnessing endogenous stem/progenitor cells for tendon regeneration. *J Clin Invest* 125: 2690–2701, 2015.

15. **Léjard V**, **Brideau G**, **Blais F**, **Salingcarnboriboon R**, **Wagner G**, **Roehrl MHA**, **Noda M**, **Duprez D**, **Houillier P**, **Rossert J**. Scleraxis and NFATc Regulate the Expression of the Pro-α1(I) Collagen Gene in Tendon Fibroblasts. *Journal of Biological Chemistry* 282: 17665–17675, 2007.

16. **Mendias CL**, **Bakhurin KI**, **Faulkner JA**. Tendons of myostatin-deficient mice are small, brittle, and hypocellular. *Proc Natl Acad Sci USA* 105: 388–393, 2008.

17. **Mendias CL**, **Gumucio JP**, **Bakhurin KI**, **Lynch EB**, **Brooks SV**. Physiological loading of tendons induces scleraxis expression in epitenon fibroblasts. *J Orthop Res* 30: 606–612, 2012.

18. **Mendias CL**, **Gumucio JP**, **Lynch EB**. Mechanical loading and TGF-β change the expression of multiple miRNAs in tendon fibroblasts. *J Appl Physiol* 113: 56–62, 2012.

19. **Murchison ND**, **Price BA**, **Conner DA**, **Keene DR**, **Olson EN**, **Tabin CJ**, **Schweitzer R**. Regulation of tendon differentiation by scleraxis distinguishes force-transmitting tendons from muscle-anchoring tendons. *Development* 134: 2697–2708, 2007.

20. **Olesen JL**, **Heinemeier KM**, **Haddad F**, **Langberg H**, **Flyvbjerg A**, **Kjaer M**, **Baldwin KM**. Expression of insulin-like growth factor I, insulin-like growth factor binding proteins, and collagen mRNA in mechanically loaded plantaris tendon. *J Appl Physiol* 101: 183–188, 2006.

21. **Pryce BA**, **Watson SS**, **Murchison ND**, **Staverosky JA**, **Dünker N**, **Schweitzer R**. Recruitment and maintenance of tendon progenitors by TGFbeta signaling are essential for tendon formation. *Development* 136: 1351–1361, 2009.

22. **Schmittgen TD**, **Livak KJ**. Analyzing real-time PCR data by the comparative CT method. *Nat Protoc* (2008). doi: 10.1038/nprot.2008.73.

23. **Schwartz AJ**, **Sarver DC**, **Sugg KB**, **Dzierzawski JT**, **Gumucio JP**, **Mendias CL**. p38 MAPK Signaling in Postnatal Tendon Growth and Remodeling. *PLoS ONE* 10: e0120044, 2015.

24. **Schweitzer R**, **Chyung JH**, **Murtaugh LC**, **Brent AE**, **Rosen V**, **Olson EN**, **Lassar A**, **Tabin CJ**. Analysis of the tendon cell fate using Scleraxis, a specific marker for tendons and ligaments. *Development* 128: 3855–3866, 2001.

25. **Scott A**, **Zwerver J**, **Grewal N**, **de Sa A**, **Alktebi T**, **Granville DJ**, **Hart DA**.

Lipids, adiposity and tendinopathy: is there a mechanistic link? Critical review. *British Journal of Sports Medicine* 49: 984–988, 2015.

26. **Shukunami C**, **Takimoto A**, **Oro M**, **Hiraki Y**. Scleraxis positively regulates the expression of tenomodulin, a differentiation marker of tenocytes. *Dev Biol* 298: 234–247, 2006.

27. **Shukunami C**, **Takimoto A**, **Oro M**, **Hiraki Y**. Scleraxis positively regulates the expression of tenomodulin, a differentiation marker of tenocytes. *Dev Biol* 298: 234–247, 2006.

28. **Tan Q**, **Lui PPY**, **Lee YW**. In vivo identity of tendon stem cells and the roles of stem cells in tendon healing. *Stem Cells and Development* 22: 3128–3140, 2013.

29. **Viukov S**, **Sharir A**, **Shwartz Y**, **Galloway JL**, **Pryce BA**, **Johnson RL**, **Tabin CJ**, **Schweitzer R**, **Zelzer E**. Bone Ridge Patterning during Musculoskeletal Assembly Is Mediated through SCX Regulation of Bmp4 at the Tendon-Skeleton Junction. 17: 861–873, 2009.

30. **Yoshimoto Y**, **Takimoto A**, **Watanabe H**, **Hiraki Y**, **Kondoh G**, **Shukunami C**. Scleraxis is required for maturation of tissue domains for proper integration of the musculoskeletal system. *Sci Rep* 7: 45010, 2017.

CHAPTER IV

Mitochondrial Dysfunction and Impaired in Muscle Regeneration in Myosteatosis

ABSTRACT

Myosteatosis is the pathological accumulation of lipid that occurs in conjunction with atrophy and fibrosis following skeletal muscle injury or disease. Little is known about the mechanisms by which lipid accumulates in myosteatosis, but many studies have demonstrated the degree of lipid infiltration negatively correlates with muscle function and regeneration. Our goal was to identify biochemical pathways that lead to muscle dysfunction and lipid accumulation in injured rotator cuff muscles, a model that demonstrates severe myosteatosis. Adult rats were subjected to a massive tear to the rotator cuff musculature. After a period of either 0 (healthy control), 10, 30, or 60 days, muscles were prepared for RNA sequencing, shotgun lipidomics, metabolomics, biochemical measures, electron microscopy, and muscle fiber contractility. Following rotator cuff injury, there was a decrease in muscle fiber specific force production that was lowest at 30d. There was a dramatic time dependent increase in triacylglyceride content. Interestingly, genes related to not only triacylglyceride synthesis, but also lipid oxidation were largely downregulated over time. Using bioinformatics techniques, we identified that biochemical pathways related to mitochondrial dysfunction and reactive

oxygen species were considerably increased in muscles with myosteatosis. Long chain acyl-carnitines and L-carnitine, precursors to beta-oxidation, were depleted following rotator cuff tear. Electron micrographs showed injured muscles displayed large lipid droplets within mitochondria at early time points, and an accumulation of peripheral segment mitochondria at all time points. Several markers of oxidative stress were elevated following rotator cuff tear. The results from this study suggest that the accumulation of lipid in myosteatosis is not a result of canonical lipid synthesis, but occurs due to decreased lipid oxidation in mitochondria. A failure in lipid utilization by mitochondria would ultimately cause an accumulation of lipid even in the absence of increased synthesis. Further study will identify whether this process is required for the onset of myosteatosis.

INTRODUCTION

Injuries to skeletal muscle are associated with atrophy of muscle fibers, and excess extracellular matrix accumulation, called fibrosis. Regeneration of skeletal muscle is a complex process and involves the coordination of many different cell types directing many processes within skeletal muscle (24). For minor injuries, muscle can heal without any intervention, and will usually recover to full function. However, more severe chronic injuries and diseases to skeletal muscle result in the progressive loss in muscle size and function, and do not heal over time. In addition to severe muscle atrophy and fibrosis, some chronic injuries also cause infiltration of lipid within and between skeletal muscle fibers, and disrupt the ability of the muscle to function normally (13, 14, 20). The pathological accumulation of lipid, along with muscle atrophy and fibrosis, is referred to as myosteatosis. This phenomenon is not new, as myosteatosis

was first recorded in 1852 in the first paper to describe Duchenne muscular dystrophy (35). Since then, advances in the detection lipid infiltration in various muscle wasting injuries and diseases have been made, yet the cellular and molecular etiology of myosteatosis remains poorly understood.

In a healthy individual, lipid accounts for approximately 0.5% of the volume of skeletal muscle, and can increase up to 7 fold in obese individuals (43) and increase similarly in athletes (16). In extreme cases of myosteatosis, the amount of lipid can exceed greater than 50% of muscle tissue volume (17). A muscle cell can deal with lipids in two fundamental ways, either utilize fatty acids for energy production, or store them as triglycerides. Lipids are typically stored in skeletal muscle in the form of tiny triglyceride-rich puncta within skeletal muscle fibers, often in close proximity to mitochondria (16, 42). Fatty acids cleaved from intracellular lipid droplets can be utilized in mitochondria for energy production through beta-oxidation and subsequent ATP generation in the electron transport chain (44). For years, two distinct populations of mitochondria were thought to exist in skeletal muscle: intermyofibrillar, which exist between myofibrils, and subsarcolemmal mitochondria, located in the space between myofibrils and the plasma membrane (7, 12, 26). Intermyofibrillar mitochondria have higher respiratory chain complex activity (12) and are thought to be more specialized for the production of energy for use in contracting myofibrils compared to subsarcolemmal mitochondria (7). More recently, mitochondria have been shown to exist in a larger network, which allows for a cell-wide coupling of energy and membrane potential (15, 36). Instead of distinct mitochondrial populations, a dense matrix of mitochondria within the myofibrils called I-band segments extend to the periphery of the cell, creating

peripheral mitochondrial segments (36). These 3-dimensionally connected segments allow for a mitochondrial reticulum to exist and form a strong electrical coupling between these different segments and across the muscle cell (3, 36).

It is not known what functional consequences are directly caused by excess lipid accumulation in skeletal muscle. There is a strong negative correlation between lipid infiltration and muscle force production (13), and excess lipid in other disorders such as diabetes and cancer can result in increased inflammation (4, 44) and decreased insulin signaling (23, 44). The objective of this study was to evaluate the cellular and molecular pathways that are involved in the progression of myosteatosis in a rat model of rotator cuff injury. The rotator cuff develops substantial myosteatosis following tear, and the condition worsens with time (14, 19). Using a variety of omics techniques, including transcriptomics, shotgun lipidomics, metabolomics, and proteomics, we assessed pathways that were enriched with myosteatosis using bioinformatics techniques. We used these techniques to test the hypothesis that myosteatosis arises due to increased lipid synthesis genes early following injury and sustained lipid accumulation leads to chronic inflammation.

METHODS

Animals. This study was approved by the University of Michigan IACUC. Forty adult male Sprague Dawley rats were used in this study (N=10 per group). Bilateral supraspinatus tears were administered as previously described (8), with a slight modification. Briefly, a deltoid-splitting transacromial approach was used to expose the supraspinatus tendon, and a tenectomy was performed, removing the tendon from its footprint on the humerus. Following tenectomy, the suprascapular nerve was located,

and approximately a 3-4mm piece of the nerve was removed, creating a nerve injury. The deltoid muscle and skin were closed and the animals were allowed to recover in their cages. After a period of either 10, 30, or 60 days, supraspinatus muscles were harvested, weighed, and prepared for either histology, single fiber contractility, mitochondrial enzyme activity measures, or minced and snap frozen in 25-50mg aliquots for biochemical measures.

RNA isolation and RNA Sequencing (RNASeq). Snap frozen aliquots of muscle tissue was homogenized in QIAzol (Qiagen, Valencia, CA) and isolated using a micro RNeasy kit (Qiagen). RNA concentration was determined using a NanoDrop 2000 (Thermo Fisher Scientific, Waltham, MA). For each sample, 250ng total RNA was delivered to the University of Michigan Sequencing Core for RNA sequencing. Sample concentrations were normalized and cDNA pools were created for each sample, and then subsequently tagged with a barcoded oligo adapter to allow for sample specific resolution. Sequencing was carried out using an Illumina-HiSeq platform (Illumina, San Diego, CA) and 50bp single end reads. Raw RNASeq data was quality checked using FastQC v0.10.0 (Barbraham Bioinformatics, Cambridge, UK), and alignment to the reference genome (rn5, UCSC), differential expression, and post-analysis diagnostics were carried out using the Tuxedo Suite software package (40). Transcripts were considered differentially expressed based on $q<0.05$ and fold change≥ 1.5.

Shotgun lipidomics and metabolomics. Aliquots of muscle tissue were delivered to the University of Michigan metabolomics core for mass spectrometry based shotgun lipidomics and metabolomics. For lipidomics, lipids were extracted from samples with a solvent mixture consisting of 2:2:2 (v/v/v) methanol:dichloromethane:water mixture at

room temperature after adding internal standard mixture. After drying, the samples were resuspended in a solution containing 1:5:85 (v/v/v) acetonitrile:water:isopropanol and 10mM ammonium acetate. Samples were then subjected to liquid chromatrography-mass spectrometry (LC-MS), and MS peaks were matched in-silico with LipidBlast (25). Quantification was performed by Multiquant software (AB-SCIEX, Framingham, MA). For metabolomics, metabolites were extracted from frozen muscle in a solvent mixture containing 8:1:1 methanol:chloroform:water (v/v/v). Hydrophilic interaction chromatography-electropray time of flight MS was used to determine polar metabolites (28). Reversed phase liquid chromatography-tandem quadrupole MS was used to measure acylcarnitines. Other metabolites were derivatized and analyzed with gas chromatography-MS. Quantification of metabolites was performed using Masshunter Quantitative Analysis software (Agilent Technologies, Santa Clara, CA).

Bioinformatics. Expression data from RNASeq measurements was imported into Ingenuity Pathway Analysis (IPA) software (Qiagen) to determine cellular and molecular pathways involved in myosteatosis. For metabolomics and lipidomic measures, MS peak data was imported into Metaboanalyst (metaboanalyst.ca, McGill University, Ontario, Canada) for data normalization and statistical analysis. Heatmaps were generated in Prism 6.0 (GraphPad Software, La Jolla, CA).

Permeablized muscle fiber contractility. Distal segments of supraspinatus muscles were prepared for single fiber contractility as described (19, 37). Ten to 20 fibers per muscle were used for experiments.

Electron Microscopy. Portions of distal supraspinatus muscles were fixed in 1% tannic acid, 1% glutaraldehyde in Sorenson's buffer, followed by post-fixation in 2%

osmium tetroxide (Electron Microscopy Sciences, EMS, Hatfield, PA). Samples were then dehydrated using a graded ethanol series and embedded in EMBed 812 resin using a graded resin (EMS) and propylene oxide series. One micron transverse sections were cut with a diamond knife ultramicrotome, and imaged using a JEOL 1400-plus transmission electron microscope with a high-resolution AMT digital camera (JEOL USA, Peabody, MA).

Hydroxyproline content. Hydroxyproline was measured from the insoluble fraction of preparation from protein isolation. Pellets were dried at 100ºC overnight, and hydroxyproline was determined as described previously (20).

Mitochondrial DNA (mtDNA) measurements. Total DNA was isolated from frozen aliquots of muscle tissue using the DNeasy Blood & Tissue Kit (Qiagen). DNA was amplified via qPCR with custom primers for mtDNA (*Fwd:*5'AGCTTAATCACAAAGCATCTGGCCT3'; *Rev:*5' TGTTGGTTGGTTGTAGGGCTAGGGT3') and beta-2-microglobulin (B2M) genomic DNA (gDNA, *Fwd:*5' GTGCTTGTCTCTCTGGCCGTCG3'; *Rev:*5' AACGCCCACTCCTTTCCCGAGA3'). Using known standards of rat DNA, standard curves were generated for each primer set to determine number of copies of either mtDNA or gDNA. The ratio of mtDNA/gDNA was calculated per sample and averaged across groups.

Mitochondrial enzymatic assays. Fifty milligrams of freshly minced supraspinatus tissue was isolated and placed in 500µL of ice cold PBS (Thermo Fisher) containing protease inhibitor. Samples were homogenized and then 100µL of 10% laurel maltoside and 400µL cold PBS with protease inhibitor was further added. Samples were incubated

on ice for 30min and then centrifuged at 12,000xg for 20 min at 4ºC. Samples were stored at -80ºC until use. On the day of measurement, samples were thawed on ice, and protein concentration was determined using a BCA assay (Thermo Fisher). Colorimetric enzymatic assays for mitochondrial complex I, II, and IV were performed as per the protocol acquired from the manufacturer (AbCam, San Francisco, CA). Sample concentration was optimized per assay in pilot experiments, and equal protein was loaded per well. Samples were measured in duplicate in a BioTek Epoch2 microplate spectrophotometer (BioTek, Winooski, VT). Optical density per minute (mOD/min) was calculated as per the manufacturer protocol.

Protein oxidation measurements. Protein was isolated from frozen aliquots of supraspinatus tissue and treated with 2,4-dinitrophenylhydrazine (Sigma-Aldrich, Dorset, United Kingdom). Glutathionylation and carbonylation of protein was measured as previously described (31). Blots were imaged using a Chemidoc (Bio-Rad), and band densitometry was measured using ImageJ (NIH).

Western blots. Protein was isolated from frozen aliquots of muscle tissue and placed in 500µL of a solution containing TPER (Thermo Fisher Scientific, Waltham, MA) with 1% NP-40 and 1% protease-phosphatase inhibitor. Samples were homogenized, vortexed at 4ºC for 30 min, then centrifuged at 12,000xg for 15 min at 4ºC. The supernatant was collected and saved at -80ºC until use. The pellets were saved for hydroxyproline assays. Protein concentration was determined with a BCA assay (Thermo Fisher). Twenty micrograms of protein were loaded into 6-12% polyacrylamide gels, and subjected to electrophoretic separation. Proteins were transferred onto nitrocellulose membranes (Bio-Rad) and blocked for 1h in 5% skim milk. Membranes

were rinsed and incubated overnight in rabbit primary antibodies (Cell Signaling, 1:1000) against either succinate dehydrogenase-A (SDHA, SDH, D6J9M), cytochrome c oxidase subunit 4 (COXIV, 3E11), Phospho-Insulin-like Growth Factor-1 Receptor (P-IGF-1R) Tyr^{1135} (DA7A8), Phospho-p44/42 MAPK (P-Erk1/2) $Tyr^{202/204}$ (A13.14.4E), Protein Kinase B (Akt) Ser^{473} (D9E), pan Akt (C67E7), Phospho-p70S6 Kinase (P-$p70^{S6K}$) Thr^{389} (108D2), P-$p70^{S6K}$ Thr^{421}/Ser^{424}, pan $p70^{S6K}$ (49D7), Phospho-ribosomal protein S6 (P-rpS6) $Ser^{235/236}$ (D57.2.2E), or pan rpS6 (5G10). After primary antibody incubation, membranes were rinsed and incubated in goat anti rabbit horseradish peroxidase-conjugated secondary antibodies (Abcam). Proteins were detected using Clarity Western ECL Substrate (Bio-Rad) and imaged on a Chemidoc (Bio-Rad).

Statistics. Differences between groups were measured using One-way ANOVAs (α=0.05), followed by Fisher's LSD post hoc sorting (α=0.05). Analyses were performed using Prism 6.0 (GraphPad). Values are presented as mean+SD.

RESULTS

Rotator cuff tear resulted in a decrease in supraspinatus mass that reached the lowest point at 30d compared to uninjured controls, with a slight increase from 30d to 60d (Figure 4.1A). There was an increase in transcripts measured by RNASeq related to muscle atrophy, atrogin-1 and MuRF-1 at 10d compared to 0d, but the expression of these transcripts returned to control levels at 30 and 60d (Figure 4.1B). Hydroxproline content was used as a measure of collagen accumulation, and compared to controls, fibrosis did not accumulate until 30d, and was elevated through 60d (Figure 4.1C). There was an increase of *Col1a1* transcript at 10d compared to control, and an increase in *Col3a1* expression at 30d compared to controls (Figure 4.1C). We also measured via

RNASeq the expression of several transcripts related to inflammation. Interleukin (IL)-1β (*Il1b*) was increased at 10 and 30d compared to control, but fell to control levels by 60d (Figure 4.1D). IL-12 (*Il12*) was increased in the chronic time points at 30 and 60d compared to controls (Figure 4.1D). IL-23 (*Il23*) and interferon-gamma receptor (IFNγ-R, *Ifngr*) were both increased at 10d and 30d compared to controls, then returned to control levels by 60d (Figure 4.1D).

For single muscle fiber contractility, there was a decrease in CSA compared to control at all time points, with 30d having the lowest CSA among groups (Figure 4.2A). Similarly, there was a decrease in both Fo (Figure 4.2B) and sFo (Figure 4.2C) at 10d and a further decrease at 30d, which increased slightly at 60d but not to the level of controls. Sarcomere ultrastructure was disrupted noticeably at all time points compared to control, where large lipid droplets seemed to affect sarcomere alignment and arrangement (Figure 4.2D). Qualitatively, many large lipid droplets were found within mitochondria at 10d and 30d, and large lipid droplets were far less abundant in the intracellular space by 60d (Figure 4.2D).

Shotgun lipidomics revealed differences in many different lipid species across groups. Cholesterol ester levels increased at 10d and 30d compared to 0d, but fell back to control levels by 60d (Figure 4.3A). Monoacylglyceride levels stayed relatively stable across groups, with slight decreases at 10d and 60d compared to 0d (Figure 4.3B). Diacylglyceride levels did not increase until 30d compared to controls, and slightly decreased at 60d compared to 30d, but at a level still higher than 10d (Figure 4.3C). Triacylglyceride (TAG) was the most abundant lipid measured by a wide margin, and there was a time-dependent increase in TAG with rotator cuff tear (Figure 4.3D). We

also measured the accumulation of common free fatty acid species and there was an increase in palmitic acid (Palmitate) and stearic acid (Stearate) at 30d and 60d compared to control and 10d (Figure 4.3E), and an increase in oleic acid (Oleate) at 30d and 60d compared to 0d (Figure 4.3E).

Transcripts measured in RNASeq datasets were uploaded into Ingenuity Pathway Analysis (IPA) software to determine pathways that were involved in the progression of myosteatosis. One of the highest scored pathways by IPA in the early phases of myosteatosis was mitochondrial dysfunction, and in the later time points PKC-theta signaling and reactive oxygen species generation were the most involved (Table 4.1). Interestingly, compared to 0d, the very lowest scored pathways from IPA at 10d was lipid beta-oxidation, and this cellular process was decreased at later time points as well (Table 4.2). Additionally, we measured the counts for transcripts in RNASeq data that relate to lipid synthesis, breakdown, and utilization. For lipid synthesis, diacylglycerol acetyl transferase (DGAT) 1 was largely unchanged until a downregulation at 60d compared to all other time points (Figure 4.4A). DGAT2 was decreased from 0 and 10d at 30 and 60d (Figure 4.4A). For lipid breakdown, lipoprotein lipase (LPL) was decreased from 0d at 30 and 60d, and hormone sensitive lipase (HSL), was unchanged among all time points (Figure 4.4B). Carnitine palmitoyl transferase (CPT) I was increased at 30d compared to control and returned to control levels at 60d (Figure 4.4C). CPT II, SDH, and COXIV were decreased at 10d compared to control (Figure 4.4C). CPTII was also decreased from control at 60d, and SDH remained decreased through the remaining time points (Figure 4.4C). COXIV returned to control levels by 60d (Figure 4.4C).

Mass spectrometry metabolomics were used to assess the changes in metabolites from beta-oxidation. Across all time points, there was a decrease in all long-chain acyl carnitine levels with injury (Figure 4.5A,B). L-carnitine levels were also decreased across all time points compared to 0d (Figure 4.5C).

Several different measures of protein abundance and activity were used to assess mitochondrial function. There was no change in either mtDNA/gDNA ratio (Figure 4.6A) or cardiolipin levels across any time point (Figure 4.6B). There was decrease in SDH protein levels with injury compared to control (Figure 4.6C), but no differences in COXIV protein abundance (Figure 4.6D). Electron micrographs revealed an accumulation of peripheral segment mitochondria in all injured time points (Figure 4.6E). To assess mitochondrial enzymatic function, we used various mitochondrial enzyme assays. Complex I activity was decreased from control at 10d, but increased to control levels by 30d and 60d (Figure 4.6F). Complex II activity decreased from control at 10d, but increased beyond control levels at 30d and 60d (Figure 4.6G). Complex IV activity also decreased at 10d compared to 0d, and activity was highest at 60d (Figure 4.6H).

To measure protein oxidation, we measured overall carbonylation and glutathionylation. Carbonylated proteins were not different across groups (Figure 4.7A), but there was an increase in glutathionylation from control at 10d and 30d, which decreased to control levels by 60d (Figure 4.7B). Additionally, while there was no change in peroxiredoxin6 (Prdx6) abundance (Figure 4.7C), there was a dramatic increase in the oxidated form of Prdx6 at 60d (Figure 4.7D).

We measured various components of the insulin like growth factor-1 (IGF-1) pathway to assess the changes in phosphorylation in key proteins and kinases along the protein synthesis cascade. There was a decrease in P-IGF-1R (Ser^{1135}) at 30d and 60d compared to 0d (Figure 4.8A). Similarly, there was a decrease in P-Akt (Ser^{473}) at 60d, but not at 30d (p=0.08), compared to controls, but no change in total Akt across groups (Figure 4.8B). There was a decrease in P-Erk1/2 (Thr^{202}/Tyr^{204}) across all time points compared to 0d (Figure 4.8C). No change was observed for P-$p70^{S6K}$ (Thr^{389}) between groups, but a decrease across all injury time points for P-$p70^{S6K}$ (Thr^{421}/Ser^{424}) compared to 0d (Figure 4.8D). Total $p70^{S6K}$ was unchanged until a slight decrease at 60d compared to 10d (Figure 4.8D). Interestingly, there was an increase in P-rpS6 ($Ser^{235/236}$) at 10d and 30d compared to control (Figure 4.8E). There was a corresponding increase in total rpS6 at 30d compared to control, but no other differences between groups (Figure 4.8E).

DISCUSSION

For over 150 years, myosteatosis was a relatively unstudied phenomenon, despite the suggestion of a limited number of studies that pathological lipid accumulation with myosteatosis correlated with muscle dysfunction (13, 14). The aim of this study was to identify previously unknown mechanisms that explain the etiology of myosteatosis in a model of rotator cuff tears in rats. The results from this study indicate that infiltrating lipid that arises in myosteatosis is not from de novo lipogenesis, but potentially from decreased lipid utilization by dysfunctional mitochondria. This study also indicates that myosteatosis in rotator cuff tears is a result from at least two distinct stages of injury. The first of which is an acute inflammatory condition marked by

mitochondrial dysfunction and intracellular lipid accumulation by 10 days. The second phase, which occurs by 30 days post injury and continues through 60 days, is a chronically inflamed environment under active remodeling and marked by extracellular lipid accumulation, oxidative stress, and widespread muscle wasting.

During more commonly studied cardiotoxin or lengthening contraction-based skeletal muscle injuries, muscles are typically fully regenerated within 30-60 days (6, 11). In the current study, myosteatosis results in a progressive loss of muscle function, sarcomere disruption, atrophy, and fibrosis that continues through 60 days following injury. Lipid levels also do not return to normal over time, as the injury is marked by a dramatic time-dependent increase in TAG species both intracellularly and extracellularly, as well as a dramatic increase in DAG at the chronic time points. Despite the increase in TAG, expression of genes related to TAG synthesis, DGAT1/2, were largely unchanged with injury, and downregulated at time points that correspond to the most lipid accumulation. The early increase in lipid can be found intracellularly within mitochondria, which appear to be greatly disrupted structurally. IPA software analysis of RNASeq data predicted that beta-oxidation was the most downregulated cellular process, and it is conceivable that in the absence of increased lipid synthesis, a lack of beta-oxidation in mitochondria can lead to a backup of lipid. Shuttling lipid into mitochondria for beta-oxidation requires the conversion of long fatty acyl-CoAs into fatty acyl-carnitines (22), and this is accomplished through the action of carnitine palmitoyl transferases (CPTs) and L-carnitine (5). Despite the dramatic accumulation of lipid across all injured time points, there was a dramatic decrease in long chain acyl-carnitines and L-carnitine measured at any point in the injury. There was an increase in

CPTI transcript at 10 days, but a decrease in CPTII transcript at 10 and 60 days compared to controls, which is conceivable given the decrease in long chain acyl-carnitines for transport by CPTII.

There is debate in the literature as to the best measure of total mitochondrial mass (27, 34), as mitochondria are constantly in a state of flux and connected in a large network (3). By two measures, mtDNA content or cardiolipin abundance, there was no change in mitochondrial mass. These would likely be more appropriate measures of mitochondrial mass than abundance of mitochondrial complex proteins, given the deficiencies in oxidation and the increase in oxidative stress. Complex II protein levels, measured by SDH abundance, was decreased from control at all time points, and at 10d could explain the drop in complex II activity at that time. But the activity of complex II increased at 30 and 60 days, times where oxidative stress was highest in the glutathionylation and oxidized Prdx6 assays, respectively. Similarly, though complex IV protein was unchanged, COXIV transcript was increased at 10 days, and complex IV activity was decreased at 10 days and increased at 60 days compared to controls. Combined, a decrease in complex I, II, and IV and a decrease in long chain acyl-carnitines could explain the lipid arising within mitochondria at the 10 day time point. In the absence of beta-oxidation, lipid would either build up in lipid droplets, in mitochondria, be exported out of the cell, or remain as intracellular fatty acids. Mitochondria have homeostatic roles outside of energy homeostasis, and can be reservoirs for the proteolysis of misfolded proteins (38). It is possible that in this particular model, or in other times of lipid excess and muscle injury, mitochondria can also be reservoirs for lipid. Mitochondrial oxidation can also be inhibited by excess lipid

(1), and could provide a mechanism by which mitochondrial dysfunction actually occurs from an initial increase in lipid, further exacerbating the problem of lipid excess. In either case, the more proximal mechanisms by which mitochondrial dysfunction arises in this model need to be studied further. Overall, it is clear that rotator cuff injury results in widespread mitochondrial dysfunction, and an inability to oxidize lipid, leading to an early increase in intracellular lipid.

In the more chronic time points in this injury model, there are also several other factors that can lead to the decrease in muscle specific force generation at 30 and 60 days post injury. Mitochondrial dysfunction continued, as oxidative stress was highest at the chronic time points, and there was an accumulation of peripheral segment mitochondria. In the two mitochondrial population model, the peripheral, or subsarcolemmal, mitochondria have decreased oxidative capacity compared to mitochondria in the myofibrillar space (7, 12, 26). In the mitochondrial reticulum model, peripheral segment mitochondria have a greater abundance of proton motive proteins, whereas the intermyofibrillar mitochondria have more ATP generating proteins for use by sarcomeres (15, 36). In the current study, the abnormal spherical mitochondria in the peripheral space of injured muscles at 30 and 60 days post injury could reflect a mitochondrial network that has been disrupted. A network of long tube-like mitochondria that undergoes fission results in an accumulation of less tubular and more spherical mitochondria at the edges of fission (32). Given the widespread mitochondrial dysfunction with myosteatosis, it is possible that the conduction of energy homeostasis is lost with injury, and fission events could explain the accumulation of mitochondria in these spaces, however this warrants further study.

In addition to continued mitochondrial dysfunction, there is a continued increase in lipid at the 30d and 60d time points compared to control and 10d. Not only does TAG continue to dramatically rise, but there is also an accumulation of non-stable lipid intermediates, such as DAG, palmitate, stearate, and oleate. Many of the available studies on the effect of these intermediates on muscle energy homeostasis falls within the diabetes literature. Lipid excess within diabetes results in the intracellular accumulation of fatty acids like palmitate, which instead of stored as TAG, build up as DAG and other intermediates, which can activate inflammatory pathways (44). DAG accumulation also activates a member of the novel family of protein kinase Cs, PKCθ (18). In diabetes, PKCθ activation inhibits insulin stimulated glucose uptake by disrupting insulin signaling (47). The inhibition of the insulin pathway by the activation of PKCθ links obesity to insulin resistance, where the excess in lipid drastically reduces insulin signaling (23). In skeletal muscle, one of the main pathways that regulates mass is the IGF-1 pathway, which shares many of the same kinases and signaling proteins as the insulin pathway (21, 39). In the current study, IPA software predicted PKCθ signaling as an enriched pathway at 30 and 60 days post injury, and there was a distinct decrease in proximal IGF-1 signaling in the chronic stages of rotator cuff tear. There was a decrease in Akt phosphorylation in the chronic time points, where DAG and palmitate were most abundant. Additionally, there was a decrease in Erk1/2 phosphorylation across all injury time points, and a decrease in the Erk-dependent phosphorylation sites (Thr^{421}/Ser^{424}) on $p70^{S6K}$. Interestingly, the mTOR dependent site on $p70^{S6K}$, Thr^{389}, was unchanged, despite a trend for increased phosphorylation at 30d compared to control ($p=0.07$). Other than a slight difference in timing for

phosphorylation between the different sites with exercise (9, 30), to our knowledge no other study has found quite a divergence in the two sites. Surprisingly, there was an increase in P-rpS6 at 10 and 30 days post injury. This could be indicative of active remodeling, as there is an increase in transcripts related to autophagy in the chronic time points of this model of muscle injury (19). Further study will identify whether PKCθ is required for the changes in IGF-1 signaling in myosteatosis.

This study has several limitations. Myosteatosis is not limited to the rotator cuff muscle group. It can occur in hamstring muscles (41), paraspinal muscles with chronic back pain (2), with degenerative diseases like Duchenne muscular dystrophy (45) and cancer (10), and in aging (29). Therefore, there may be some differences in the etiology of myosteatosis in these different tissues and disease states, but likely these findings may help identify common themes for the development of myosteatosis in other injuries and diseases. Additionally, this study assessed myosteatosis in a model of combined tenectomy and neurectomy, but did not decipher the effects of each individually. However, we chose the combined approach due to the collective mechanical injury and neurodegenerative components that lead to myosteatosis in humans. In humans, the wasting of skeletal muscle with myosteatosis does not improve with time (13, 14, 33), but in rats there seems to be a small increase in specific force generation around 60d following injury compared to 30d. It is not clear whether this will continue to improve, but based on sustained oxidative stress, inflammation, and sarcomere disruption even at 60d, it is unlikely that the muscle will be able to fully regenerate even in the rat model. Despite these limitations, this study provided substantial insight into the mechanisms of myosteatosis over the course of a chronic degenerative injury.

Myosteatosis is a degenerative disorder that results in chronic muscle wasting, and can get worse with time. The early phases of myosteatosis arise due to a decrease in mitochondrial function, where lipid droplets form in myofibers and within mitochondria, and muscles have a widespread decrease in lipid beta-oxidation. Shuttling lipid into droplets may initially serve as a protective effect for the cell, as this would prevent the cell from high concentrations of reactive fatty acid molecules and lipid intermediates (46, 48). However, over time, decreased beta-oxidation would render the muscle cell incapable of decreasing lipid levels, and sustained damaged mitochondria results in increased oxidative stress. This further expansion of oxidative stress, lipid, and inflammation results in dramatic atrophy of the muscle fiber, and a chronic degenerative condition. Combined, this results in a temporal decrease in muscle function, which does not return at time points where muscle function is restored in non-lipid accumulating injuries (6, 11).

In order to develop therapies for the treatment of muscle wasting in myosteatosis, a better understanding of the cellular and molecular mechanisms behind the accumulation of lipid accumulation and muscle function is required. The results of this study provide the framework for the development of therapies to increase muscle function and regeneration in patients with myosteatosis. With further study of the mechanism and translatability in humans, methods that target IGF-1 signaling would be an attractive therapeutic direction that could help not only rotator cuff tears, but a much wider range of muscle injuries and diseases that affect millions of people in the world.

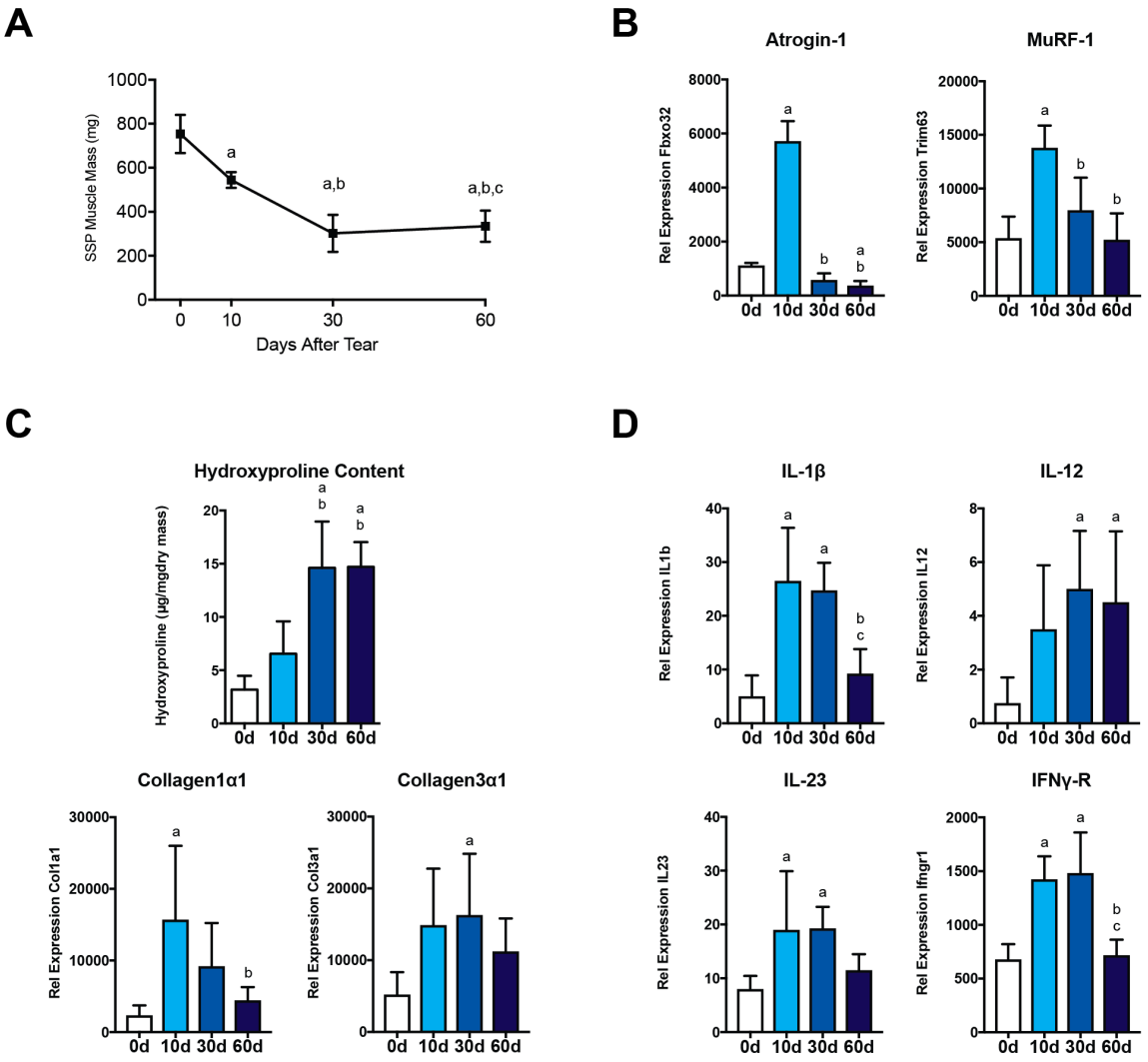

Figure 4.1. Measures of atrophy, fibrosis, and inflammation over time following rotator cuff tear. (A) Supraspinatus (SSP) mass after isolation from torn rotator cuff muscles. (B) Expression of transcripts measured by RNA Sequencing related to muscle atrophy. (C) Hydroxyproline content, a commonly used measure of collagen content or fibrosis, following rotator cuff tear, and expression of type I and III collagen transcripts measured by RNA Sequencing. (D) Expression of transcripts measured by RNA Sequencing related to inflammation. Data are presented mean+SD. a, Different from 0d; b, Different from 10d; c, Different from 30d ($P < 0.05$).

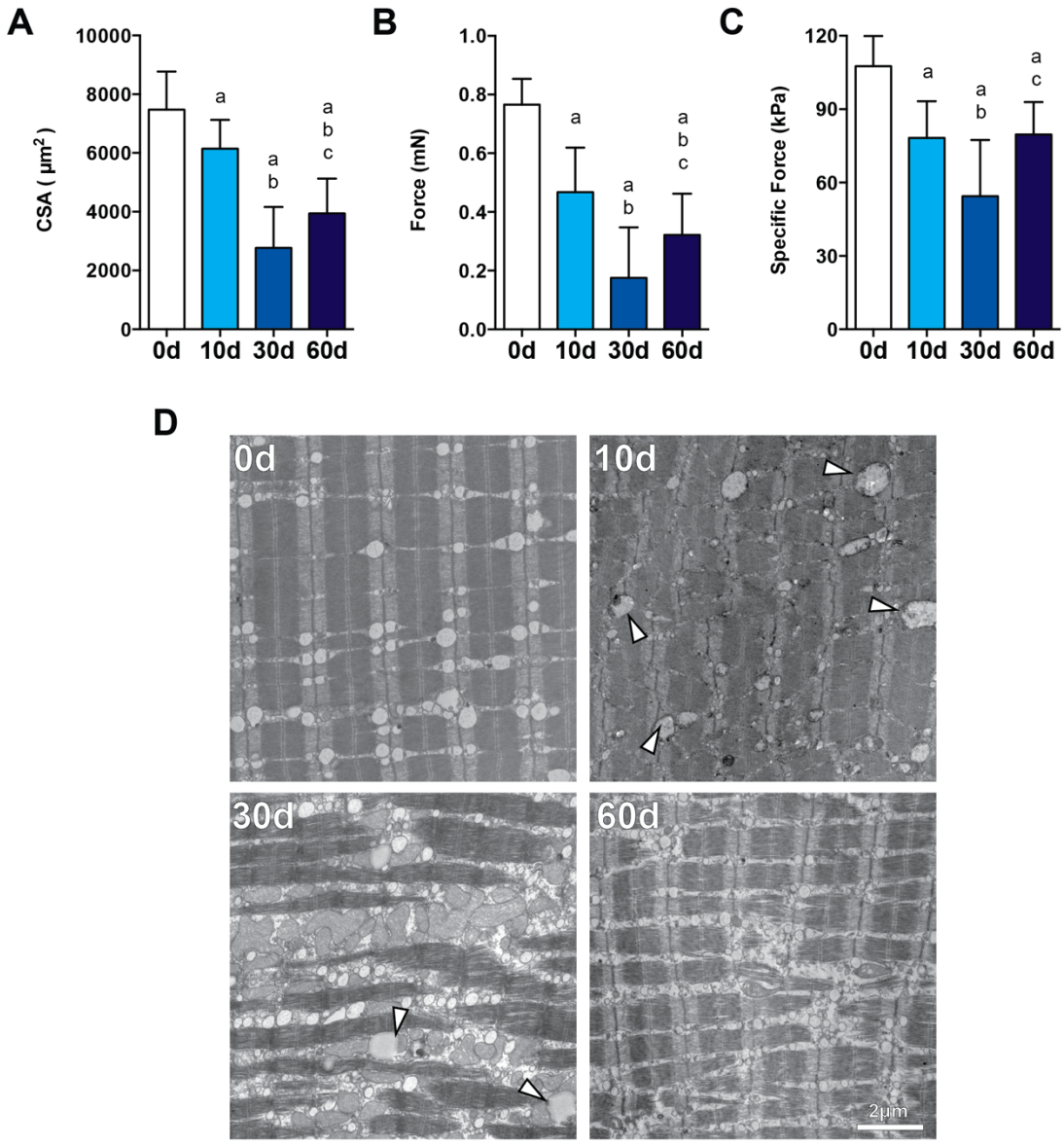

Figure 4.2. Changes in single fiber contractility and sarcomere ultrastructure over time following rotator cuff tear. (A) Cross sectional area (CSA), (B) maximum isometric force, and (C) specific force of permeablized muscle fibers from supraspinaus muscles following tear. Data are presented mean+SD. a, Different from 0d; b, Different from 10d; c, Different from 30d ($P < 0.05$). (D) Representative images of sarcomere ultrastructure in supraspinatus muscles following rotator cuff tear. White arrows indicate lipid-laden mitochondria. Scale bar is 2μm

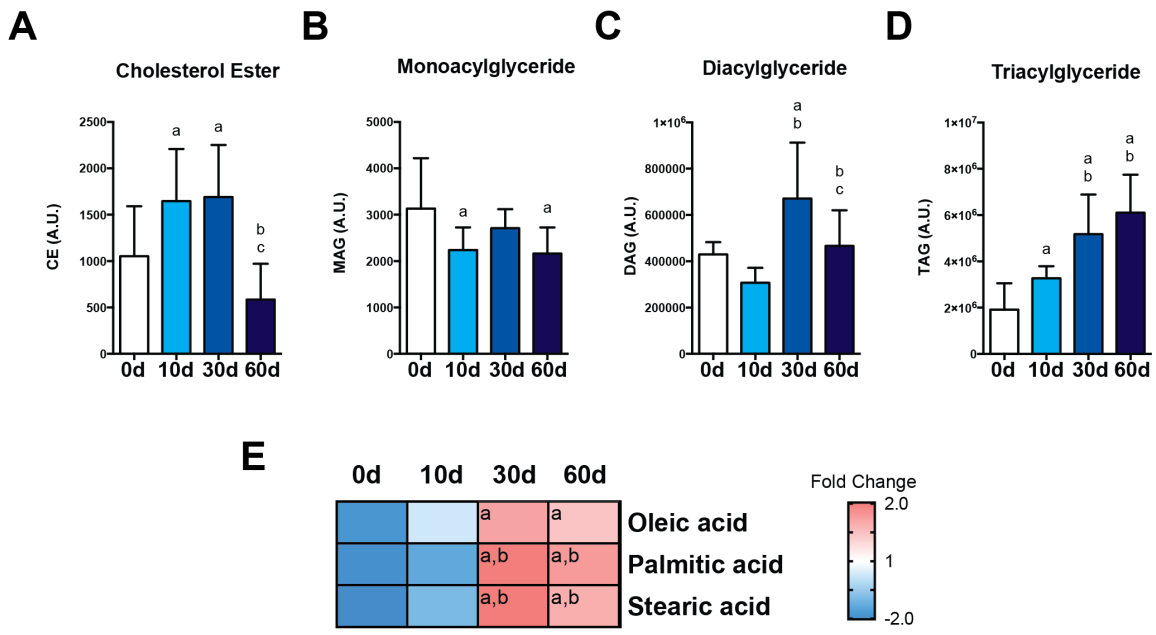

Figure 4.3. Changes in lipid species over time following rotator cuff tear. Sum of peak intensities of major lipid classes including (A) cholesterol ester, (B) monoacylglyceride (MAG), (C) diacylglyceride (DAG), and (D) triacylglyceride (TAG) measured by shotgun lipidomics. Data are presented mean+SD. a, Different from 0d; b, Different from 10d; c, Different from 30d ($P < 0.05$). (E) Heatmap of changes in fatty acid species measured by metabolomic analyses. a, Different from 0d; b, Different from 10d ($P < 0.05$).

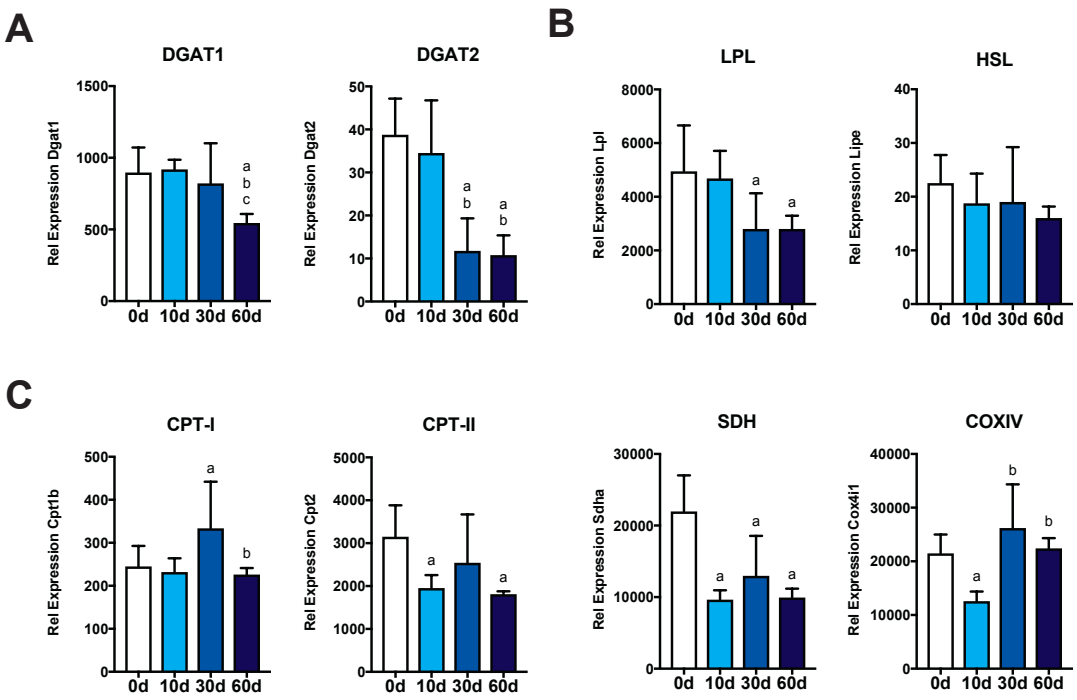

Figure 4.4. Expression of transcripts measured by RNASeq at each time point following rotator cuff tear. Transcripts that correspond to (A) lipid synthesis, (B) lipolysis, and (C) lipid utilization. Data are presented mean+SD. a, Different from 0d; b, Different from 10d; c, Different from 30d ($P < 0.05$).

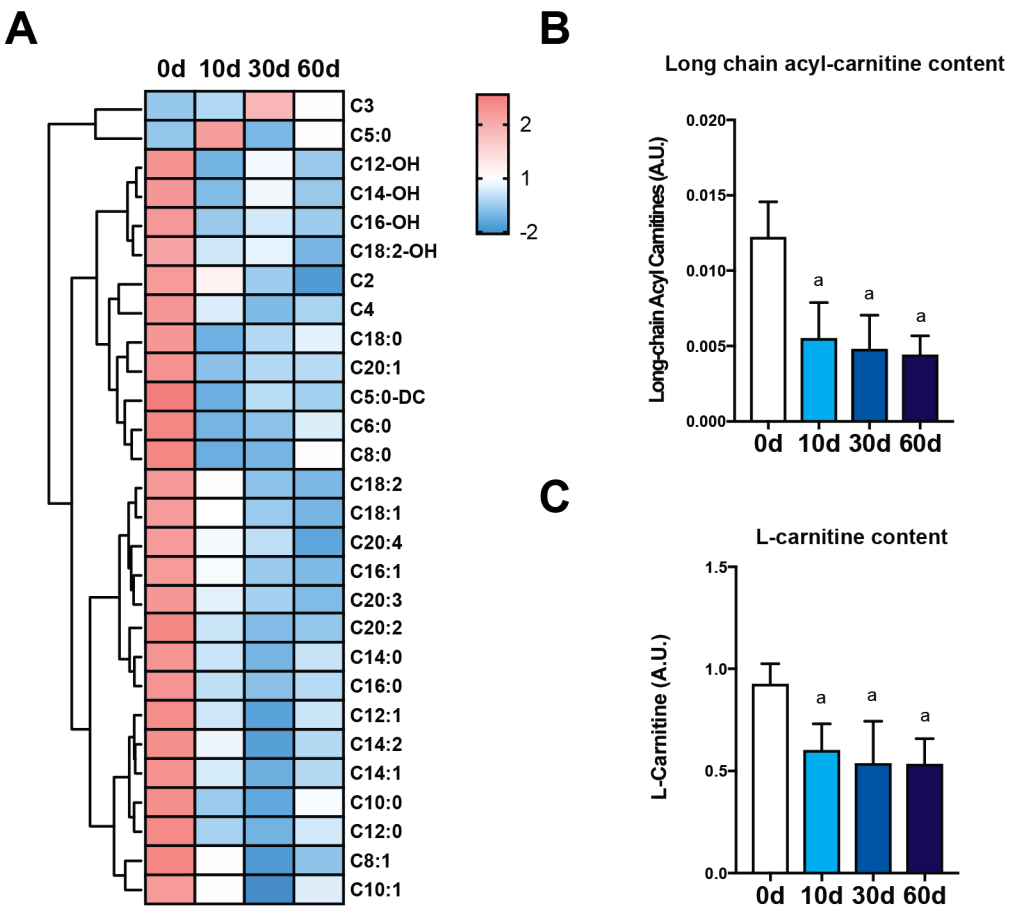

Figure 4.5. Decreases in acyl-carnitine species following rotator cuff tear. (A) Heatmap of acyl-carnitine species in torn rotator cuff muscles. (B) Quantification of mass spec peak intensity values for (B) all long chain (C>5) acyl-carnitines, and (C) L-carnitine. Data are presented mean+SD. a, Different from 0d (P <0.05).

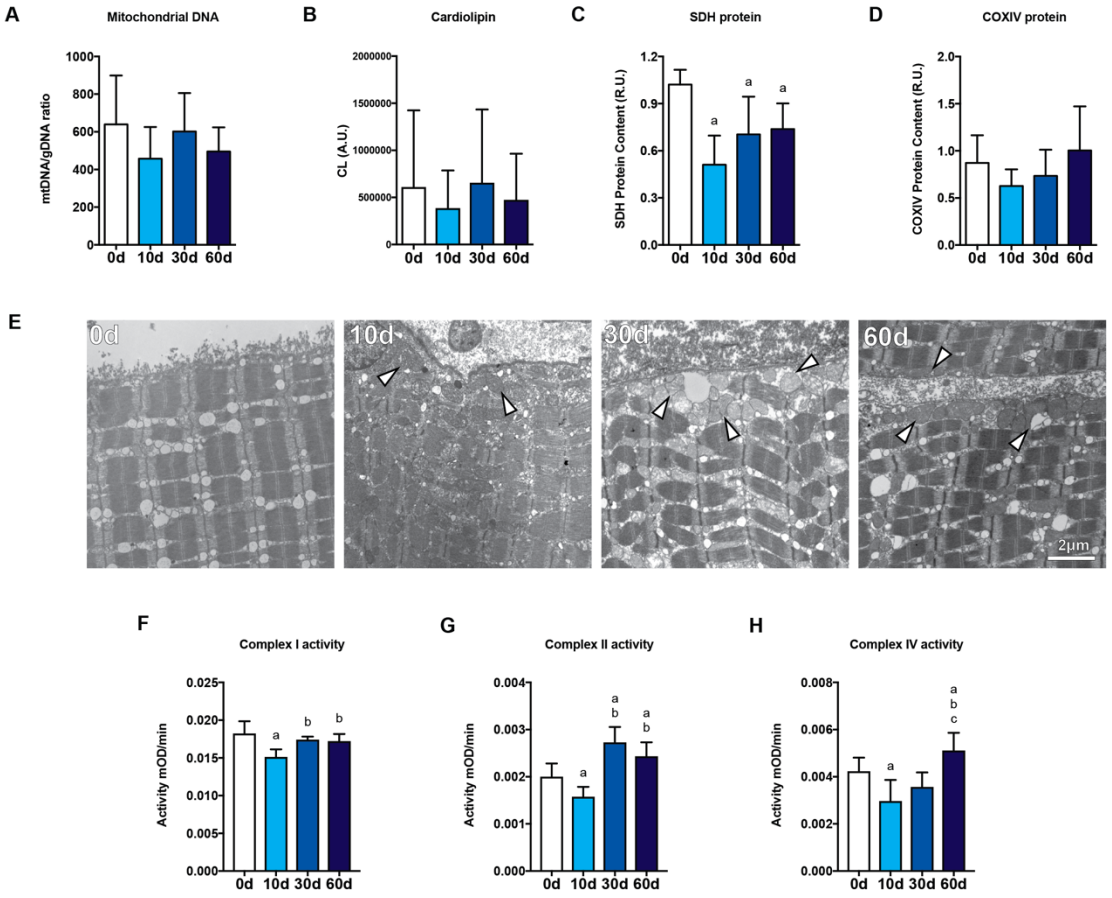

Figure 4.6. Mitochondrial levels, localization, and enzyme activity over time following rotator cuff tear. (A) Mitochondrial DNA:genomic DNA ratio using specific primers against mtDNA and genomic beta-2-microglobulin and (B) Cardiolipin levels as measures of mitochondrial mass in torn rotator cuff muscles. (C) Western blot analysis of SDH or (D) COXIV proteins from supraspinatus muscle homogenates. (E) Representative EM images of subsarcolemmal mitochondria in supraspinatus muscles following rotator cuff tear. White arrows indicate accumulation of peripheral space mitochondria. Scale bar is 2μm. Mitochondrial enzyme assay for (F) complex I, (G) complex II, and (H) complex III. For A-D and F-H, Data are presented mean+SD. a, Different from 0d; b, Different from 10d; c, Different from 30d ($P < 0.05$).

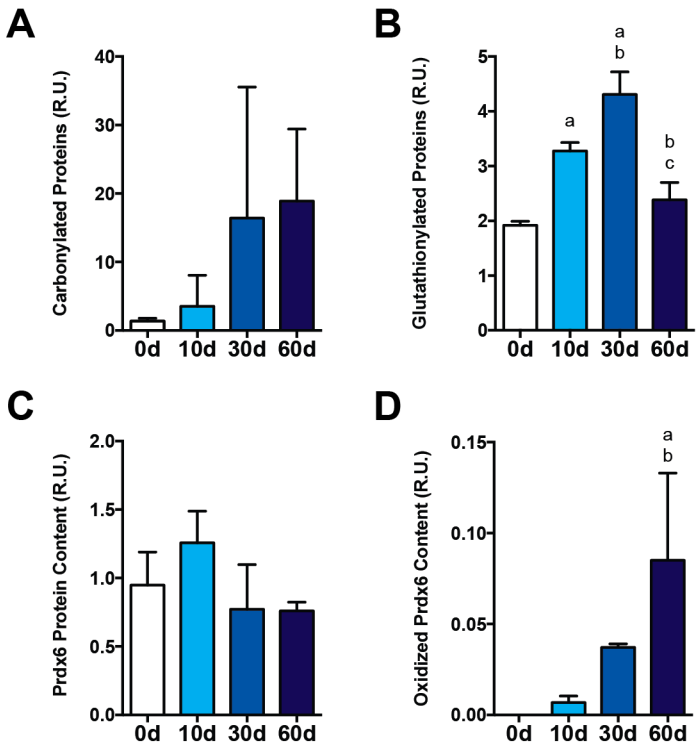

Figure 4.7. Markers of oxidative stress over time following rotator cuff tear. Protein (A) carbonylation and (B) glutathionylation, (C) Peroxiredoxin 6 protein content and (D) oxidized peroxiredoxin 6 accumulation in supraspinatus muscles following rotator cuff tear. Mitochondrial enzyme assay for (A) complex I, (B) complex II, and (C) complex III. Data are presented mean+SD. a, Different from 0d; b, Different from 10d; c, Different from 30d ($P < 0.05$).

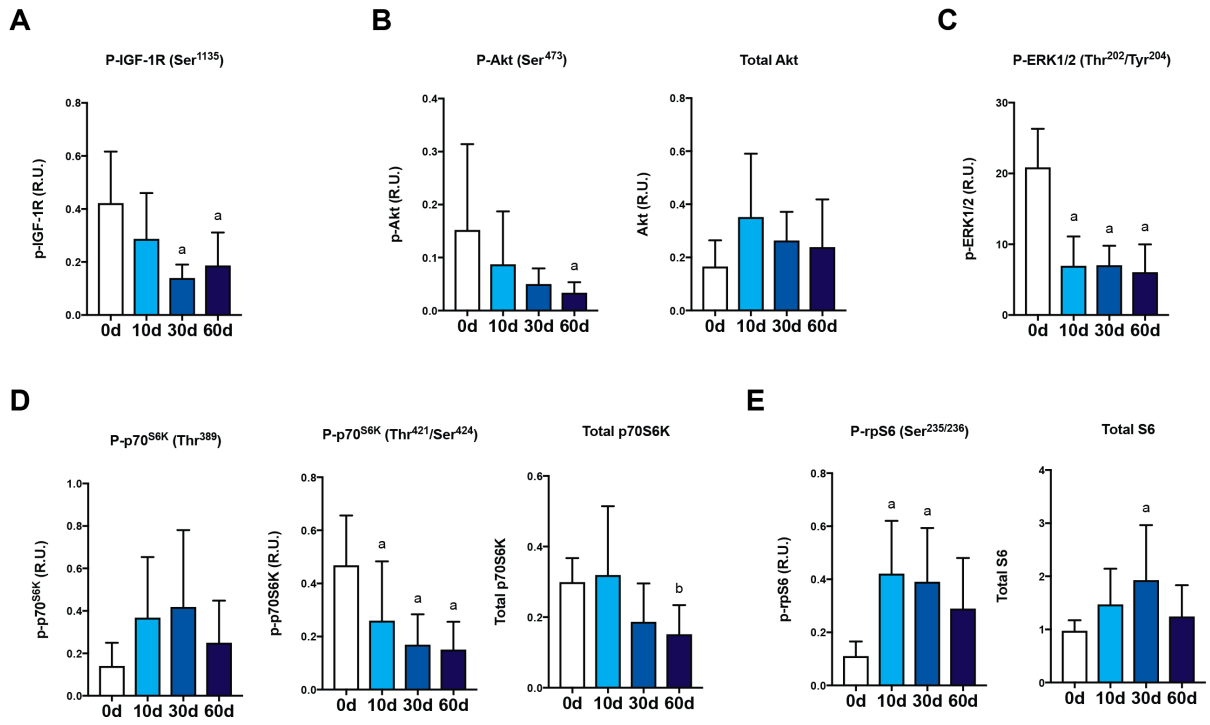

Figure 4.8. Decreased proximal IGF-1 signaling after rotator cuff tear. Western blot quantification of (A) phospho-IGF-1 receptor, (B) phospho-Akt (Ser473), and total Akt abundance, (C) phospho-Erk1/2 (Thr202/Tyr204), (D) phospho-p70S6K (Thr389 and Thr421/Ser424) and total p70S6K abundance, and (E) phospho-ribosomal protein S6 and total rpS6 abundance. Data are presented mean+SD. a, Different from 0d; b, Different from 10d; c, Different from 30d ($P < 0.05$).

Table 4.1. IPA output of canonical pathways in torn rotator cuff muscles compared to control muscles. P-values indicate test against 0d.

Time Point	Canonical Pathway	p-value
10d	Mitochondrial Dysfunction	2.21E-25
	Oxidative Stress Response	1.26E-14
30d	PKC-theta Signaling	1.58E-13
	Macrophage Activation	6.31E-19
60d	Macrophage Activation	7.94E-15
	PKC-theta Signaling	3.10E-10

Table 4.2. IPA output of cellular processes and predicted pathway activation state in torn rotator cuff muscles compared to control muscles. P-values indicate test against 0d.

Cellular Process	Time Point	Predicted Activation State	p-value
Oxidation of Lipid	10d	Decreased	6.64E-08
	30d	Decreased	1.78E-08
	60d	Decreased	2.72E-07
Beta-Oxidation of Fatty Acid	10d	Decreased	1.21E-07
	30d	Decreased	1.90E-08
	60d	N/A	NS

REFERENCES

1. **Aon MA**, **Bhatt N**, **Cortassa SC**. Mitochondrial and cellular mechanisms for managing lipid excess. *Front Physiol* 5: 432, 2014.

2. **Aubrey J**, **Esfandiari N**, **Baracos VE**, **Buteau FA**, **Frenette J**, **Putman CT**, **Mazurak VC**. Measurement of skeletal muscle radiation attenuation and basis of its biological variation. *Acta Physiologica* 210: 489–497, 2014.

3. **Bakeeva LE**, **Chentsov YS**, **Skulachev VP**. Mitochondrial framework (reticulum mitochondriale) in rat diaphragm muscle. *Biochim. Biophys. Acta* 501: 349-369, 1978.

4. **Bozza PT**, **Viola JPB**. Lipid droplets in inflammation and cancer. *Prostaglandins Leukot Essent Fatty Acids* 82: 243–250, 2010.

5. **Bremer J**. Carnitine--metabolism and functions. *Physiol Rev* 63: 1420–1480, 1983.

6. **Carlson BM**, **Faulkner JA**. The regeneration of skeletal muscle fibers following injury: a review. *Medicine & Science in Sports & Exercise* 15: 187–198, 1983.

7. **Cogswell AM**, **Stevens RJ**, **Hood DA**. Properties of skeletal muscle mitochondria isolated from subsarcolemmal and intermyofibrillar regions. *Am J Physiol* 264: C383–9, 1993.

8. **Davis ME**, **Stafford PL**, **Jergenson MJ**, **Bedi A**, **Mendias CL**. Muscle fibers are injured at the time of acute and chronic rotator cuff repair. *Clin Orthop Relat Res* 473: 226–232, 2015.

9. **Deldicque L**, **Atherton P**, **Patel R**, **Theisen D**, **Nielens H**, **Rennie MJ**, **Francaux M**. Decrease in Akt/PKB signalling in human skeletal muscle by resistance exercise. *Eur J Appl Physiol* 104: 57–65, 2008.

10. **Ewaschuk JB**, **Almasud A**, **Mazurak VC**. Role of n-3 fatty acids in muscle loss and myosteatosis. *Applied physiology, nutrition, and metabolism = Physiologie appliquée, nutrition et métabolisme* 39: 654–662, 2014.

11. **Faulkner JA**, **Davis CS**, **Mendias CL**, **Brooks SV**. The aging of elite male athletes: age-related changes in performance and skeletal muscle structure and function. *Clin J Sport Med* 18: 501–507, 2008.

12. **Ferreira R**, **Vitorino R**, **Alves RMP**, **Appell HJ**, **Powers SK**, **Duarte JA**, **Amado F**. Subsarcolemmal and intermyofibrillar mitochondria proteome differences disclose functional specializations in skeletal muscle. *Proteomics* 10: 3142–3154, 2010.

13. **Gerber C**, **Schneeberger AG**, **Hoppeler H**, **Meyer DC**. Correlation of atrophy

and fatty infiltration on strength and integrity of rotator cuff repairs: a study in thirteen patients. *J Shoulder Elbow Surg* 16: 691–696, 2007.

14. **Gladstone JN**, **Bishop JY**, **Lo IKY**, **Flatow EL**. Fatty infiltration and atrophy of the rotator cuff do not improve after rotator cuff repair and correlate with poor functional outcome. *American Journal of Sports Medicine* 35: 719–728, 2007.

15. **Glancy B**, **Hartnell LM**, **Malide D**, **Yu Z-X**, **Combs CA**, **Connelly PS**, **Subramaniam S**, **Balaban RS**. Mitochondrial reticulum for cellular energy distribution in muscle. *Nature* 523: 617–620, 2015.

16. **Goodpaster BH**, **He J**, **Watkins S**, **Kelley DE**. Skeletal muscle lipid content and insulin resistance: evidence for a paradox in endurance-trained athletes. *Journal of Clinical Endocrinology & Metabolism* 86: 5755–5761, 2001.

17. **Goutallier D**, **Postel JM**, **Bernageau J**, **Lavau L**, **Voisin MC**. Fatty muscle degeneration in cuff ruptures. Pre- and postoperative evaluation by CT scan. *Clin Orthop Relat Res* : 78–83, 1994.

18. **Griffin ME**, **Marcucci MJ**, **Cline GW**, **Bell K**, **Barucci N**, **Lee D**, **Goodyear LJ**, **Kraegen EW**, **White MF**, **Shulman GI**. Free fatty acid-induced insulin resistance is associated with activation of protein kinase C theta and alterations in the insulin signaling cascade. *Diabetes* 48: 1270–1274, 1999.

19. **Gumucio JP**, **Davis ME**, **Bradley JR**, **Stafford PL**, **Schiffman CJ**, **Lynch EB**, **Claflin DR**, **Bedi A**, **Mendias CL**. Rotator cuff tear reduces muscle fiber specific force production and induces macrophage accumulation and autophagy. *J Orthop Res* 30: 1963–1970, 2012.

20. **Gumucio JP**, **Korn MA**, **Saripalli AL**, **Flood MD**, **Phan AC**, **Roche SM**, **Lynch EB**, **Claflin DR**, **Bedi A**, **Mendias CL**. Aging-associated exacerbation in fatty degeneration and infiltration after rotator cuff tear. *J Shoulder Elbow Surg* 23: 99–108, 2014.

21. **Gumucio JP**, **Mendias CL**. Atrogin-1, MuRF-1, and sarcopenia. *Endocrine* 43: 12–21, 2013.

22. **Holloway GP**, **Luiken JJFP**, **Glatz JFC**, **Spriet LL**, **Bonen A**. Contribution of FAT/CD36 to the regulation of skeletal muscle fatty acid oxidation: an overview. *Acta Physiologica* 194: 293–309, 2008.

23. **Itani SI**, **Ruderman NB**, **Schmieder F**, **Boden G**. Lipid-Induced Insulin Resistance in Human Muscle Is Associated With Changes in Diacylglycerol, Protein Kinase C, and IκB-α. *Diabetes* 51: 2005–2011, 2002.

24. **Järvinen TA**, **Järvinen M**, **Kalimo H**. Regeneration of injured skeletal muscle after the injury. *Muscles Ligaments Tendons J* 3: 337–345, 2013.

25. **Kind T**, **Liu K-H**, **Do Yup Lee**, **DeFelice B**, **Meissen JK**, **Fiehn O**. LipidBlast - in-silico tandem mass spectrometry database for lipid identification. *Nat Meth* 10: 755–758, 2013.

26. **Koves TR**, **Noland RC**, **Bates AL**, **Henes ST**, **Muoio DM**, **Cortright RN**. Subsarcolemmal and intermyofibrillar mitochondria play distinct roles in regulating skeletal muscle fatty acid metabolism. *Am J Physiol, Cell Physiol* 288: C1074–C1082, 2005.

27. **Larsen S**, **Nielsen J**, **Hansen CN**, **Nielsen LB**, **Wibrand F**, **Stride N**, **Schroder HD**, **Boushel R**, **Helge JW**, **Dela F**, **Hey-Mogensen M**. Biomarkers of mitochondrial content in skeletal muscle of healthy young human subjects. *J Physiol (Lond)* 590: 3349–3360, 2012.

28. **Lorenz MA**, **Burant CF**, **Kennedy RT**. Reducing Time and Increasing Sensitivity in Sample Preparation for Adherent Mammalian Cell Metabolomics. *Anal Chem* 83: 3406–3414, 2011.

29. **Marcus RL**, **Addison O**, **Kidde JP**, **Dibble LE**, **Lastayo PC**. Skeletal muscle fat infiltration: impact of age, inactivity, and exercise. *J Nutr Health Aging* 14: 362–366, 2010.

30. **Markworth JF**, **Vella LD**, **Figueiredo VC**, **Cameron-Smith D**. Ibuprofen treatment blunts early translational signaling responses in human skeletal muscle following resistance exercise. *J Appl Physiol* 117: 20–28, 2014.

31. **McDonagh B**, **Tyther R**, **Sheehan D**. Carbonylation and glutathionylation of proteins in the blue mussel Mytilus edulis detected by proteomic analysis and Western blotting: Actin as a target for oxidative stress. *Aquatic Toxicology* 73: 315–326, 2005.

32. **Mears JA**, **Lackner LL**, **Fang S**, **Ingerman E**, **Nunnari J**, **Hinshaw JE**. Conformational changes in Dnm1 support a contractile mechanism for mitochondrial fission. *Nat Struct Mol Biol* 18: 20–26, 2010.

33. **Mendias CL**, **Roche SM**, **Harning JA**, **Davis ME**, **Lynch EB**, **Sibilsky Enselman ER**, **Jacobson JA**, **Claflin DR**, **Calve S**, **Bedi A**. Reduced muscle fiber force production and disrupted myofibril architecture in patients with chronic rotator cuff tears. *J Shoulder Elbow Surg* 24: 111–119, 2015.

34. **Menshikova EV**, **Ritov VB**, **Fairfull L**, **Ferrell RE**, **Kelley DE**, **Goodpaster BH**. Effects of Exercise on Mitochondrial Content and Function in Aging Human Skeletal Muscle. *J Gerontol A Biol Sci Med Sci* 61: 534–3154, 2006.

35. **Meryon E**. On Granular and Fatty Degeneration of the Voluntary Muscles. *Med Chir Trans* 35: 73–84.1, 1852.

36. **Patel KD**, **Glancy B**, **Balaban RS**. The electrochemical transmission in I-Band

segments of the mitochondrial reticulum. *Biochimica et Biophysica Acta (BBA) - Bioenergetics* 1857: 1284–1289, 2016.

37. **Roche SM**, **Gumucio JP**, **Brooks SV**, **Mendias CL**, **Claflin DR**. Measurement of Maximum Isometric Force Generated by Permeabilized Skeletal Muscle Fibers. *J Vis Exp* : e52695–e52695, 2015.

38. **Ruan L**, **Zhou C**, **Jin E**, **Kucharavy A**, **Zhang Y**, **Wen Z**, **Florens L**, **Li R**. Cytosolic proteostasis through importing of misfolded proteins into mitochondria. *Nature* 266: 18051, 2017.

39. **Sandri M**. Signaling in muscle atrophy and hypertrophy. *Physiology (Bethesda)* 23: 160–170, 2008.

40. **Trapnell C**, **Roberts A**, **Goff L**, **Pertea G**, **Kim D**, **Kelley DR**, **Pimentel H**, **Salzberg SL**, **Rinn JL**, **Pachter L**. Differential gene and transcript expression analysis of RNA-seq experiments with TopHat and Cufflinks. *Nat Protoc* 7: 562–578, 2012.

41. **Vourazeris JD**, **Lawless MW**, **Markert RJ**, **Stills HF**, **Boivin GP**. Semitendinosus muscle fatty infiltration following tendon harvest in rabbits. *J Orthop Res* 31: 1234–1239, 2013.

42. **Wang H**, **Sreenivasan U**, **Sreenevasan U**, **Hu H**, **Saladino A**, **Polster BM**, **Lund LM**, **Gong D-W**, **Stanley WC**, **Sztalryd C**. Perilipin 5, a lipid droplet-associated protein, provides physical and metabolic linkage to mitochondria. *Journal of Lipid Research* 52: 2159–2168, 2011.

43. **Watt MJ**, **Hoy AJ**. Lipid metabolism in skeletal muscle: generation of adaptive and maladaptive intracellular signals for cellular function. *AJP: Endocrinology and Metabolism* 302: E1315–28, 2012.

44. **Watt MJ**. Storing up trouble: does accumulation of intramyocellular triglyceride protect skeletal muscle from insulin resistance? *Clin Exp Pharmacol Physiol* 36: 5–11, 2009.

45. **Willcocks RJ**, **Rooney WD**, **Triplett WT**, **Forbes SC**, **Lott DJ**, **Senesac CR**, **Daniels MJ**, **Wang DJ**, **Harrington AT**, **Tennekoon GI**, **Russman BS**, **Finanger EL**, **Byrne BJ**, **Finkel RS**, **Walter GA**, **Sweeney HL**, **Vandenborne K**. Multicenter prospective longitudinal study of magnetic resonance biomarkers in a large duchenne muscular dystrophy cohort. *Ann Neurol* 79: 535–547, 2016.

46. **Yen C-LE**, **Stone SJ**, **Koliwad S**, **Harris C**, **Farese RV**. Thematic review series: glycerolipids. DGAT enzymes and triacylglycerol biosynthesis. *The Journal of Lipid Research* 49: 2283–2301, 2008.

47. **Yu C**, **Chen Y**, **Cline GW**, **Zhang D**, **Zong H**, **Wang Y**, **Bergeron R**, **Kim JK**, **Cushman SW**, **Cooney GJ**, **Atcheson B**, **White MF**, **Kraegen EW**, **Shulman GI**.

Mechanism by which fatty acids inhibit insulin activation of insulin receptor substrate-1 (IRS-1)-associated phosphatidylinositol 3-kinase activity in muscle. *Journal of Biological Chemistry* 277: 50230–50236, 2002.

48. **Zhang C**, **Klett EL**, **Coleman RA**. Lipid signals and insulin resistance. *Clinical Lipidology* 8: 659–667, 2013.

CHAPTER V

Conclusion

SUMMARY

The purpose of this dissertation was to better understand the basic biology of tendon growth in adulthood, as well as identify mechanisms that lead to muscle dysfunction following rotator cuff. For tendon, the overall lack of knowledge in basic tendon biology restricted our ability to understand the molecular changes in tendon during injury. For muscle, the etiology of myosteatosis and consequences on muscle function was unknown, preventing the development of targeted strategies to ameliorate the disorder. The studies in this dissertation filled in considerable gaps in the understanding of basic tendon biology, and the progression of skeletal muscle myosteatosis. Additionally, this body of work established several new directions for future research that not only apply to rotator cuff injuries and tendinopathies, but a wide variety of musculoskeletal disorders.

FINDINGS AND FUTURE DIRECTIONS- TENDON

Until the last decade, studying adult tendon biology was extremely challenging due to the lack of tendon markers use for study. The approach taken by our lab was to identify markers that were important for tendon development *in utero*, and study these markers in adult tendon. The basic helix-loop-helix transcription factor, scleraxis, offered an attractive target due to its requirement for limb tendon development and it was the

earliest detectible tendon marker available (8). Early studies in our lab showed that scleraxis expression markedly decreased within tendon during adulthood compared to adolescent and young mice. However, during physiological loading, scleraxis expression was dramatically increased in the outermost region of the tendon, called the epitenon (13). There was a correlation between scleraxis expression and increased tendon CSA, but it was not known if scleraxis was required for tendon adaptation in adults. The findings of this dissertation offered substantial insight into the mechanobiology of adult tendon, using an established model of skeletal muscle hypertrophy, which also substantially increases tendon size.

The studies in Chapter II found that following synergist ablation, tendon grows by the formation of an immature tendon matrix, called a neotendon, from the epitenon outwards, similar to the rings of a tree. Within the neotendon were an abundance of scleraxis+ cells, many of which were proliferative. This was associated with increased scleraxis and type I collagen expression. Despite the load applied, the cells within the original tendon matrix did not re-enter the cell cycle, and the original tendon area did not change. Other lab groups posited that tendon contained different populations of cells: tenoblasts, which are proliferative and decreased with age, and tenocytes, which are terminally withdrawn from the cell cycle, but participated in ECM remodeling and maintenance (9, 16). The studies in Chapter II offered *in vivo* evidence for multiple populations of cells distinguished by their proliferative capacity. Increased scleraxis expression in these proliferative cells also showed that scleraxis likely had a central role in the growth and adaptation of tendon to mechanical loading.

To assess whether scleraxis was required for tendon adaptation, we utilized a line of transgenic mice that allowed for the conditional inactivation of scleraxis in Chapter III. After administering tamoxifen to knock-out scleraxis, following synergist ablation, tendons from transgenic mice displayed dramatically decreased growth due to a blunted neotendon compared to controls. The expression of several matrix-related genes was decreased in scleraxis mutant mice, and electron micrographs revealed aberrant collagen fibril alignment in mutant animals compared to controls. The most interesting finding was the accumulation of CD146+ mesenchymal stem cells in the neotendon of mutant animals. The expression of tenomodulin, which is to date the best marker for mature tendon fibroblasts, was decreased in mutant animals, suggesting a failure in proper tenogenic differentiation. These data provided, for the first time, insight into the role of scleraxis in the differentiation of adult tendon stem cells. These data indicate that scleraxis may be an important member of the tenogenic program, which starts from a CD146+ stem cell, differentiating into a proliferative, scleraxis+ fibroblast, then losing scleraxis expression, increasing tenomodulin expression, and becoming a differentiated tenocyte.

The studies in this dissertation provided substantial insight into scleraxis biology in the adult tendon, but more research is needed. Future studies will further expand the role of scleraxis in adult tendon biology, and the differentiation of tendon progenitors. We are currently examining the role of scleraxis in the differentiation of CD146+ cells *in vitro*, by separating CD146+ cells from tail tendons, and plating these cells in a 3D matrix of type I collagen. After time in culture, these cells temporally express scleraxis, and tenomodulin (Figure 1). While preliminary with only an N of 2, this protocol shows

tremendous promise in studying the tenogenic capacity of CD146+ cells *in vitro*. We plan on isolating CD146+ cells from $Scx^{flox/flox}$:$R26^{CreERT2/CreERT2}$ ($Scx^{\Delta/\Delta}$) mice and repeating this study with the addition of 4HT in culture, to assess whether scleraxis is required for the tenogenic capacity of these cells. Further, we are underway in creating $CD146^{CreERT2}$ mice, which we can cross to the available $Rosa26^{Ai9}$ mice, that contain a conditional activation cassette for the fluorescent protein, tdTomato. This new mouse would allow us to lineage trace CD146 cells through the process of neotendon formation during plantaris overload, and determine if indeed that this population is the tendon progenitor cell pool. Additionally, crossing $CD146^{CreERT2}$ mice to $Rosa26^{DTA}$ mice would allow for the ablation of CD146 cells to see if they are required for the expansion in neotendon following plantaris overload. The $Rosa26^{DTA}$ mouse expresses a modified form of the diphtheria toxin receptor (2), and after the addition of diphtheria toxin can kill off only cells that express the receptor, in this case CD146+ cells. Another important set of experiments would be to isolate tendon progenitors and perform experiments to identify the upstream regulators of scleraxis. We can identify potential upstream transcription factors *in silico* using the scleraxis promoter, and knock out top candidates in a series of *in vitro* experiments. The factor or factors that lead to a loss in scleraxis expression would be strong candidates for the upstream regulator of scleraxis, and could be overexpressed in other mesenchymal cell populations to determine if it is a master regulator of the tenogenic cell fate.

There is also evidence that scleraxis may be an attractive therapeutic target for the treatment of tendinopathies. Studies in our lab using human subjects have also identified that scleraxis may be important for normal tendon homeostasis, and loss of

scleraxis could lead to painful tendinopathies. We obtained biopsies from the biceps tendon of patients during rotator cuff surgery. The biceps are not part of the rotator cuff, and served as a control for tendon tissue. However, some of the biceps tendons of patients displayed tendinosis from pre-operative imaging. Interestingly, but perhaps not surprisingly given the studies outlined in this dissertation, the epitenon of these tendinopathic biopsies displayed a complete lack of scleraxis compared to healthy tendon biopsies (Figure 2). Therefore, scleraxis may also be important in the proper growth and maintenance of adult tendon in humans, and could potentially be re-administered into tendinopathic tendons as a therapy for these painful conditions.

FINDINGS AND FUTURE DIRECTIONS- SKELETAL MUSCLE

Most of the literature on rotator cuff myosteatosis relies on a recording system for the severity of lipid infiltration known as Goutallier scoring (6). The scale ranges from 0, or no lipid, to 4, indicating severely more lipid than muscle. Countless studies use this system to grade the severity of rotator cuff injuries and identify very strong negative correlations between the severity of lipid and muscle function (4, 5). Despite the importance of muscle function to regeneration and recovery from injury, there were very few studies that actually tested what the molecular consequences of myosteatosis were. Other than in rotator cuff injuries, myosteatosis can occur following injury to hamstring muscles (17), paraspinal muscles (1), with diseases like Duchenne muscular dystrophy (14, 18) and cancer (3), and in aging (12). Therefore, understanding the mechanisms by which lipid infiltration leads to muscle wasting could have an effect on a much larger body of musculoskeletal diseases, not just the rotator cuff. Identifying how lipid arises, and the consequences of ectopic lipid on muscle function, protein homeostasis, and

metabolism, will be useful in the development of therapies to reduce myosteatosis in patients. Additionally, it is still not known why the rotator cuff exhibits such a high degree of myosteatosis compared to other more commonly studied muscle injury models, and this question may require a substantial amount of research to address.

Studies in Chapter IV aimed to assess the molecular mechanisms of lipid infiltration in skeletal muscle during myosteatosis. Using large scale omics approaches, we identified several new mechanisms by which lipid accumulates and affects muscle function and metabolism. Using RNA Sequencing (RNASeq) and bioinformatics, we identified mitochondrial dysfunction as a highly-enriched pathway, and interestingly, despite the massive increase in lipid with injury, lipid oxidation was predicted by analysis software to be the most decreased pathway with injury. We assessed several measures of mitochondrial content, localization, and function and determined that myosteatosis conferred a lack of beta-oxidation, an increase in oxidative stress, and an accumulation of mitochondria in the peripheral space of muscle fibers. There was a decrease in long-chain acyl carnitines, which are required for the import of lipid into mitochondria for beta-oxidation, yet electron micrographs showed that early after injury, many lipid droplets accumulated inside mitochondria. Recent studies have shown that mitochondria can be reservoirs for misfolded protein in yeast with heat shock protein dysfunction (15), so it is conceivable that mitochondria can perform similar functions with lipid during myosteatosis. An accumulation of lipid in mitochondria as a scavenging mechanism could lead to an inability to oxidize them, exacerbating the accumulation of lipid further. Future studies will identify whether indeed this mechanism exists in mammalian cells, by knocking out heat shock proteins and measuring mitochondrial

lipid accumulation. Additionally, as mice can also be used to study rotator cuff myosteatosis (11), we can use transgenic mice that overexpress heat shock proteins and measure lipid accumulation in mitochondria in the early days following rotator cuff tear. This would provide substantial insight into whether lipid accumulation is a cause or consequence of mitochondrial dysfunction. To test this in a rat model, dysfunctional mitochondria can be isolated from torn rotator cuff muscles and injected into healthy rotator cuff. This would also identify if dysfunctional mitochondria were sufficient for the accumulation of lipid in a rat model.

The studies in Chapter IV also provided important insight into the long-term repercussions of lipid accumulation. Bioinformatics analysis identified protein kinase C-theta (PKCθ) signaling as an enriched pathway in the chronic stages of myosteatosis. Not much is known about this pathway in the context of skeletal muscle myosteatosis, but several studies have studied PKCθ signaling in skeletal muscle with obesity in type II diabetes. During lipid excess with diabetes, lipid intermediates build up within the muscle cell, activating PKCθ, which inhibits the insulin pathway (19). The insulin like growth factor-1 (IGF-1) pathway shares many of the same members of the signaling cascade as insulin, and the IGF-1 pathway is one of the main determinants of skeletal muscle mass (7). Therefore, it is possible that excess lipid in myosteatosis also activates PKCθ and leads to a decrease in IGF-1 signaling, further causing muscle weakness and atrophy. Indeed, components of IGF-1 signaling were reduced with injury, and future studies can address this further. Using primary rat myotubes, we plan to test the impact of excess lipid on PKCθ signaling and muscle atrophy. After the addition IGF-1 to cells, we can measure the effect of free fatty acids on IGF-1 signaling

components and myotube size. Additionally, we will use inhibitors of PKCθ to identify if PKCθ is required for changes in lipid induced muscle atrophy and IGF-1 signaling. This would provide a much greater understanding of the mechanisms by which sustained ectopic lipid in chronic rotator cuff tears leads to deficits in muscle function.

Clinically, the studies outlined here may provide several avenues for therapies for myosteatosis. Most patients that present with myosteatosis have developed a chronic form of the disorder, where lipid infiltration and muscle wasting is already progressed. Persistent muscle weakness and atrophy is a major drawback in the ability to successfully treat these injuries and reduce patient recovery times. Therefore, improving the regeneration of skeletal muscle following surgical intervention will decrease failure rates. Therapies that aim to increase beta-oxidation will likely help patients with acute myosteatosis and decrease subsequent lipid accumulation. However, for chronic situations, strategies to increase IGF-1 signaling would potentially be promising therapies to increase muscle size and regeneration for chronically wasted muscles. This would require further research towards specific therapeutic targets and methods of administration of such therapies in order to translate from pre-clinical models to human treatment.

CONCLUSIONS

Diseases and injuries to the musculoskeletal system are the leading cause of disability for people in the United States, and account for over half of chronic conditions for individuals over 50 (20). By 2030, the number of individuals over 65 is expected to double, therefore there will likely always be a requirement for research towards the development of therapies for musculoskeletal conditions. The studies in this dissertation

made considerable advancements in the understanding of musculoskeletal physiology. These data will serve as the framework to better understand musculoskeletal conditions involving tendinopathies and muscle myosteatosis, and likely have a much wider reach than these disorders.

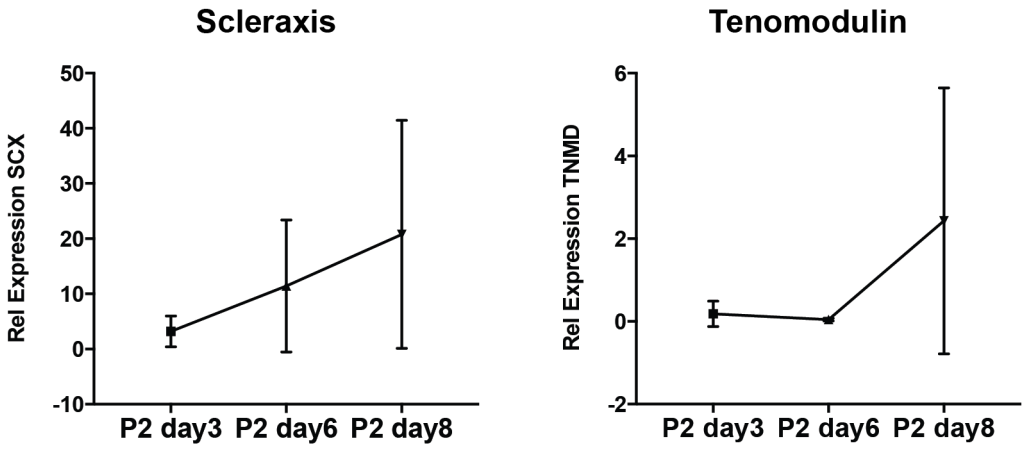

Figure 5.1. Expression of scleraxis and tenomodulin in a cohort (N=2) of isolated CD146+ cells in culture. Cells were passaged into 3D type I collagen gel and isolated 3, 6, and 8 days following passaging.

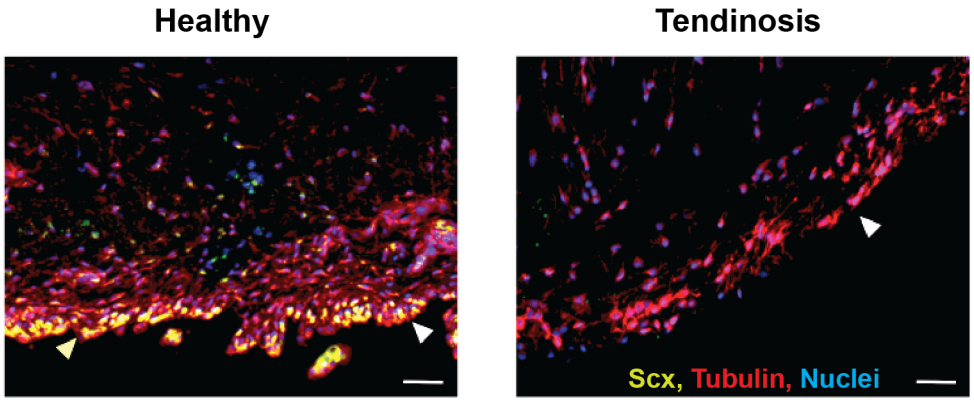

Figure 5.2. Immunohistochemical images of biceps tendon biopsies from patients with healthy (left) or tendinopathic (right) tendon. Scleraxis (green), tubulin (red), nuclei (blue). White arrows indicate cells in the epitenon.

REFERENCES

1. **Aubrey J**, **Esfandiari N**, **Baracos VE**, **Buteau FA**, **Frenette J**, **Putman CT**, **Mazurak VC**. Measurement of skeletal muscle radiation attenuation and basis of its biological variation. *Acta Physiologica* 210: 489–497, 2014.

2. **Buch T**, **Heppner FL**, **Tertilt C**, **Heinen TJAJ**, **Kremer M**, **Wunderlich FT**, **Jung S**, **Waisman A**. A Cre-inducible diphtheria toxin receptor mediates cell lineage ablation after toxin administration. *Nat Meth* 2: 419–426, 2005.

3. **Ewaschuk JB**, **Almasud A**, **Mazurak VC**. Role of n-3 fatty acids in muscle loss and myosteatosis. *Applied physiology, nutrition, and metabolism = Physiologie appliquée, nutrition et métabolisme* 39: 654–662, 2014.

4. **Gerber C**, **Schneeberger AG**, **Hoppeler H**, **Meyer DC**. Correlation of atrophy and fatty infiltration on strength and integrity of rotator cuff repairs: a study in thirteen patients. *J Shoulder Elbow Surg* 16: 691–696, 2007.

5. **Gladstone JN**, **Bishop JY**, **Lo IKY**, **Flatow EL**. Fatty infiltration and atrophy of the rotator cuff do not improve after rotator cuff repair and correlate with poor functional outcome. *American Journal of Sports Medicine* 35: 719–728, 2007.

6. **Goutallier D**, **Postel JM**, **Bernageau J**, **Lavau L**, **Voisin MC**. Fatty muscle degeneration in cuff ruptures. Pre- and postoperative evaluation by CT scan. *Clin Orthop Relat Res* : 78–83, 1994.

7. **Gumucio JP**, **Mendias CL**. Atrogin-1, MuRF-1, and sarcopenia. *Endocrine* 43: 12–21, 2013.

8. **Huang AH**, **Lu HH**, **Schweitzer R**. Molecular regulation of tendon cell fate during development. *J Orthop Res* 33: 800–812, 2015.

9. **Ippolito E**, **Natali PG**, **Postacchini F**, **Accinni L**, **De Martino C**. Morphological, immunochemical, and biochemical study of rabbit achilles tendon at various ages. *J Bone Joint Surg Am* 62: 583–598, 1980.

10. **Jain NB**, **Wilcox RB**, **Katz JN**, **Higgins LD**. Clinical examination of the rotator cuff. *PM R* 5: 45–56, 2013.

11. **Liu X**, **Laron D**, **Natsuhara K**, **Manzano G**, **Kim HT**, **Feeley BT**. A mouse model of massive rotator cuff tears. *The Journal of Bone and Joint Surgery* 94: e41–10, 2012.

12. **Marcus RL**, **Addison O**, **Kidde JP**, **Dibble LE**, **Lastayo PC**. Skeletal muscle fat infiltration: impact of age, inactivity, and exercise. *J Nutr Health Aging* 14: 362–366, 2010.

13. **Mendias CL**, **Gumucio JP**, **Bakhurin KI**, **Lynch EB**, **Brooks SV**. Physiological

loading of tendons induces scleraxis expression in epitenon fibroblasts. *J Orthop Res* 30: 606–612, 2012.

14. **Meryon E**. On Granular and Fatty Degeneration of the Voluntary Muscles. *Med Chir Trans* 35: 73–84.1, 1852.

15. **Ruan L**, **Zhou C**, **Jin E**, **Kucharavy A**, **Zhang Y**, **Wen Z**, **Florens L**, **Li R**. Cytosolic proteostasis through importing of misfolded proteins into mitochondria. *Nature* 266: 18051, 2017.

16. **Tan Q**, **Lui PPY**, **Lee YW**. In vivo identity of tendon stem cells and the roles of stem cells in tendon healing. *Stem Cells and Development* 22: 3128–3140, 2013.

17. **Vourazeris JD**, **Lawless MW**, **Markert RJ**, **Stills HF**, **Boivin GP**. Semitendinosus muscle fatty infiltration following tendon harvest in rabbits. *J Orthop Res* 31: 1234–1239, 2013.

18. **Willcocks RJ**, **Rooney WD**, **Triplett WT**, **Forbes SC**, **Lott DJ**, **Senesac CR**, **Daniels MJ**, **Wang DJ**, **Harrington AT**, **Tennekoon GI**, **Russman BS**, **Finanger EL**, **Byrne BJ**, **Finkel RS**, **Walter GA**, **Sweeney HL**, **Vandenborne K**. Multicenter prospective longitudinal study of magnetic resonance biomarkers in a large duchenne muscular dystrophy cohort. *Ann Neurol* 79: 535–547, 2016.

19. **Yu C**, **Chen Y**, **Cline GW**, **Zhang D**, **Zong H**, **Wang Y**, **Bergeron R**, **Kim JK**, **Cushman SW**, **Cooney GJ**, **Atcheson B**, **White MF**, **Kraegen EW**, **Shulman GI**. Mechanism by which fatty acids inhibit insulin activation of insulin receptor substrate-1 (IRS-1)-associated phosphatidylinositol 3-kinase activity in muscle. *Journal of Biological Chemistry* 277: 50230–50236, 2002.

20. **The Burden of Musculoskeletal Diseases in the United States**. Amer Academy of Orthopaedic Surgeons, 2008.